AD-A140 434 JOINT SERVICES ELECTRONICS PROGRAM(U) OHIO STATE UNIV 1/3
COLUMBUS ELECTROSCIENCE LAB DEC 83 ESL-710816-15
N00014-78-C-0049

UNCLASSIFIED F/G 9/5 NL

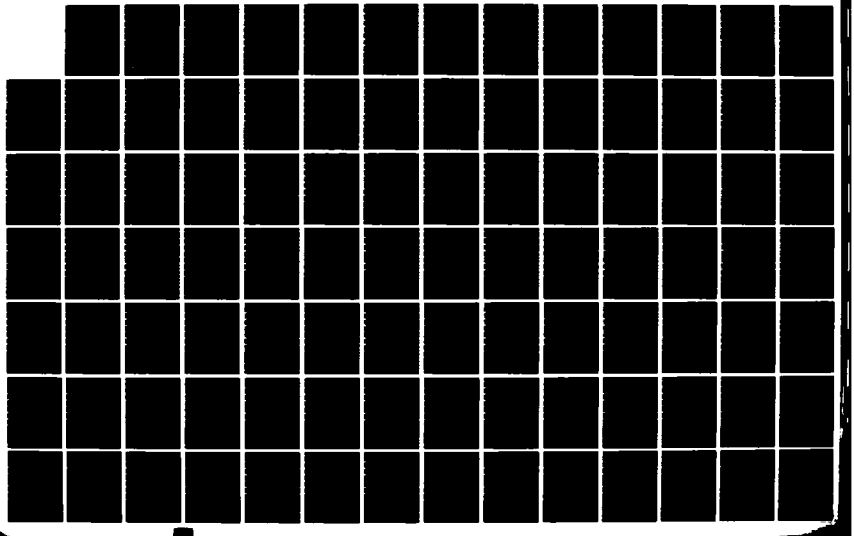

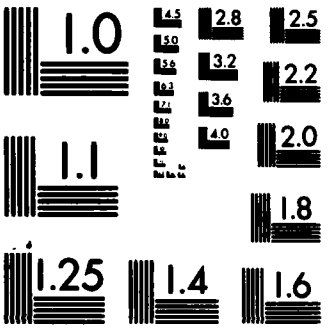

(12)

OSU

The Ohio State University

JOINT SERVICES ELECTRONICS PROGRAM

AD A140434

The Ohio State University

ElectroScience Laboratory

Department of Electrical Engineering
Columbus, Ohio 43212

Sixth Annual Report 710816-15

Contract N00014-78-C-0049

December 1983

DTIC FILE COPY

Department of the Navy
Office of Naval Research
800 Quincy Street
Arlington, Virginia

NOTICES

When Government drawings, specifications, or other data are used for any purpose other than in connection with a definitely related Government procurement operation, the United States Government thereby incurs no responsibility nor any obligation whatsoever, and the fact that the Government may have formulated, furnished, or in any way supplied the said drawings, specifications, or other data, is not to be regarded by implication or otherwise as in any manner licensing the holder or any other person or corporation, or conveying any rights or permission to manufacture, use, or sell any patented invention that may in any way be related thereto.

50272-101

REPORT DOCUMENTATION PAGE	1. REPORT NO. 1	2.	3. Recipient's Accession No. A140 434
4. Title and Subtitle: JOINT SERVICES ELECTRONICS PROGRAM			5. Report Date: December 1983
			6.
7. Author(s)			8. Performing Organization Rept. No. ESL 710816-15
9. Performing Organization Name and Address: The Ohio State University ElectroScience Laboratory, Department of Electrical Engineering, Columbus, Ohio 43212			10. Project/Task/Work Unit No.
			11. Contract(C) or Grant(G) No. (C) N00014-78-C-0049 (G)
12. Sponsoring Organization Name and Address: Department of the Navy, Office of Naval Research, 800 North Quincy Street, Arlington, Virginia 22217			13. Type of Report & Period Covered: Annual Report 11/82-11/83
			14.

15. Supplementary Notes

16. Abstract (Limit: 200 words)

This report presents the sixth annual summary of research at Ohio State sponsored by the Joint Services Electronics Program (JSEP). The research is in the area of electromagnetics and the specific topics are: (1) Diffraction Studies; (2) Hybrid Techniques; (3) Integral Equation Studies; (4) Time Domain; and (5) Transient Signature Measurements of Radar Targets for Inverse Scattering Research.

17. Document Analysis a. Descriptors

b. Identifiers/Open-Ended Terms

Electromagnetics	Surface Current	Polarization	Transient Signature
Diffraction	Antennas	Radar Target	
Hybrid Techniques	Time Domain	Inverse Scattering	

c. COSATI Field/Group

18. Availability Statement	19. Security Class (This Report) Unclassified	21. No. of Pages 201
	20. Security Class (This Page) Unclassified	22. Price

(See ANSI-Z39.18) See Instructions on Reverse OPTIONAL FORM 272 (4-77) (Formerly NTIS-35) Department of Commerce

TABLE OF CONTENTS

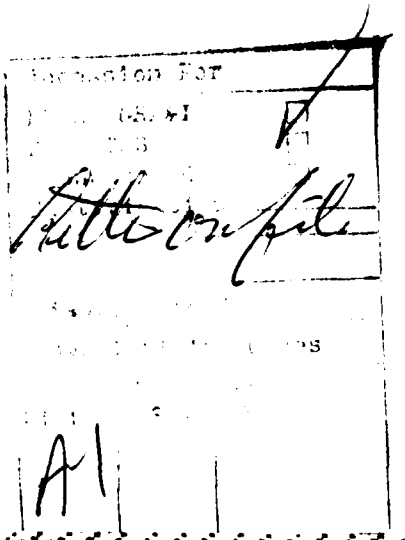

LIST OF TABLES

LIST OF FIGURES

I. INTRODUCTION

This report presents the sixth annual summary of research at Ohio State sponsored by the Joint Services Electronics Program (JSEP). The research is in the area of electromagnetics and the specific topics are: (1) Diffraction Studies; (2) Hybrid Techniques; (3) Integral Equation Studies; (4) Time Domain; and (5) Transient Signature Measurements of Radar Targets for Inverse Scattering Research.

The following sections summarize the significant accomplishments of the program (Section II) and the research by work unit (Section III). Researchers and their publications are listed under each work unit. A listing of the present research programs at the Laboratory and all reports and papers published by the Laboratory during the past year are given in the appendices.

II. SIGNIFICANT ACCOMPLISHMENTS

Our major research area continues to be the analysis of electromagnetic radiation and scattering. Associated with this primary goal is a substantial program for improving our experimental capabilities. This was supported in part by the JSEP program and has expanded recently with other sponsorship so that our anechoic chamber compact scattering range is probably the best of its kind at the present time. This is emphasized by the fact that we have provided information to Scientific Atlanta (the reflector manufacturer) for improving these facilities. We have also been contacted by several other manufacturers requesting assistance in building the next generation of compact ranges. It is noted that the stepped frequency concept originated under JSEP was then developed using the compact range under separate funding by ONR. Additional improvements were made under funding from NASA. This has indeed been a most rewarding area of research.

The analysis is being directed more and more to the study of the interaction of electromagnetic fields and penetrable materials. This is being pursued from (a) a high frequency asymptotic viewpoint, (b) a surface impedance model, (c) a moment method approach and (d) a hybrid approach.

However, the studies of diffraction by conducting bodies using the Uniform Geometrical Theory of Diffraction (UTD) continue to be a very substantial part of our research activities. The general problems consist of the radiation from antennas mounted close to perfectly

conducting edges (and also the scattering from objects positioned at edges), as well as paraxial edge diffraction and slope diffraction by perfectly-conducting convex cylinders. The radiation studies have helped us to develop more general computer codes on other programs for the analysis of antennas on or near complex structures (e.g., aircraft and ships). The scattering work is helping on programs involving radar cross section studies and target identification. This work is basic to the development of computer codes for calculating the patterns of reflector antennas and antennas on aircraft, missiles, satellites, ships and in other environments, and for calculating the scattered fields of a wide range of complex objects.

As we have observed, some of the above efforts have been supported by other sources of funding but are a direct offspring of the Joint Services Electronics Program. Such topics include but are not limited to:

a) improved RCS pattern measurement techniques,

b) analysis of the scattered fields of aerospace vehicles, and

c) use of transient techniques for low frequency target center isolation.

Computer codes based on the high frequency asymptotic techniques for antennas mounted on various types of vehicles are now used through out the aerospace industry. A long term goal in the electromagnetic scattering studies is to evolve computer codes comparable to those

for antenna patterns now in general use by the aerospace industry. One special code has been developed for this purpose but requires substantial knowledge of the GTD and of the pertinent scattering mechanism by the user.

The time domain studies in electromagnetics are also continued. Research in both theoretical and experimental methods are providing substantial rewards. The theoretical program involves:

1. Complex Natural Resonance and Geometrical Procedures
2. Evaluation of Complex Natural Resonances via Rational Function Approximants
3. Transient Current Density on a Conducting Sphere
4. Cavity Studies, and
5. K-Pulse Studies.

The time domain experimental program is directed toward assembling complete complex scattering data on several canonical target shapes. The complete target signature data increases substantially in value when the waveform can be interpreted and scattering mechanisms can be identified. These experimental results are of sufficient quality that this has become practical. Indeed, they have been used several times this past year on related projects when unexpected high scattered fields were obtained for aircraft targets to identify and reduce these high scattering mechanisms.

Continued research in time domain reflection will produce a more complete understanding of the interaction of electromagnetic fields with complex targets and will also improve our target identification capabilities.

Nine graduate students have been involved in the above research over the past year. Over the past four years, with the support of the JSEP at Ohio State, there have been 10 students granted the M.Sc. degree in Electrical Engineering and 9 students granted the Ph.D. degree in Electrical Engineering.

III. RESEARCH SUMMARY

A. Diffraction Studies

Researchers: R.G. Kouyoumjian, Professor (Phone: (614) 422-7302)

P.H. Pathak, Assistant Professor

N. Wang, Senior Research Associate

R. Tiberio, Visiting Professor and Consultant

R. Paknys, Graduate Research Associate

M. Buyukdura, Graduate Research Associate

Accomplishments

During the present contract period, the work accomplished in extending the uniform geometrical theory of diffraction (UTD) has been substantial. This research, and the technical papers based on this research which have recently appeared (or have been accepted for publication) are described below.

1. Diffraction by Non-Conducting Surfaces

a. Smooth dielectric covered and impedance convex surface

A study of the electromagnetic radiation and scattering from a conducting surface with dielectric coating is of great interest in that it provides an understanding of the effects of the loading on the scattered fields. An interesting application of coating is to control the electromagnetic scattering characteristics from conducting bodies such as an aircraft, missile, satellite, etc. Also, it is useful in predicting the radar cross-section of structures made of composite materials or conducting bodies coated with dielectric materials.

In the case of a conducting surface coated with a thin layer of dielectric with a uniform thickness, the surface can be conveniently viewed as an impedance surface with a constant surface impedance. We have developed a high frequency solution for the problem and were able to predict the resonance phenomena of the radar cross-section of a circular cylinder with a constant surface impedance. It was found that surface waves with almost pure imaginary propagation constant traverse around the cylinder surface with diminishing attenuation, and interfere with each other constructively such that they add in phase to give the distinctive resonance phenomena in the radar cross-section. Numerical values for the propagation constant of the surface wave, which are related to the Regge poles of the impedance cylinder, have been found. Also, a criterion for predicting resonance has been established and

the correlations between the resonance, the Regge poles, and the natural frequencies of the impedance cylinder have been demonstrated.

It should be noted that the surface-impedance model is valid only for low-loss, thin dielectric sheets over the conducting surfaces. For a coating with moderate thickness, a more accurate approach is being pursued. More recently, work has been carried out on the investigation of the radar cross-section of a conducting cylinder coated by a dielectric layer of uniform thickness.

Using the standard Watson's transformation technique, the rigorous eigenfunction solution for the coated circular cylinder is cast into a ray solution. The backscattered field from the coated cylinder, illuminated with an incident plane wave, is obtained by summing the geometrical-optics contribution and the surface-wave contributions which include all the multiply-encircled surface waves. The parameter of fundamental importance associated with surface-wave fields is the propagation constant of the surface wave. The propagation constant is related to the Regge poles of the coated cylinder. By a combination of numerical procedures, these Regge poles were obtained by solving the high frequency approximation of the resonance equation for the dielectric coated conducting cylinder.

For thick enough coatings, the surface waves moving around the cylinder resemble those trapped in a planar, grounded, dielectric slab. It is found that the dominant surface waves have a small attenuation rate so that all the multiply-encircled waves must be taken into

consideration in a self-consistent fashion. As a consequence, resonances appear in the scattering cross section. The surface wave interpretation of the resonance phenomenon and the condition for predicting the resonance frequencies are now understood. The normalized radar cross section of the coated cylinder obtained from the high frequency ray solution has been shown to compare well with the eigenfunction result.

As a continuation and extension of the work involving the backscattering from the coated cylinder, efforts have been directed to the problems of radiation and bistatic scattering from smooth, dielectric covered and/or impedance convex surfaces. The ultimate goal here is to develop a uniform high-frequency solution for the electromagnetic fields due to an antenna radiating in the presence of a loaded convex surface. This solution could be expressed in terms of an integral representation similar to the Fock-type integrals which appeared in the solution for the perfectly-conducting, smooth, convex surfaces [1,2,3] except that the Fock integral now contains a denominator in the Fock integrand which yields a resonant condition in terms of the impedance or dielectric loading. Far from the geometrical shadow boundaries, the integrals can be well approximated by the geometrical optics (GO) solution in the illuminated region and by the surface (creeping) or ray modal residue series solution in the shadow region, respectively. However, within the transition region, i.e., in the neighborhood of the shadow boundaries, only the integral representation provides the correct solution. Furthermore, this

transition integral joins smoothly with the GO solution in the lit region and reduces to the surface ray modal or residue series solution in the shadow region. Thus, the essential task is to develop an efficient method for evaluating this Fock-type transition integral associated with the smooth, dielectric-covered and impedance type convex surface.

The Fock (transition) integral g(x,q), associated with the canonical problem of the radiation by a two dimensional (2-D) magnetic line source on a circular cylinder with a constant surface impedance boundary condition, has been derived and evaluated. Some numerical results for g(x,q) are presented in Figure A-1. Referring to Figure A-1, our results for a lossy curved surface (A = 0.5, 1.0) compare well with those obtained by Wait and Conda [4]. Note that g(x,q) represents the field radiated by the line source on the cylinder, or it also represents the field induced on the surface of the cylinder by a distant line source (located off the surface) via reciprocity. For a reactive surface that supports a surface wave, our results (q>0) confirm the fact that a reactive surface is more efficient than the conducting surface for guiding the electromagnetic energy. Notice that in Figure A-1, the curve denoted by q=0 is for the case of a perfectly conducting curved surface. Here, q is a parameter related to the value of the surface impedance and the cylinder radius. The shadow boundary is located at x=0 in Figure A-1. The above material taken from [5] has now been extended in the current time frame as is discussed in the following paragraphs.

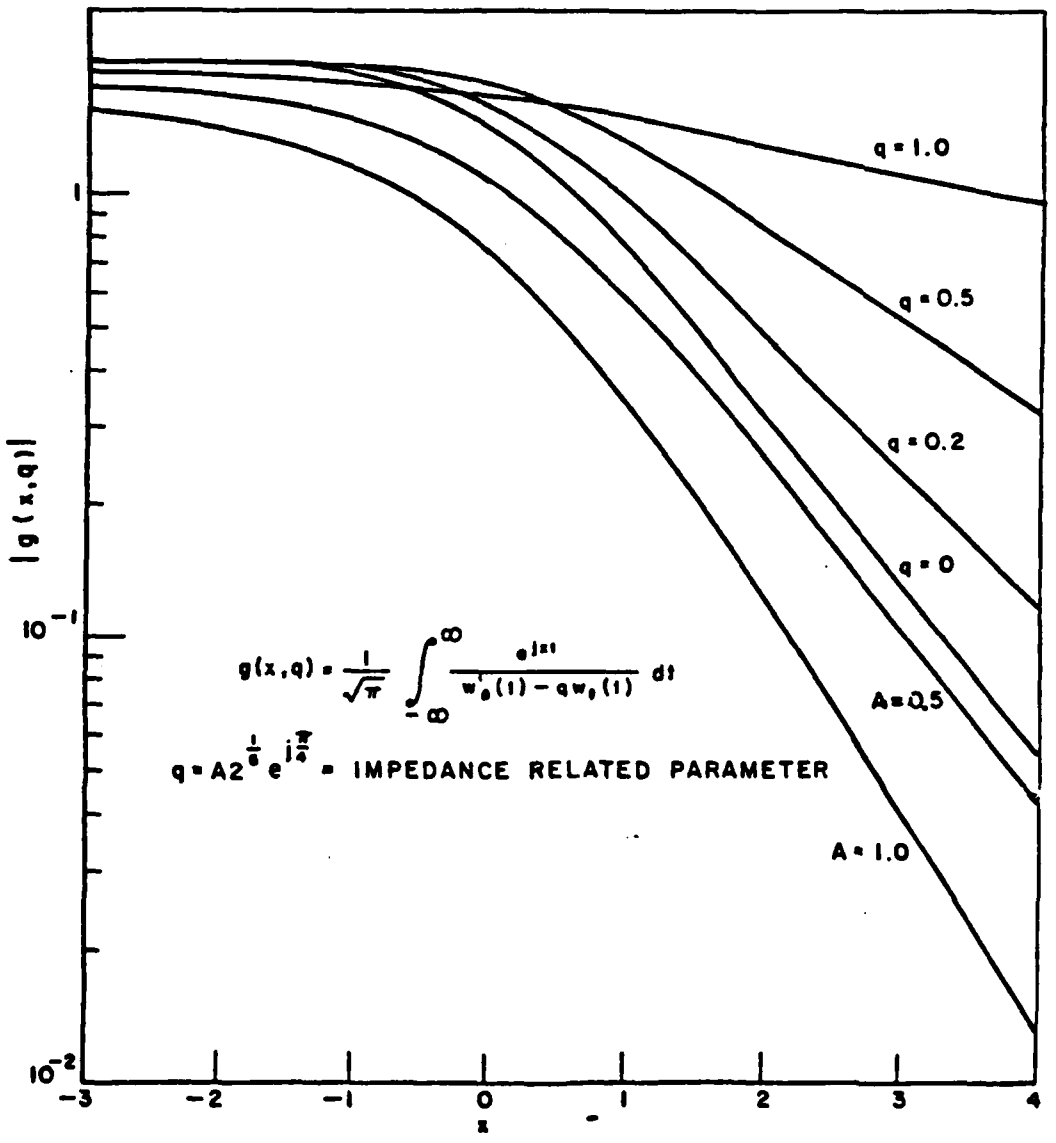

Figure A-1. The transition integral |g(x,q)|.

The newly developed transition integral g(x,z) has been employed to calculate the high frequency radiation patterns due to a two dimensional magnetic line source mounted on a circular cylinder with surface impedance Z_s. Figures A-2 through A-5 compare the patterns obtained by the eigenfunction solution (solid line) and the high frequency GTD solution (dash line). It should be noted that the high frequency GTD solution contains the newly developed transition integral g(x,q), where

$$q = -i\left(\frac{ka}{2}\right)^{1/3} \frac{Z_s}{\eta_0} \quad .$$

Notice the agreement between the two solutions is satisfactory for $Z_s = R_s + j\,X_s$ up to 10 + j 200. However, for Z_s = 10 + j 300, the high frequency GTD solution does not yield accurate results. The discrepency is introduced by the approximation used for the Hankel function $H_\nu^{(2)}(x)$, namely

$$H_\nu^{(2)}(x) \sim \frac{j}{\sqrt{\pi}} \left(\frac{2}{x}\right)^{1/3} W_1(t)$$

and

$$H_\nu^{(2)'}(x) \sim -\frac{j}{\sqrt{\pi}} \left(\frac{2}{x}\right)^{2/3} W_1'(t)$$

where $W_1(t)$ and $W_1'(t)$ are the Airy integrals defined by [4]

$$W_1(t) = \frac{1}{\sqrt{\pi}} \int_{\Gamma_1} ds\; e^{st - s^3/3}$$

and

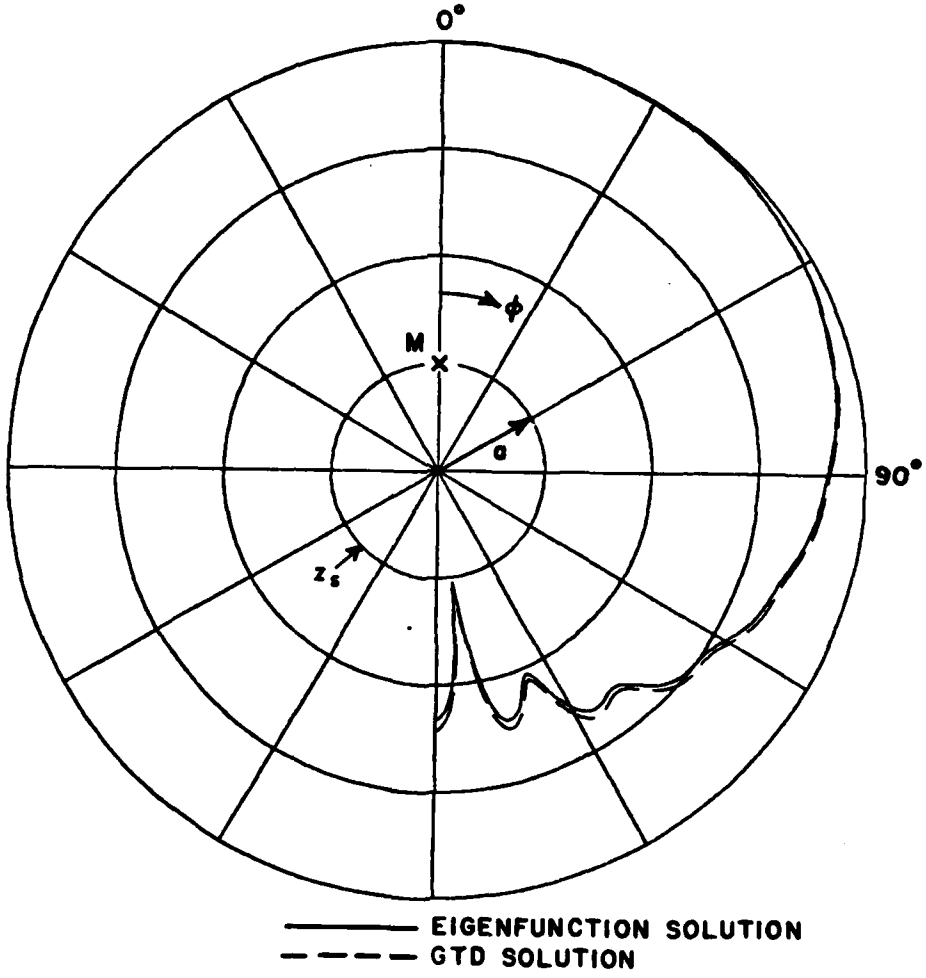

Figure A-2. Pattern due to a magnetic line source radiating from a circular cylinder with surface impedance $Z_S=R_S+jX_S$. ka = 10, Z_S = 10Ω.

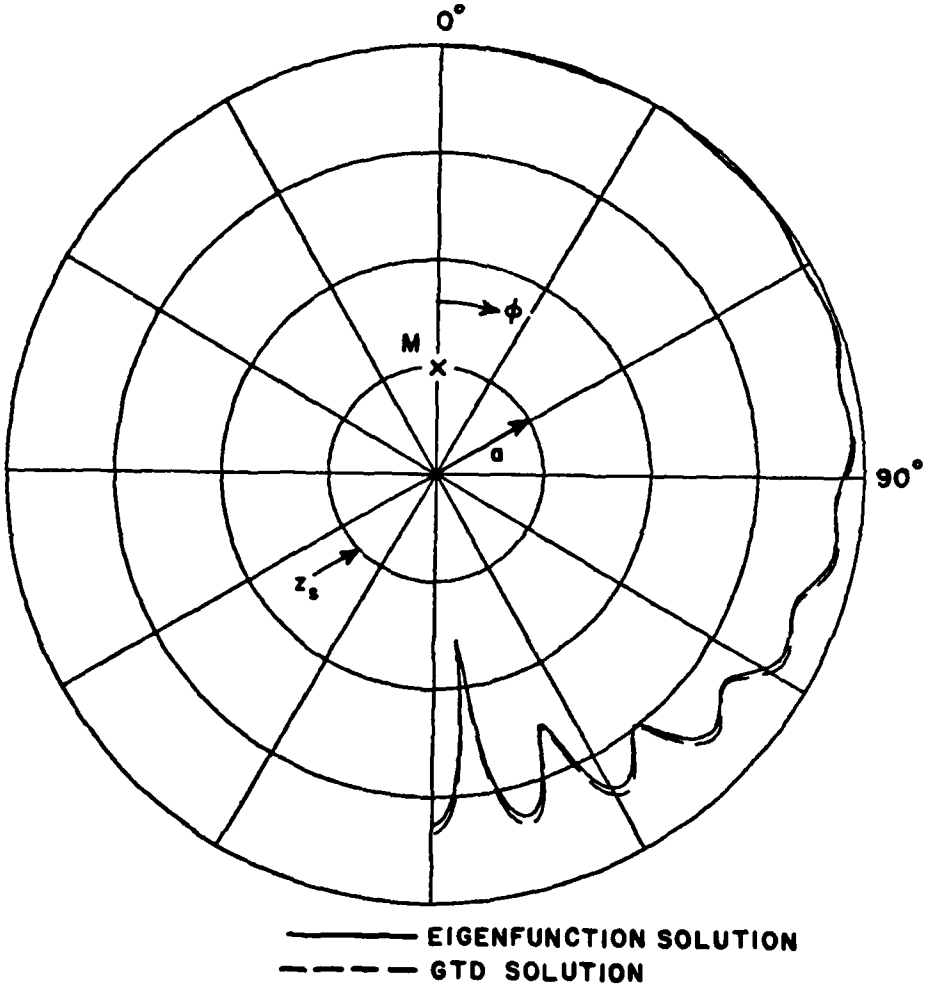

Figure A-3. Pattern due to a magnetic line source radiating from a circular cylinder with surface impedance $Z_S=R_S+jX_S$. ka = 10, Z_S = 10 + j 100.

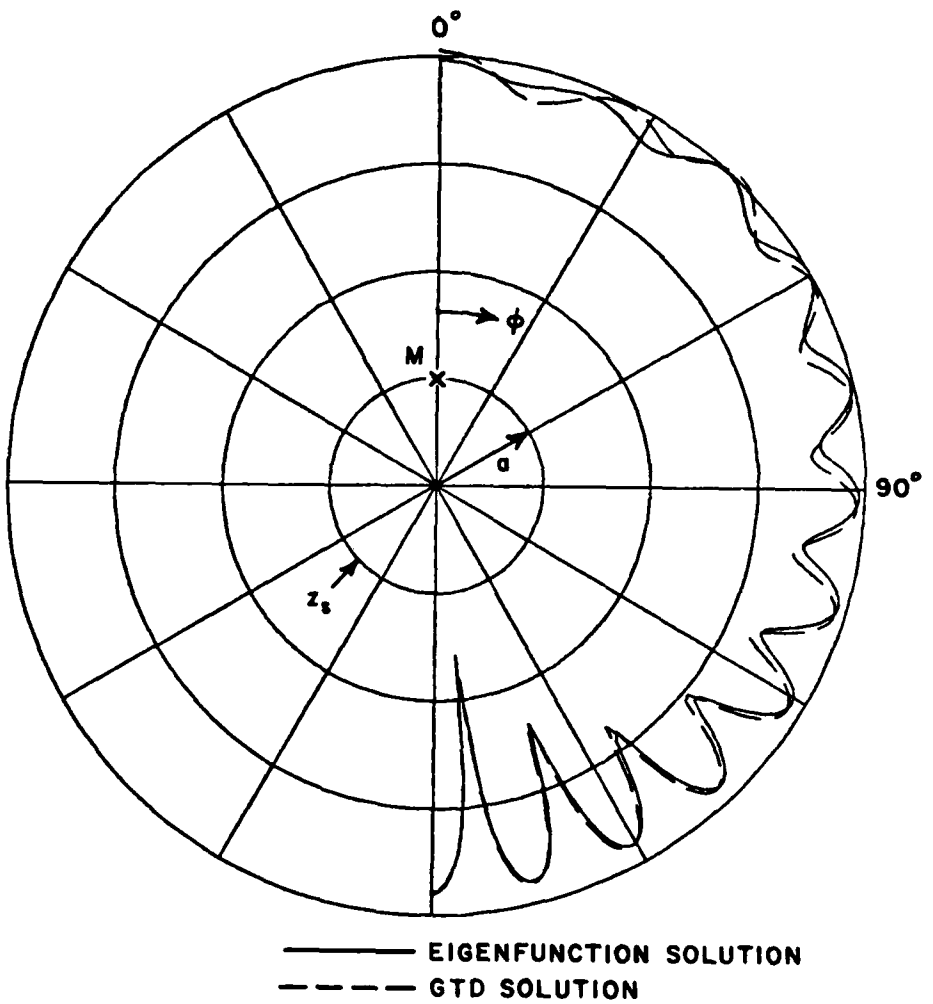

Figure A-4. Pattern due to a magnetic line source radiating from a circular cylinder with surface impedance $Z_S=R_S+jX_S$. ka = 10, Z_S = 10 + j 200.

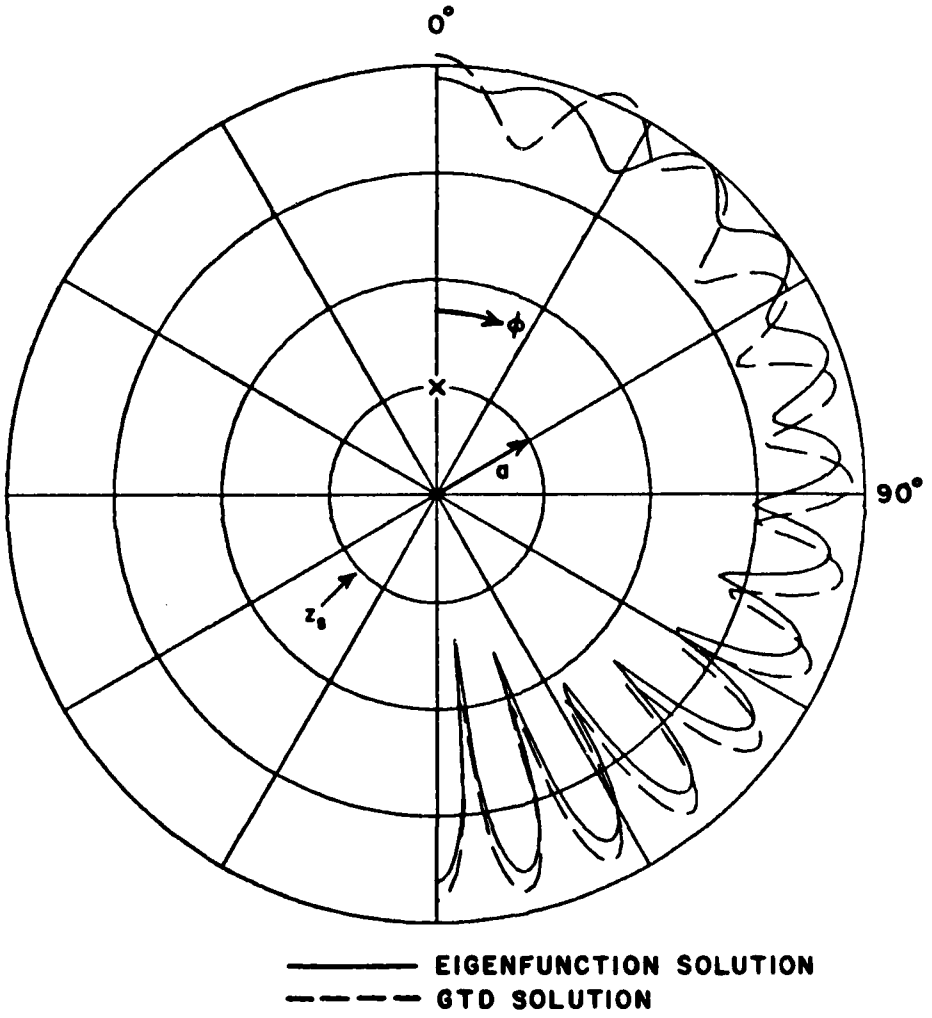

Figure A-5. Pattern due to a magnetic line source radiating from a circular cylinder with surface impedance $Z_S=R_S+jX_S$. ka = 10, Z_S = 10 + j 300.

$$W_1'(t) = \frac{1}{\sqrt{\pi}} \int_{\Gamma_1} s\, ds\, e^{st-s^3/3}$$

in the notation of Fock where the quantity t is defined by

$$t = \left(\frac{2}{x}\right)^{1/3} (\nu - x) .$$

It turns out that for large reactance X_s, the curved surface supports surface waves which are tightly trapped. As a consequence, a better approximation for the function $H_\nu^{(2)}(x)$,

$$H_\nu^{(2)}(x) \sim \frac{j}{\sqrt{\pi}} \left(\frac{2}{x}\right)^{1/3} \left\{W_1(t) - \frac{1}{60m^2}\left[4tW_1(t) + t^2 W_1'(t)\right]\right\}$$

$$H_\nu^{(2)'}(x) \sim -\frac{j}{\sqrt{\pi}} \left(\frac{2}{x}\right)^{2/3} \left\{W_1'(t) + \frac{1}{60m^2}\left[4tW_1'(t) + (6-t^3)W_1(t)\right]\right\} ,$$

should be employed [5] in the analysis.

During the previous year, the high frequency GTD solution has been modified to include the higher-order terms resulted from the approximations employed for the Hankel functions. Figures A-6 through A-9 compare the new GTD solution and the eigenfunction solution. It is seen that the agreement between the two solutions is excellent.

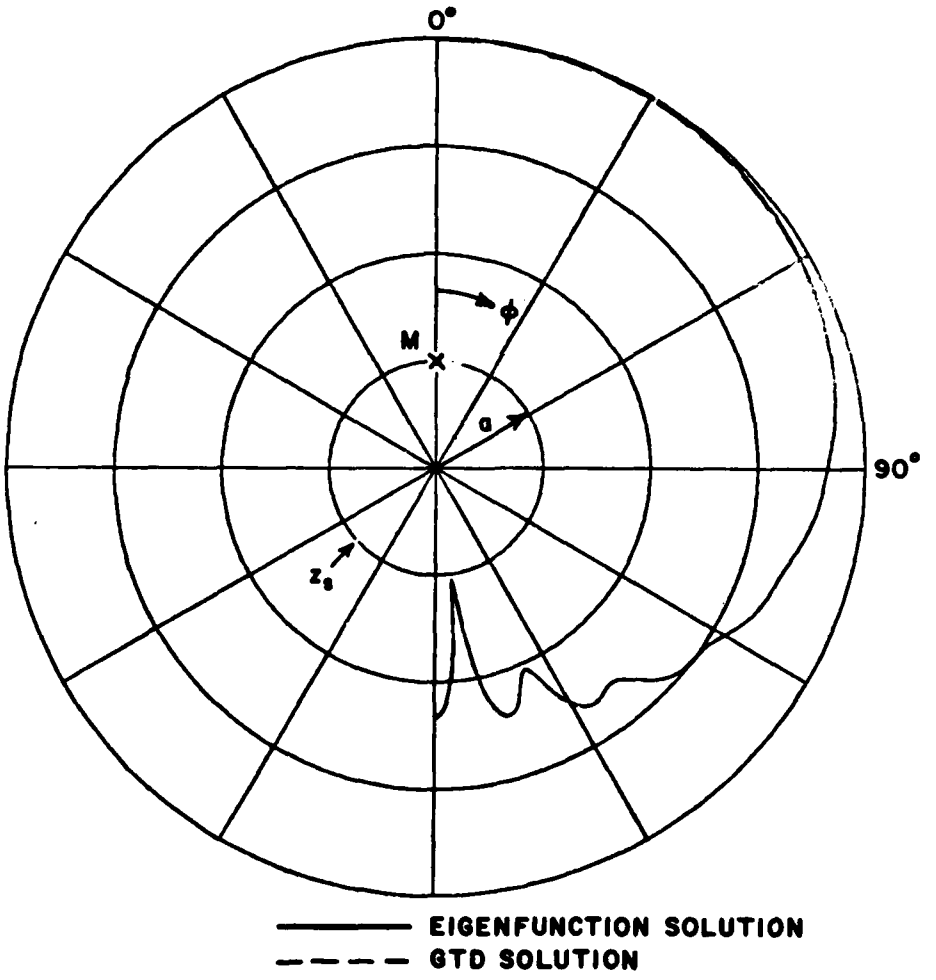

Figure A-6. Pattern due to a magnetic line source radiating from a circular cylinder with surface impedance $Z_S=R_S+jX_S$. ka = 10, Z_S = 10.

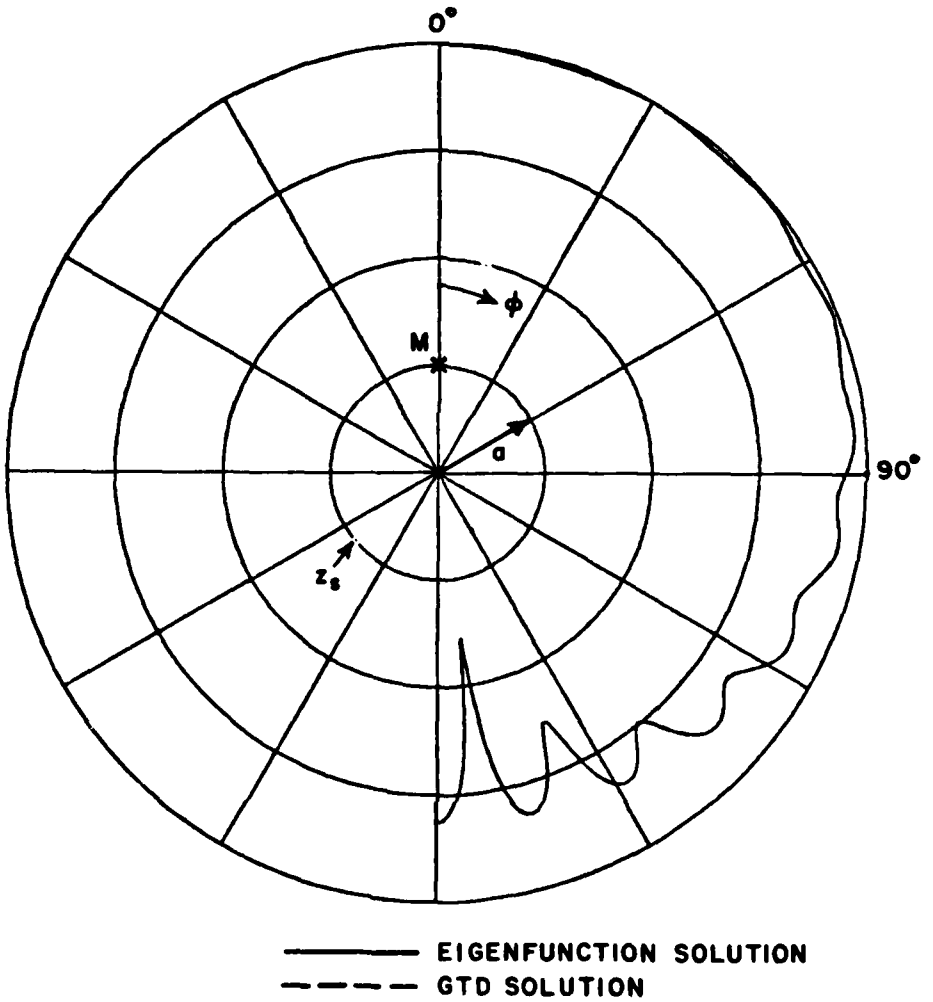

Figure A-7. Pattern due to a magnetic line source radiating from a circular cylinder with surface impedance $Z_S=R_S+jX_S$. ka = 10, Z_S = 10 + j 100.

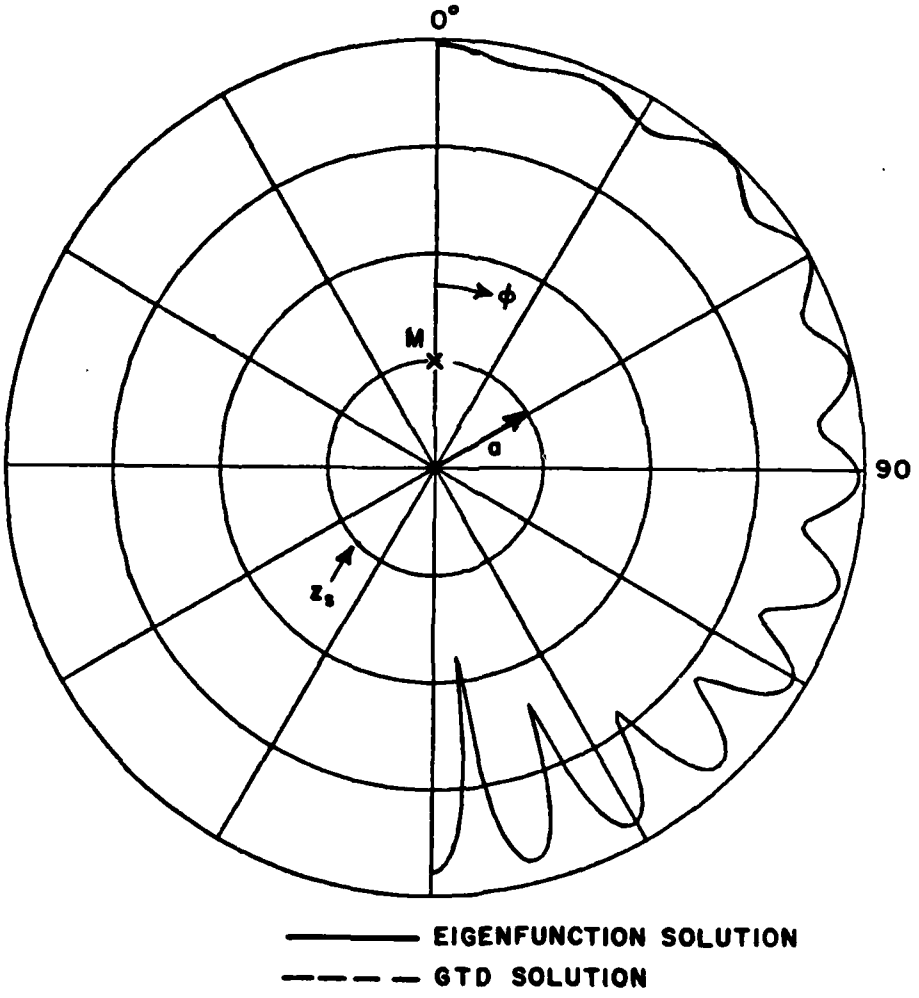

Figure A-8. Pattern due to a magnetic line source radiating from a circular cylinder with surface impedance $Z_S=R_S+jX_S$. ka = 10, Z_S = 10 + j 200.

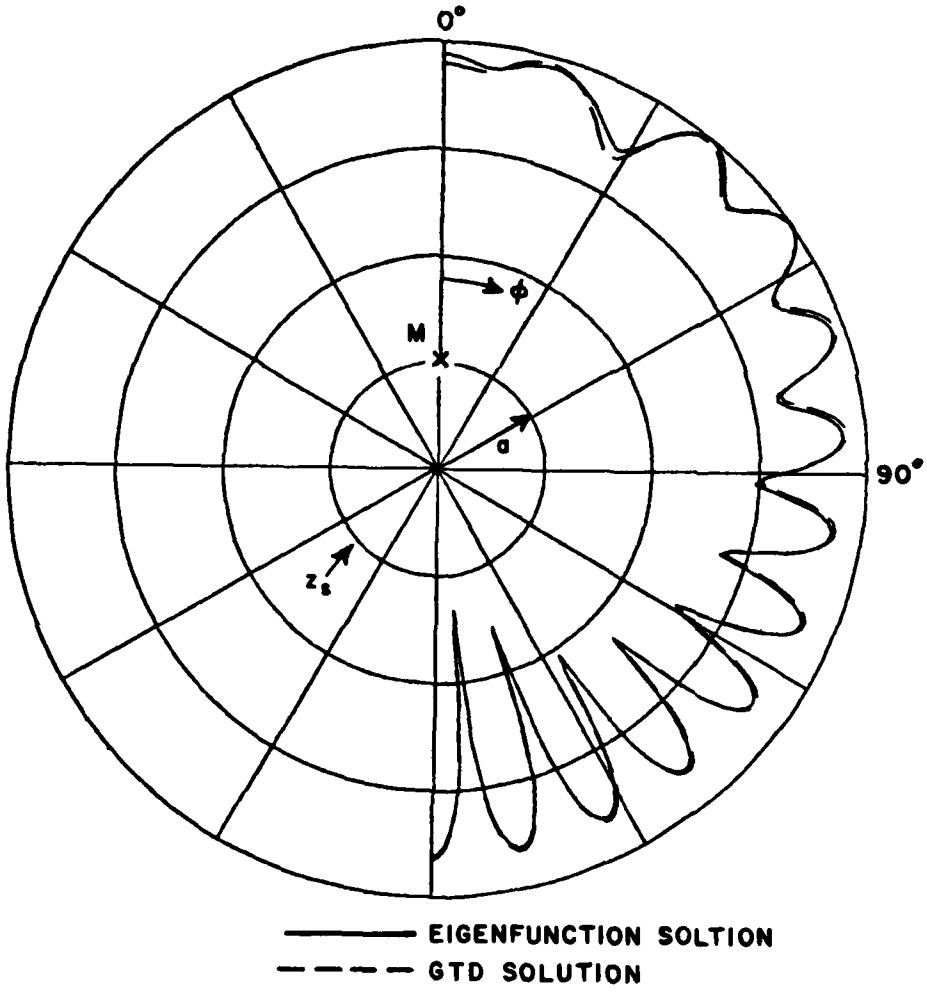

Figure A-9. Pattern due to a magnetic line source radiating from a circular cylinder with surface impedance $Z_S=R_S+jX_S$. ka = 10, Z_S = 10 + j 300.

Another topic of interest is the mutual coupling between antennas mounted on a conducting surface covered with a layer of dielectric material. Work has been in progress to study the surface impedance model of the dielectric-coated surface. It is known that the surface impedance model provides a convenient tool to study the electromagnetic characteristics of the surface waves associated with the dielectric-coated surface. Some preliminary results for the surface fields due to a magnetic line source located on a circular cylinder with reactive surface impedance have been obtained. Figure A-10a presents the surface fields as a function of angular separation from the source, using the normalized surface impedance, $n_s = Z_s/Z_o$, as a parameter. It can be seen from Figure A-10a that an increase in the value of the inductive impedance gives rise to surface waves which are more tightly trapped on the surface. As a consequence, the field intensity increases in the shadow regions with an increase in the inductive reactance of the surface and also the standing-wave feature is more profound. Work also has been carried out to isolate the dominant contribution to the surface field on the cylinder. Figure A-10b shows the "one-ray" solution of the problem given in Figure A-10a. Work is now in progress to study the high frequency characteristics of the one-ray solution. It should be noted that this one-ray solution is related to the universal transition integral

$$\int_t \frac{W_2(t)e^{-jXt}}{W_2'(t)-qW_2(t)}\,dt \quad .$$

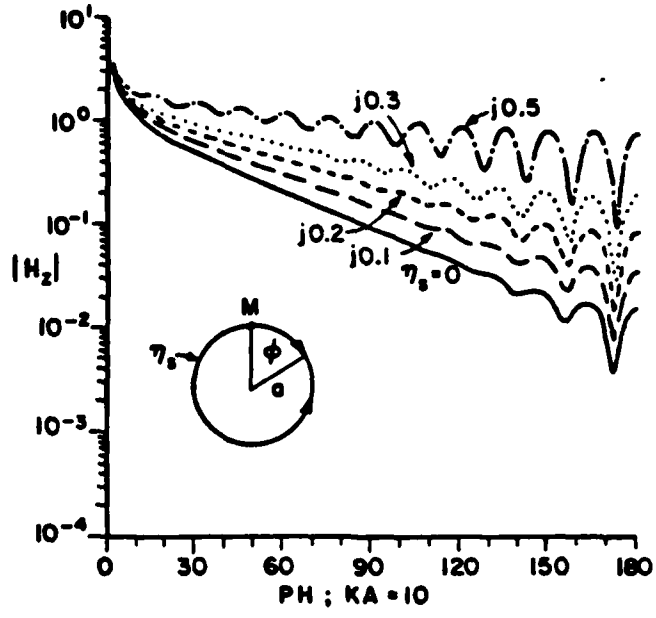

Figure A-10a. Surface field produced by a magnetic line source M on the circular cylinder with a surface impedance η_s (eigenfunction solution).

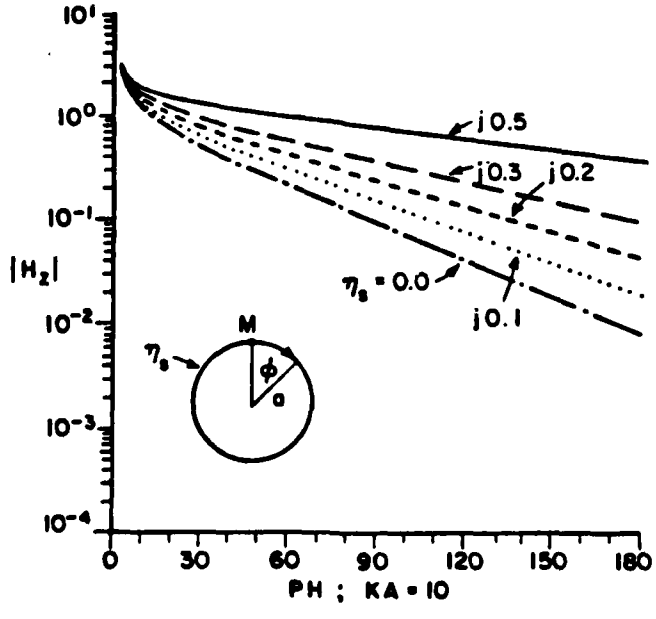

Figure A-10b. Dominant (one-ray) contribution to the surface field produced by a magnetic line source M on a circular cylinder with a surface impedance η_s.

b. Discontinuity of surface immpedance

The problems of EM scattering by discontinuities in surface impedance arise not only in the control of the RCS of perfectly conducting structures by impedance loading, but they also arise, for example, in the design of flush mounted aircraft/missile antennas with a thin coating (or a radome), of finite extent, and in the studies for improving the isolation among a pair of flush mounted antennas by placing an absorber (which can be modeled by a lossy impedance surface) in between those two antennas.

A problem of interest in the area of scattering is that of plane wave diffraction by a strip with two face impedance (i.e., the impedance on the two sides of the strip can, in general, be different). This problem has been analyzed for the special case of grazing incidence; the analysis for illumination at aspects away from grazing on the strip is actually simpler than the case of grazing incidence. It is noted that the analysis in the forward scatter direction for grazing incidence is complicated because the diffraction from the leading edge produces a non-ray optical field at the trailing edge; consequently, the diffraction of this non-ray optical field from the trailing edge which contributes to the field diffracted in the forward direction must be handled carefully. Here, the diffraction of the non-ray optical field is analyzed via a spectral extension of the geometrical theory of diffraction. A paper has been written recently which describes this work; namely:

"Scattering by a Strip with Two Face Impedances at Edge-On Incidence", by R. Tiberio, F. Bessi, G. Manara, and G. Pelosi, accepted for publication in J. Radio Science.

The geometrical theory of diffraction solution employed in the above analysis (which is formulated in the spectral domain) is based on the work of Maliuzhinets [6]. The result for the diffraction coefficient available from Maliuzhinets work, dealing with the problem of the diffraction of a plane wave by a wedge with two face impedances, is non-uniform. Consequently, Maliuzhinets results had to be modified here so that it would remain uniformly valid across the geometrical optics incident and reflection shadow boundaries formed by the edge of the wedge.

A second configuration of interest which has also been investigated recently, and which is somewhat related to the previous one, deals with the problem of diffraction of an electromagnetic plane wave by the edges of an impedance surface patch on a planar perfectly-conducting boundary of infinite extent. In this investigation, an asymptotic high frequency solution for the surface field is obtained again using the spectral theory in conjunction with a uniform version of Maliuzhinets result [6]. Both the TE and TM polarizations are considered in this two-dimensional problem, and the contribution from the bound surface waves (on the impedance surface) is included in the solution. Furthermore, this analysis is further extended to treat the diffraction by a planar

three-part impedance surface in which diffracted rays are produced by the illumination at the edges of the impedance surface patch that lies in the middle of that planar three-part impedance surface. A paper describing this work has been written recently, namely:

"High Frequency Scattering From the Edges of Impedance Discontinuities on a Flat Plane", by R. Tibereo and G. Pelosi, IEEE Transactions on Antennas and Propagation, Vol. AP-31, No. 4, pp. 5910-596, July 1983.

In addition to the above problems, work has been completed on the analysis of the scattering of an EM plane and surface waves by a planar, two part impedance surface in which one part is a perfect electric or magnetic conductor and the other part is characterized by a non-zero surface impedance. This two-dimensional analysis is based on the Wiener-Hopf procedure with Weinstein's method of factorization [7]. These Wiener-Hopf based solutions, which have been obtained for both the TE and TM polarizations, provide uniform (GTD) diffraction coefficients for the discontinuity in surface impedance, and besides being solutions to important canonical problems, they are also crucial to the development of uniform GTD solutions for the important problems of the diffraction by a thin dielectric or ferrite half plane, and by a thin dielectric or ferrite half plane on a perfectly conducting surface. The problem of the diffraction by a thin dielectric or ferrite half plane is discussed later in part c.

An analysis of the high frequency EM radiation by a magnetic line (or line dipole) source on a uniform impedance surface which partially covers a smooth perfectly-conducting convex surface has been performed in the past. A manuscript describing this work,

"An Approximate Asymptotic Analysis of the Radiation from Sources on Perfectly-Conducting Convex Cylinders with an Impedance Surface patch", by L. Ersoy and P.H. Pathak,

has nearly been completed. The preceding work is of interest, for example, in the study of fuselage mounted airborne slot antennas for the purposes of controlling the field radiated near the horizon (or shadow boundary) over that in the absence of the patch.

The work on the diffraction problems described above, dealing with structures possessing a discontinuity in surface impedance, will be continued in the future phases of this study in order to extend these solutions to treat more general situations (e.g., to treat 3-D problems).

c. Diffraction by the edge of a thin dielectric or ferrite half plane

The diffraction by a thin dielectric or ferrite half plane is an important canonical problem in the study of the diffraction of electromagnetic waves by penetrable bodies with edges. The excitation chosen for studying this problem is either an electromagnetic plane wave, or a surface wave incident along the dielectric surface; both types of excitation are considered. For sufficiently thin dielectric or ferrite half planes, solutions based on the Wiener-Hopf technique have been obtained where one initially approximates the effect of the thin dielectric or ferrite slab by an equivalent impedance boundary condition. The Wiener Hopf solutions to the latter canonical problems dealing with the two part impedance surface were briefly mentioned in the previous part (b) dealing with discontinuities in surface impedance. The present analysis begins by bisecting the semi-infinite dielectric or ferrite half plane by an electric wall in the first case, and by a magnetic wall in the second case. The problem of plane (or surface) wave diffraction by the dielectric or ferrite half plane is then constructed by appropriately superimposing the corresponding solutions for the electric and magnetic wall bisections, respectively. This procedure is expected to yield a dielectric half-plane diffraction coefficient which is more accurate than the one obtained by Anderson for the case of an incident electric plane wave field which is parallel

to the edge of the thin dielectric half plane [8], because the latter analysis employs an approximate "equivalent" polarization current sheet model for the thin dielectric half plane. The approximation in [8] contains only a part of the information present in the more general approach being employed in our work; consequently, it is found that the previous analysis in [8] yields a diffraction coefficient which is valid only for an extremely thin dielectric half plane. Furthermore, the equivalent polarization current approximation leads to a rather complicated Wiener-Hopf analysis when the magnetic field is parallel to the edge; the latter case has not been treated by Anderson [8]. It is also noted that the Wiener-Hopf factors for the case treated by Anderson [8] do not appear to be well behaved for near edge-on plane-wave incidence. In contrast, the Wiener-Hopf factors being employed in our work are based on Weinstein's factorization procedure [7] which appears to overcome the difficulties present in [8]. Furthermore, the present work includes both dielectric as well as ferrite half planes.

At the present time, the diffraction coefficients for the two-dimensional case of both TE and TM plane and surface wave excitation of the thin dielectric and ferrite half-planes have been obtained, and they have been tested for accuracy for the dielectric case. Also, these results have been extended to treat a moderately thick dielectric or ferrite half plane which is excited not only by plane and surface wave fields, but also by a cylindrical wave (or line source excited) field. The thickness is allowed to be such that only the first TE and

TM surface wave can exist. The Uniform GTD (UTD) solution obtained for the thin dielectric or ferrite half plane suggests an ansatz upon which the aforementioned extensions to the moderately thick dielectric or ferrite half plane, and also to cylindrical wave illumination are based. In addition to extending the 2-D analysis to treat moderately thick dielectric and ferrite half planes, work has also been completed to include loss in the dielectric and ferrite half planes. The final result for the lossy case is almost as simple to use as the lossless case.

A typical numerical result for the diffraction of a cylindrical wave by a moderately thick dielectric strip that is based on the present UTD solution is shown in Figure A-11. The UTD based result in Figure A-11 is compared with an independent numerical moment-method solution of an integral equation pertaining to this line source excited lossy dielectric strip geometry. Since the line source illuminates the strip at near grazing angles of incidence in Figure A-11, it is especially important in this near grazing incidence case to include surface wave diffraction effects as well. The contribution of all the dominant singly and multiply diffracted rays is included for calculating the pattern in Figure A-11. It is noted from the pattern in Figure A-11 that the total UTD field is continuous at the reflection and transmission shadow boundaries as it should be; furthermore, the very close agreement between the totally independent UTD and moment-method

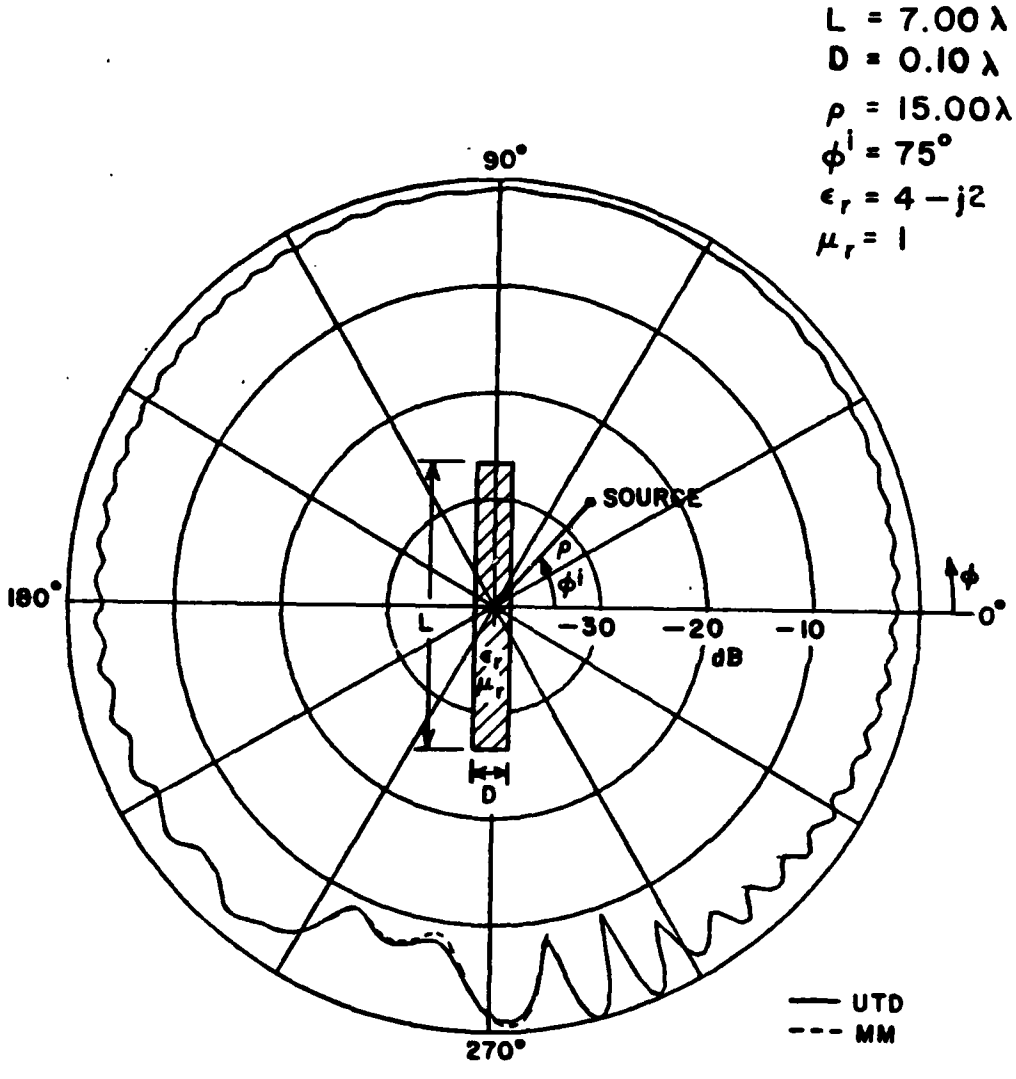

UTD

MM

Figure A-11a. Far zone pattern of an electric line source in the near zone of a lossy dielectric strip.

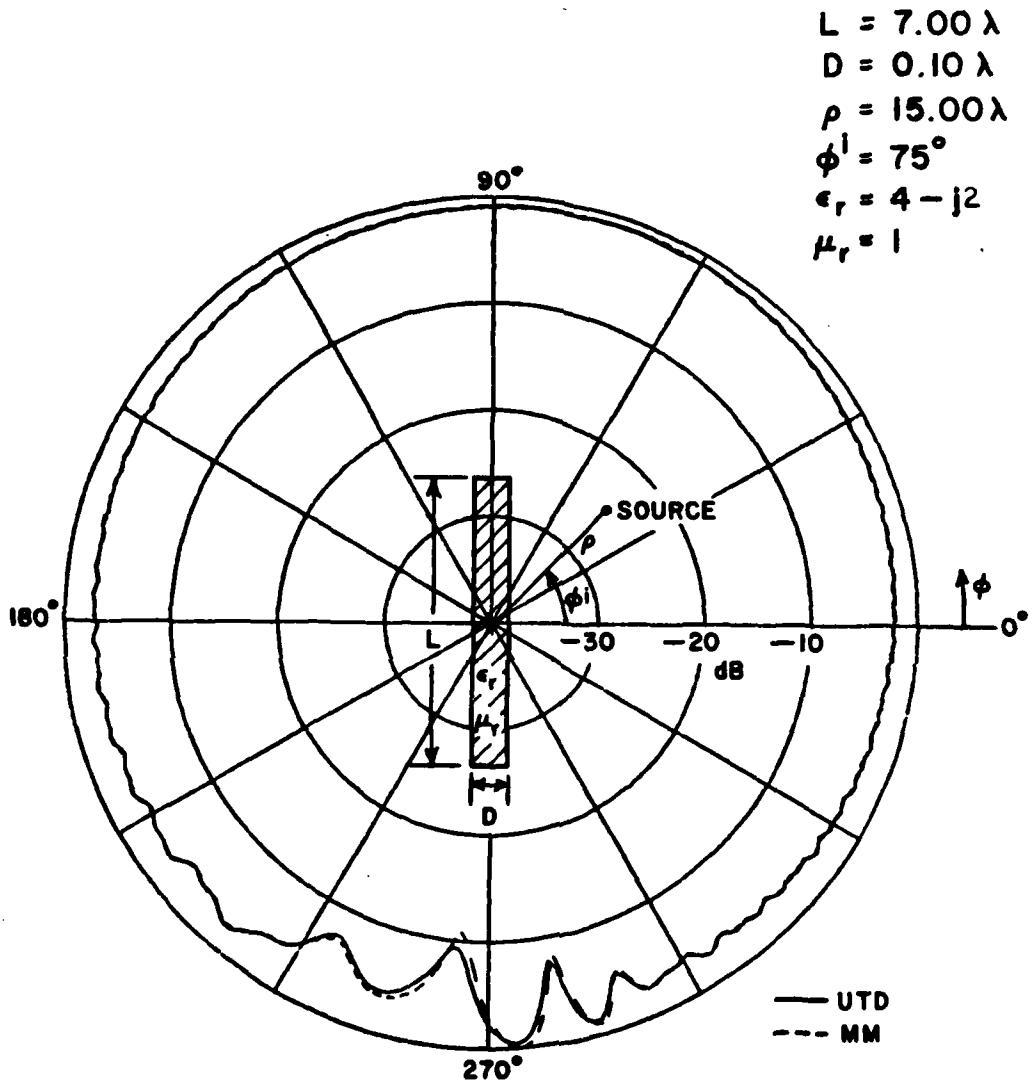

UTD

MM

Figure A-11b. Far zone pattern of a magnetic line source in the near zone of a lossy dielectric strip.

solution in Figure A-11 (and also in other cases which are not shown here) is indeed gratifying. The effects of surface wave diffraction become more pronounced in the lossless case.

Work is currently in progress to treat the three-dimensional (3-D) problems of the diffraction of obliquely incident plane, conical, and spherical waves, and obliquely incident surface waves by a thin (or at most moderately thick) dielectric half-plane. These important generalizations are not trivial because an obliquely incident plane wave is expected to launch both TE and TM type surface waves at the edge of the dielectric half plane. In other words, mode coupling between TE and TM surface waves obliquely incident on the edge of a dielectric half plane is possible. Consequently, the generalization of the two-dimensional (2-D) solutions to treat the corresponding three-dimensional (3-D) problems is not straightforward. It is also noted that even though a relationship exists between the 2-D and 3-D solutions, this is not a direct relationship of the type which would allow the 3-D solutions to be constructed in a simple way from the 2-D solutions as is possible for the case of a perfectly conducting half plane. The 3-D dielectric half plane diffraction solution may also be of interest in the area of integrated optics and millimeter wave integrated circuits where open dielectric guiding structures are employed.

2. Diffraction by Perfectly-Conducting Surfaces

a. Vertex diffraction

The analysis of vertex diffraction is important because one frequently encounters situations where an antenna radiates in the presence of planar structures with edges which terminate in a vertex (or corner). Also, flat plates with edges are used to model aircraft wings and vertical or horizontal stabalizers for calculating the patterns of antennas on aircraft. In these problems, the antenna pattern is affected both by edge diffraction and by the diffraction at the vertices.

A typical vertex in a planar, perfectly-conducting surface is shown in Figure A-12. A more general vertex in a planar surface is formed by the intersection of two otherwise smooth, curved edges. The angle α is the internal angle formed by the tangents to each of the curved edges at the vertex.

The asymptotic high-frequency analysis of electromagnetic vertex diffraction is rather complicated. Vertices not only shadow the incident field, but they also shadow the edge diffracted fields. The shadow boundary of an edge diffracted field is a conical surface whose tip coincides with the vertex and whose axis is an extension of the shadowed edge. The vertex introduces a diffracted ray which penetrates the shadow regions; moreover, the vertex diffracted field must also compensate the discontinuties in the incident and edge diffracted

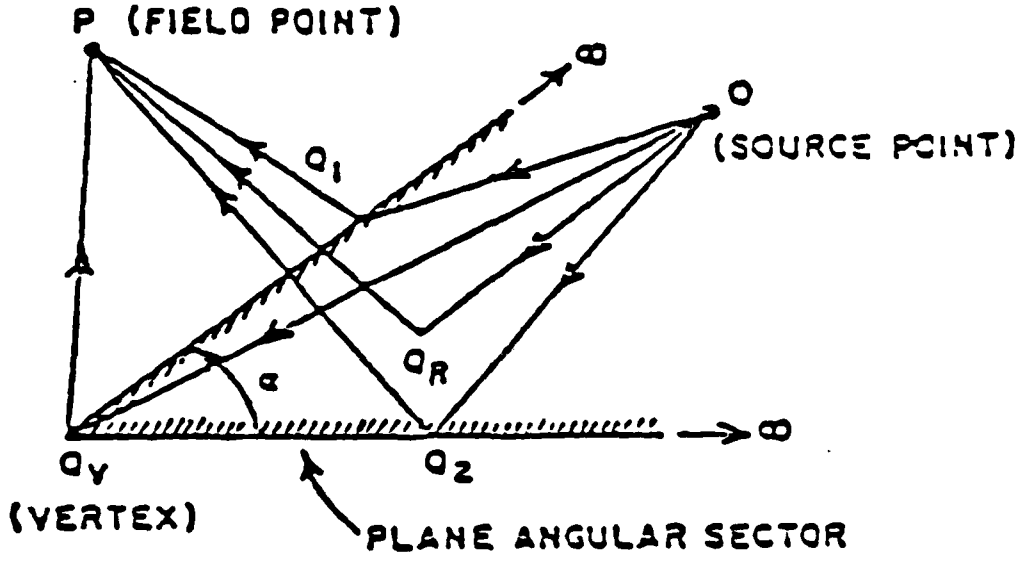

Figure A-12. Various rays associated with the reflection and diffraction by a plane angular sector.

fields at their shadow boundaries. At these boundaries the vertex diffracted field assumes its largest magnitude and, hence, its greatest importance. If the vertex diffracted field is omitted in the GTD solution, then substantial discontinuities connected with the shadowing of the incident and edge diffracted fields may occur in the calculated radiation pattern.

A simple, approximate vertex diffraction coefficient which appears to work reasonably well in certain cases has been obtained at the ElectroScience Laboratory [9,10]. However, this result has been found heuristically using a combination of theory and experiment; it therefore needs to be improved in order to be useful in the general situations

encountered in practice. Nevertheless, this diffraction coefficient offers some clues for constructing the more refined and useful vertex diffraction coefficient, which we expect to obtain from asymptotic analysis.

The objective of this research is a uniform asymptotic solution for the electromagnetic field scattered by the vertex, which can be interpreted ray optically in terms of contributions from the critical points Q_R, Q_1, Q_2 and Q_V. The approach is to approximate the current away from the edges by the geometrical optics current. Near the edges, but away from the vertex, the local half-plane current is used and near the vertex the first few terms of the eigenfunction solution [11] are employed. The integral representation of the field radiated by these currents is then approximated by the stationary phase method to obtain the fields diffracted and reflected from the critical points.

Recently a method for asymptotically evaluating the field of the current near an edge was investigated; an eigenfunction representation of the edge current was used. The preliminary results are encouraging and if the method is successful, it will be applied to the eigenfunction representation of the current near the vertex to obtain the vertex diffraction coefficient.

During the past year, the confluence of the critical points was examined using the geometrical optics current everywhere on the vertex.

When all the critical points are close to each other, then the expression obtained for the transition function is so complicated it does not appear to be useful. An effort is being made to simplify this expression.

As was mentioned earlier, a convergent (eigenfunction) solution is needed to represent the current near the vertex. Also, a convergent solution is of great value in numerically checking the approximate high-frequency solutions obtained by asymptotic methods. Therefore, an effort has been made to accurately determine the dyadic Green's function for the plane angular sector.

To find the dyadic Green's function we begin by expanding it in terms of a complete set of vector wave functions which are solutions of the vector wave equation along with the radiation condition and the boundary conditions on the surface containing the vertex. The vector wave functions, in turn, are expressed in terms of scalar wave functions which are solutions to the scalar wave equation with the appropriate boundary conditions. Both Neumann and Dirichlet type boundary conditions must be satisfied to yield a complete set of vector wave functions. The final step of the solution involves separating the scalar wave equation in the sphero-conal coordinate system. The resulting separated equations include the spherical Bessel equation and two Lame' equations (one with periodic boundary conditions and the other with nonperiodic ones) which are coupled through the two eigenvalues

which are actually the separation constants. It is precisely these eigenvalue pairs which serve as the summation index of the dyadic Green's function.

The solution is thus ultimately reduced to solving for the eigen-values and eigenfunctions of the separated Lame' equations. It is then a straightforward procedure to construct the vector wave functions and hence the dyadic Green's function. Once this is found one can proceed to investigate a wide variety of problems because of the versatility and general nature of the Green's function solutions.

There is no known closed form solution to the Lame' equations and one is therefore attracted to an infinite series solution. Earlier work [11] used Fourier sine and cosine series representations, but these resulted in the need to solve two simultaneous, infinite continued-fraction equations for the eigenvalues and eigenvectors. This solution proves to be numerically formidable, and indeed, almost impossible for higher order eigenvalues because of the rapidly varying nature of the continued fractions. However, Sahalos has used these representations [12] and reports that he has developed methods of calculation which are more efficient and accurate. We plan to study his methods before doing further work on this problem; it may be adequate for purpose of calculating the dyadic Green's function for the plane angular sector.

During the past two years we have worked on the special case of the dyadic Green's function where $\alpha = \pi$ and the plane angular sector reduces to a half plane. This is discussed in the following section.

b. Paraxial diffraction

i) At edges

As was mentioned in the last section, the dyadic Green's function for the plane angular sector can be applied to the half-plane by letting the sector angle go to 180°. The Lame' differential equations decouple and the eigenvalues and eigenfunctions are easily found; furthermore, this solution can be extended to the wedge without difficulty. The advantage of this spherical wave solution for the dyadic Green's function of the wedge over that given in [13] is that it can be used when the field and the source point are close to the edge. This should make it possible to extend the UTD solution to the paraxial region, i.e., to grazing incidence on the edge, and to study the propagation of edge waves. These waves are important in analyzing the scattering from plates illuminated at or near grazing incidence or in treating the coupling between monopoles or slots near the edge of a wedge.

During the past year, a paper was written on the spherical wave representation of the dyadic Green's function for the perfectly-conducting wedge [14]; its use to determine the fields in the paraxial region was also described. A summary of this paper was presented at the 1983 International URSI Symposium [15].

The use of this dyadic Green's function to treat the scattering from an object at the edge of the wedge was described in the preceding annual report; again the paraxial region was of special interest. A

T-Matrix method was proposed for non-spherical objects. In the period covered by this report, the method was tested by choosing a sphere whose center is displaced along the edge from the origin of the coordinate system. This simulates the difficulties encountered in treating a non-spherical scatterer by this method.

Calculations of the echo area σ (normalized with respect to wavelength λ) are shown in Figures A-13a,b. The direction of incidence makes an angle of 30° with respect to the edge of the wedge (half-plane case), the radius of the sphere is 0.25λ, and its center is displaced 0.125λ from the origin of the coordinate system. The incident and scattered electric fields are polarized in the θ-direction in Figure A-13a and in the ϕ-direction in Figure A-13b. The echo area curves are seen to be in excellent agreement with those calculated from an (exact) eigenfunction solution. This establishes confidence in our T-Matrix solution.

Recently some work has been done on the problem of multiple scattering where there are two or more objects arrayed along the edge of the wedge.

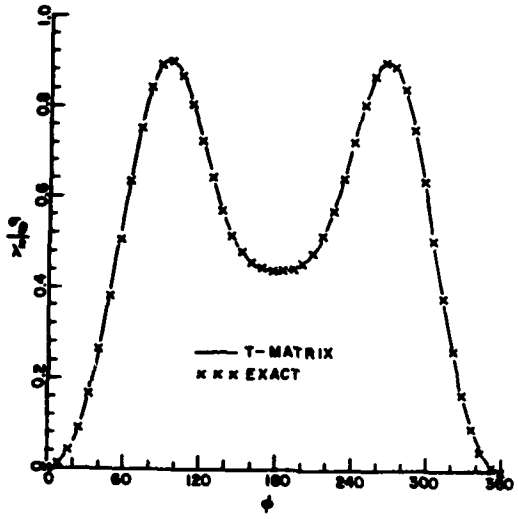

Figure A-13a. Backscatter from a spherical boss at the edge of a half plane. Incident field polarized in the θ-direction.

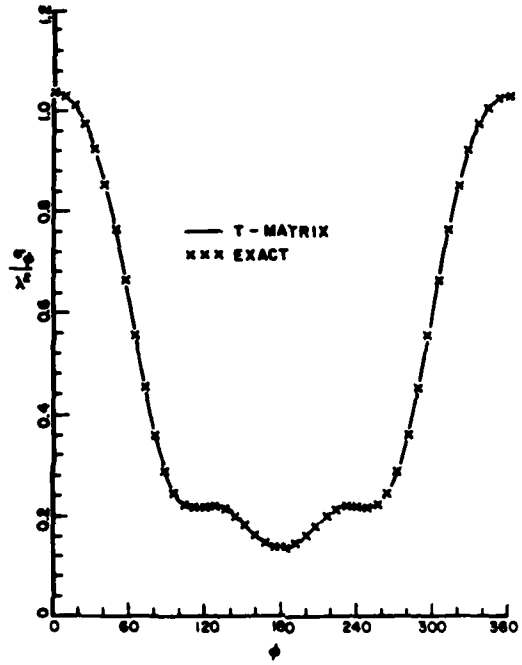

Figure A-13b. Backscatter from a spherical boss at the edge of a half plane. Incident field polarized in the φ-direction.

ii) At smooth, quasi-cylindrical surfaces

Several papers were written (under the JSEP program) and published [1,2,3] which describe Uniform GTD (UTD) solutions for the diffraction by perfectly-conducting convex surfaces. In particular, efficient UTD solutions for the problems of the radiation from sources both off and on a convex surface and the mutual coupling between sources on a convex surface were presented in [1,2,3]. These UTD solutions, for the problems of scattering, radiation, and mutual coupling, which are associated with the radiation by antennas in the presence of an arbitrary, smooth perfectly-conducting convex surface that is electrically large represent an important and useful contribution to the area of ray methods for analyzing the EM radiation and scattering from complex structures. It is noted that the effects of surface ray torsion on the diffracted fields are explicitly identified in these solutions. Here, the diffracted fields are associated with surface rays as well as with rays shed from the surface rays. It is noted that these surface rays on a convex surface traverse geodesic paths which in general are torsional; i.e., the surface ray paths are twisted (or they do not lie in a plane).

While the above mentioned UTD solutions for sources on or off a smooth perfectly-conducting convex surface are valid under very general conditions, they must be modified within the paraxial regions. For example, these solutions must be modified for an observation point

(either on or off the surface) which lies in the paraxial region of an elongated or cigar shaped (quasi-cylindrical) convex surface whenever the rays from the source to that observation point traverse paths which lie within the paraxial zone. At the present time, the solution for the surface fields of a source on the convex surface has been extended so as to be valid within the paraxial region of quasi-cylindrical, or elongated convex surfaces. The surface field (or mutual coupling related) solution provides the electric current density which is induced by a source on the same surface. Such a surface current density can be incorporated into the usual radiation integral to find the field radiated by this current; that step has also been performed presently. Thus, the field radiated by the source on the surface has been obtained via an asymptotic high frequency evaluation of the radiation integral containing this surface current density which remains valid in the paraxial zone. The asymptotic evaluation of this radiation integral associated with a general convex surface has been done carefully in order to obtain a simple and useful uniform solution for the radiated field. It may be remarked that previous attempts by others, which have been reported earlier, were not very successful in asymptotically evaluating such radiation integrals associated with a general convex surface. We have found that such previous attempts did not lead to very useful results because of a simplifying assumption which is inherent in their work. Our present analysis reveals that such an asymptotic analysis must be done by a different approach which circumvents the

inherent approximation present in the previously reported approaches to obtain meaningful results. The solution to the problem of EM radiation in the paraxial zone by sources on a convex surface is therefore currently nearing completion. When the work on the radiation problem is completed, it will be extended subsequently to deal with the problem of EM scattering within the paraxial regions in almost the same manner as the radiation solution was obtained via an extension of the surface field (mutual coupling related) solution through the use of the radiation integral.

c. Slope diffraction

If the field incident at the edge of a wedge or the shadow boundary of a convex surface has a rapid spatial variation, a slope diffraction term must be added to the ordinary UTD. The slope diffraction term is proportional to the spatial derivatives of the incident field. It ensures that the spatial derivatives of the resulting radiation pattern are continuous at the shadow and reflection boundaries so that there are no "kinks" in the calculated pattern.

The derivation of slope diffraction terms for ordinary wedges formed by plane surfaces and for convex cylinders has been described in the two preceding annual reports, and a dissertation based on this work has been written [16]. During the present period, the rough draft of a paper on this subject has been written and there has been an effort to extend the solution to a curved wedge formed by curved surfaces.

d. Diffraction by a discontinuity in surface curvature

The diffraction by an edge in a perfectly conducting surface formed by a discontinuity in surface, such as occurs in the cone sphere and the hemispherically capped cylinder, contributes strongly to the radiation in the vicinity of the reflection boundary where it compensates for the discontinuity in the reflected field. It may also contribute strongly to the axial backscatter from a body of revolution with a discontinuity in surface curvature. The geometry of the problem is depicted in Figure A-14.

A diffraction coefficient for the discontinuity in surface curvature has been described in the two preceding annual reports. The solution is restricted to the case where the direction of incidence is normal to the edge. The purpose of the present work to obtain a simpler expression for this diffraction coefficient and to generalize it to the oblique incidence case.

It has been noted by Chu [17] that the curved wedge diffraction coefficient obtained by Kouyoumjian and Pathak [18] can be used to calculate the diffraction by a discontinuity in surface curvature in the vicinity of the reflection boundary. Although the first two terms in the curved wedge diffraction coefficient vanish in this case, the second pair of terms associated with the reflected field do not. They correctly compensate the discontinuity in the reflected field at the reflection boundary. However, outside the transition region of the

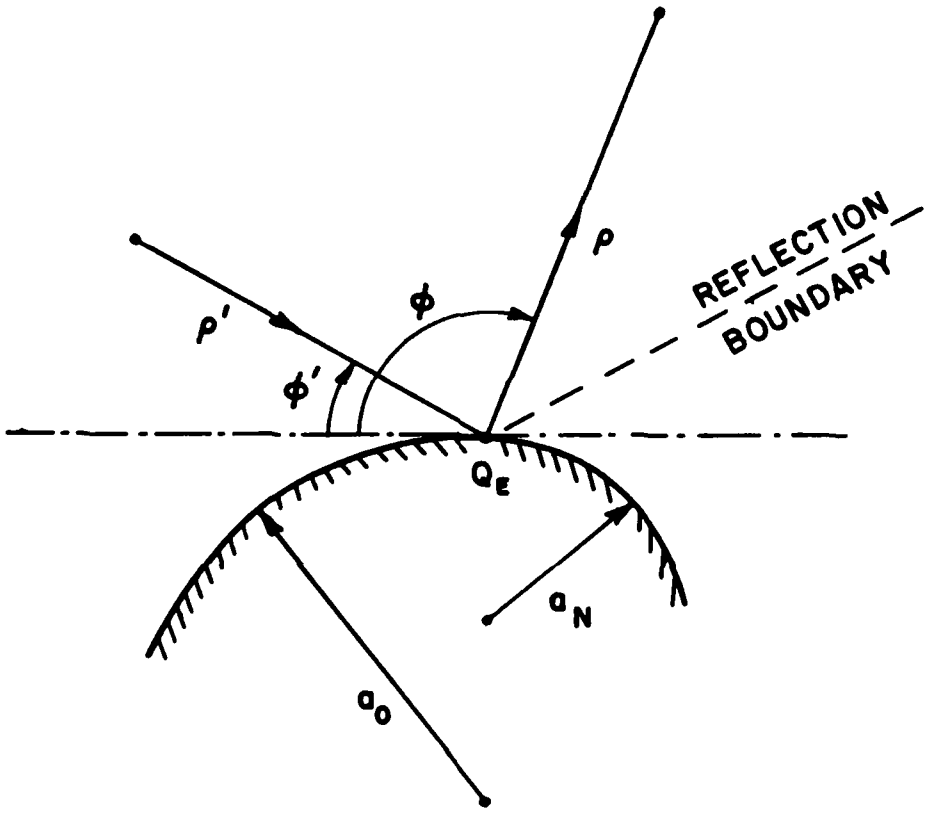

Figure A-14. Diffraction by a discontinuity in surface curvature.

reflection boundary, the diffracted field obtained by this method does not reduce to the correct, non-uniform asymptotic form given by Senior [19]. Starting with the expression for the curved wedge diffraction coefficient, a diffraction coefficient for the discontinuity in curvature was derived, which reduces to the solution given by Senior away from the reflection boundary and exactly compensates the discontinuity in the reflected field at the reflection boundary. It can be used at oblique incidence and is computationally simpler than the diffraction coefficient described in the 1982 annual report. Away from grazing incidence and diffraction, the two diffraction coefficients give virtually the same numerical results. This is demonstrated in Figures A-15a and A-15b where the soft and hard diffraction coefficients, respectively, are plotted as a function of ϕ. In these figures, the direction of incidence is normal to the edge, $\phi'=60°$, $\alpha_0=10\lambda$, $\alpha_N=5\lambda$, and the field point is in the far zone.

Since the new diffraction coefficient is based on the curved edge diffraction coefficient, it can not be used when the direction of incidence or diffraction grazes the surface unless the surface in question is planar. It is expected that this restriction can be removed by incorporating the generalized reflection coefficient given by Pathak [20] into the solution.

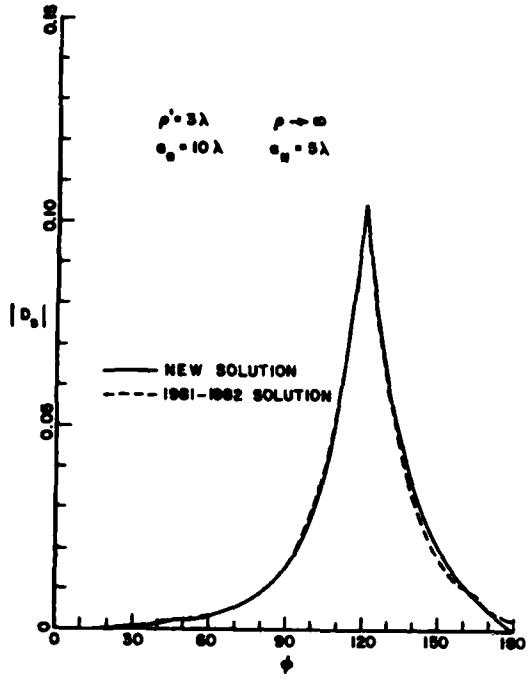

Figure A-15a. The field diffracted by a discontinuity in surface curvature. E field parallel to the edge.

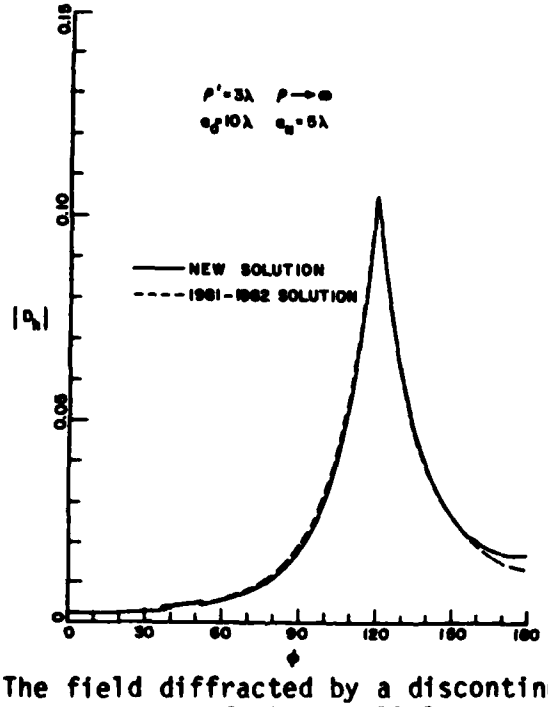

Figure A-15b. The field diffracted by a discontinuity in surface curvature. H field parallel to the edge.

3. Diffraction of Non-Ray Optical Fields (Source Close to An Edge)

In the conventional form of the Uniform GTD, it is assumed that the incident field is a ray-optical field, which implies that it is polarized in a direction perpendicular to the incident ray. In general, this requires that the source of the incident field be sufficiently far from the point of diffraction so that the component of the incident field parallel to its ray path (the component in the radial direction from the source) is negligible at the diffraction point. However, in some applications this is not the case, e.g., a monopole antenna may be mounted at or very close to the edge of a ship or the edges of wings and stabilizers. This case is also of interest in the development of the Hybrid GTD/Moment Method solution, where it is desired to calculate the input impedance of a wire antenna close to an edge.

An asymptotic solution for the diffraction of the fields of electric and magnetic dipoles close to the edge of a wedge has been obtained. The basic approach is to determine the field close to the edge of the wedge; the far field of the dipole is then found using reciprocity. The asymptotic analysis of the diffracted field proceeds as done earlier [18] except that higher order terms are retained. The diffraction coefficient has the form of a 3x2 matrix which contains radial and cross-polarized components. This solution has been used to accurately calculate the fields of dipoles which are only a few tenths of a wavelength from the edge [21]. In the present period, this result

has been improved further and the components of the diffraction coefficient have been expressed more compactly. This work has just recently been extended to the case of spherical wave illumination of the wedge.

The dyadic Green's function described in section 2.b converges rapidly when the source point is close to the edge and so it is convenient to employ it to numerically check the solutions described in the preceding paragraph; extensive comparisons of this type have been carried out. It is hoped that the two types of solutions for edge diffraction can be combined so that we will have a more useful computational algorithm for edge diffraction. This is particularly important in the paraxial region where the high frequency solutions described in the last paragraph lose accuracy.

4. Caustic Field Analysis

The GTD is a very convenient and accurate procedure for analyzing high frequency radiation, scattering, and diffraction problems. However, the GTD suffe·s from a limitation inherent in ray methods; namely, it cannot be employed directly to evaluate fields at and near focal points or caustics of ray systems. The fields at caustics must, therefore, be found from separate considerations [22,23].

In certain problems such as in the diffraction by smooth, closed convex surfaces or by surfaces with a ring-type edge discontinuity, it is possible to employ the GTD indirectly to evaluate the fields in the caustic regions via the equivalent ring current method [24,25]. However, even the equivalent ring current method fails if the incident or reflection shadow boundaries are near or on a caustic.

The recently developed uniform GTD (or UTD) solution for the scattering and diffraction of waves by a convex surface [1,2,3] offers clues as to how it may be employed indirectly to obtain the far zone fields in caustic regions where the surface is illuminated by a distant source. In the latter case, the shadow boundary and caustic transition regions tend to overlap. The far zone fields in the near axial direction of a closed surface of revolution illuminated by an axially directed plane wave can be expressed in terms of an equivalent ring current contribution plus a dominant term which may be interpreted as an "effective aperture integral". The latter integral can be evaluated in

closed form. In the near zone, where the shadow boundary and caustic directions are sufficiently far apart, only the equivalent ring current contribution must remain significant. Presently, such a solution has been developed for the special case of axial incidence on a rotationally symmetric convex surface (or revolution). The generalization of that solution to treat non-axial incidence and also closed convex surfaces which are not necessarily surfaces of revolution forms the subject of future investigation.

Another related and interesting problem which is presently under study involves the analysis of high frequency electromagnetic diffraction by perfectly conducting planar surfaces (or plates) with a smooth convex boundary. In this problem, the planar face of the plate gives rise to caustic effects. For certain aspects, the caustic and specular reflection directions can coincide so that a direct use of UTD becomes invalid. The present study is aimed at determining a proper modification of the UTD so that a new and efficient equivalent current method can be used in these situations. Away from the caustic and confluence of caustic and specular directions, the modified UTD solution must reduce to the conventional GTD solution. More related problems involving a confluence of diffracted ray caustic and geometrical optical shadow boundary transition regions will be investigated in the future phases of this work.

5. Electromagnetic Dyadic Green's Function

Electromagnetic dyadic Green's functions are useful in that they allow one to calculate the fields of an arbitrary source distribution in a systematic fashion. In the case of special Green's dyadics which account for the source radiation in the presence of any boundaries, i.e., structures, they form the starting point for the asymptotic high frequency analysis of canonical problems in the uniform geometrical theory of diffraction (or UTD). In the latter application, it is implied that a Green's dyadic for the canonical geometry is known in the first step; this Greens' dyadic is then generally transformed into a useful form in terms of appropriate integrals if it is not originally available in that form (since it could originally be given as a series expansion), and finally, the intgrals are evaluated asymptotically to extract the high frequency UTD solution of interest.

A relatively simple method has been developed recently for constructing the complete eigenfunction expansion of time-harmonic electric ($\bar{E}$) and magnetic ($\bar{H}$) fields within exterior or interior regions containing an arbitrarily oriented electric current point source. In particular, since these fields $\bar{E}$ and $\bar{H}$ pertain to the case of point source excitation, they yield directly the complete eigenfunction expansion of the corresponding electric and magnetic dyadic Green's functions $\bar{\bar{G}}_e$ and $\bar{\bar{G}}_m$ that are associated with $\bar{E}$ and $\bar{H}$, respectively.

The expansion of $\bar{\bar{G}}_e$ and $\bar{\bar{G}}_m$ obtained here is expressed in terms of only the solenoidal type eigenfunctions which satisfy the required boundary and radiation conditions. In addition, the expansion of $\bar{\bar{G}}_e$ also contains an explicit dyadic delta function term which is required for making that expansion complete at the source point. This explicit dyadic delta function term in $\bar{\bar{G}}_e$ is obtained readily in the present approach from a simple condition that the eigenfunction expansion must satisfy at the source point, provided one interprets that condition in the sense of distribution theory.

A paper has been wtitten on the above topic, namely

"On the Eigenfunction Expansion of Electromagnetic Dyadic Green's Functions", by P.H. Pathak, IEEE Transactions on Antennas and Propagation, AfP-31, No. 6, pp. 837-846, November 1983.

REFERENCES

[1] Pathak, P.H., W.D. Burnside and R.J. Marhefka, "A Uniform GTD Analysis of the Scattering of Electromagnetic Waves by a Smooth Convex Surface", IEEE Transactions on Antennas and Propagation, Vol. AP-28, No. 5, September 1980, pp. 631-642.

[2] Pathak, P.H., N.N. Wang, W.D. Burnside and R.G. Kouyoumjian, "A Uniform GTD Solution for the Radiation from Sources on a Perfectly-Conducting Convex Surface", IEEE Transactions on Antennas and Propagation, Vol. AP-29, No.4, July 1982, pp. 609-621.

[3] Pathak, P.H. and N.N. Wang, "Ray Analysis of Mutual Coupling Between Antennas on a Convex Surface", IEEE Transactions on Antennas and Propagation, Vol. AP-29, No. 6, November 1981, pp. 911-922.

[4] Wait, J.R. and A. M. Conda, "Pattern of an Antenna on a Curved Lossy Surface", IEEE Transactions on Antennas and Propagation, Vol. AP-6, No. 4, October 1958, pp. 348-359.

[5] "Joint Services Electronics Program", Fifth Annual Report 710816-12, December 1982, The Ohio State University ElectroScience Laboratory, Department of Electrical Engineering; prepared under Contract N00014-78-C-0049 for the Department of the Navy, Office of Naval Research, 800 Quincy Street, Arlington, Virginia 22217.

[6] Maliuzhinets, G.D., "Excitation, Reflection and Emission of Surface Waves from a Wedge with Given Face Impedances", Sov. Phys. Dokl., 3(4), pp. 752-755, 1959.

[7] Weinstein, L.A., The Theory of Diffraction and the Factorization Method, The Golem Press, Boulder, Colorado, 1969.

[8] Anderson, I., "Plane Wave Diffraction by a Thin Dielectric Half Plane", IEEE Trans. Antennas and Propagation, Vol. AP-27, p. 584-589, September 1979.

[9] Kouyoumjian, R.G., P.H. Pathak and W.D. Burnside (1981), "A Uniform GTD for the Diffraction by Edges, Vertices and Convex Surfaces", Theoretical Methods for Determining the Interaction of Electromagnetic Waves with Structures, ed. J.K. Skwirzynski, Sijthoff and Noordhoff, Alphen aan den Rijn, The Netherlands.

[10] Burnside, W.D. and P.H. Pathak, "A Corner Diffraction Coefficient", to be published.

[11] Satterwhite, R. and R.G. Kouyoumjian, "Electromagnetic Diffraction by a Perfectly-Conducting Plane Angular Sector", Report 2183-2, 1970, The Ohio State University ElectroScience Laboratory, Department of Electrical Engineering; prepared under Contract AF 19(628)-5929 for Air Force Cambridge Research Laboratories.

[12] Sahalos, J., Private Communication.

[13] Tai, C.T., Dyadic Green's Functions in Electromagnetic Theory, Intext Educational Publishers, 1971.

[14] Kouyoumjian, R.G. and O.M. Buyukdura, "A Spherical Wave Representation for the Dyadic Green's Function of a Perfectly-Conducting Wedge", to be published.

[15] Kouyoumjian, R.G. and O.M. Buyukdura, "Paraxial Edge Diffraction", 1983 International URSI Symposium held 23-26 August at Santiago de Compostela, Spain.

[16] Veruttipong, Thavath, "Diffraction at Edges and Convex Surfaces Illuminated by Fields with a Rapid Spatial Variation", Ph.D. Dissertation, The Ohio State University, 1982.

[17] Chu, T.T., "First Order Geometrical Theory of diffraction Analysis of the Scattering by Smooth Structures", Ph.D. Dissertation, The Ohio State University, 1983.

[18] Kouyoumjian, R.G. and P.H. Pathak, "A Uniform Geometrical Theory of Diffraction for an Edge in a Pefectly-Conducting Surface", Proc. IEEE, Vol. 62, pp. 1448-1461, 1974.

[19] Senior, T.B.A., "The Diffraction Matrix for a Discontinuity in Curvature", IEEE Trans. Antennas and Propagation, Vol. 20, p. 326, May 1972.

[20] Pathak, P.H., "An Asymptotic Analysis of the Scattering of Plane Waves by a Smooth Convex Cylinder", Radio Science, Vol. 14, p. 419, May 1979.

[21] Kouyoumjian, R.G., G. Pelosi and R. Tibereo, "An Extension of the Uniform GTD for the Diffraction by a Wedge Illuminated by a Dipole Close to Its Edge", Alta Frequenza, Vol. II, January-February, 1983, pp. 24-33.

[22] Kay, I. and J.D. Keller, "Asymptotic Evaluation of the Field at a Caustic", J. Appl. Physics, Vol. 25, No. 7, pp. 876-886, July 1954.

[23] Ludwig, D., "Uniform Asymptotic Expansions at a Caustic", Commun. Pure Appl. Math, 19, pp. 215-25, 1966.

[24] Burnside, W.D. and L. Peters, Jr., "Radar Cross Section of Finite Cones by the Equivalent Current Concept with Higher Order Diffraction", J. Radio Science, Vol. 7, No. 10, pp. 943-948, October 1972.

[25] Knott, E.F. and T.B.A. Senior, "A Comparison of Three High-Frequency Diffraction Techniques", Proc. IEEE, Vol. 62, No. 11, pp. 1468-1474, November 1974.

B. Hybrid Techniques

Researchers: P.H. Pathak, Assistant Professor
(Phone: (614) 422-6097)
C.D. Chuang, Senior Research Associate
S. Shrikanth, Graduate Research Associate

A General Description of Hybrid Techniques

The method of moments (MM) provides a means of solving electromagnetic boundary value problems in terms of a set of simultaneous linear equations. In general, the electromagnetic boundary value problem is formulated as an integral equation for the unknown surface fields on the antenna or scatterer and the integral equation is then reduced to a system of equations by expanding the unknown in terms of a basis set and by enforcing this expansion to satisfy the boundary conditions in some average sense through the use of testing functions. However, the MM procedure can become inefficient and cumbersome if the number of unknowns (coefficients of the expansion or basis functions) becomes large as is the case for antennas or scatterers which are not small in terms of wavelength. On the other hand, the geometrical theory of diffraction (GTD) exploits the local nature of high frequency wave propagation, diffraction and radiation, thereby reducing the antenna radiation or scattering problem to calculating the fields associated with just a few rays emanating from edges, tips, and shadow boundaries (of smooth convex surfaces), and also from other discontinuities in the

geometrical and electrical properties of the antenna or scatterer. Although the GTD is a high frequency technique, it works rather well, even for structures which are only moderately large in terms of the wavelength. However, the use of the GTD is limited by the number of available diffraction coefficients for characterizing a particular type of electrical and/or geometrical discontinuity. It is obvious that a procedure is desirable which would overcome the limitations of the individual MM and GTD approaches. Such a procedure, referred to as the "hybrid" GTD-MM procedure, can indeed overcome the limitations of the individual MM and GTD approaches by actually combining the best features of both methods. In particular, GTD provides the form of the local field over any part of the antenna or scattering structure, which is at least moderately large in terms of the wavelength; hence, the form of the GTD field could be viewed as a set of basis functions for the expansion of the unknowns in the MM formulation. The unknown coefficient associated with this type of GTD basis or expansion functions is then the diffraction coefficient for the surface field calculations if the unknown in the integral equation happens to be the surface field. Thus, by using the local GTD field form outside the region where the structure is small in terms of the wavelength, the number of unknowns is thereby vastly reduced in the MM procedure. The expansion for the unknown within regions (of the structure) which are small in terms of wavelength, is of course, done according to the conventional MM approach (perhaps using a subsectional basis set such as rectangular pulses, etc). Clearly, the hybrid GTD-MM procedure can

solve problems far more efficiently than the MM procedure as the frequency increases. Also, it can provide a useful check on future diffraction coefficients as and when they become available.

While the hybrid GTD-MM procedure will in general be employed to obtain diffraction coefficients, other hybrid techniques which combine ray methods and numerical methods different from the MM procedure will also be studied. Thus, in a broader sense, the area of hybrid techniques will emphasize useful combinations of high frequency or ray techniques with numerical methods for solving a variety of interesting and useful electromagnetic radiation and scattering problems.

Presently, two classes of diffraction problems are being investigated; namely, the diffraction by perfectly-conducting structures involving special edge or tip type discontinuities, and the diffraction by discontinuities associated with the junction of dielectric and perfectly-conducting structures which are connected in special ways. In particular, the problems in the first catagory are the problems of diffraction by a discontinuity in surface curvature (e.g., the smooth join of a half plane and a cylinder); by an edge-type discontinuity in an otherwise smooth convex surface; by the tip of a cone-type structure; by the tip of a semi-infinite wire; and by an aperture in a thick screen (and related configurations). The problems in the second catagory are the problems of diffraction by a truncated dielectric slab recessed in a perfectly-conducting structure as in Figure B-1(a), by the junction of a dielectric half plane which is joined to a thick perfectly-conducting half plane as in Figure B-1(b); and the problem

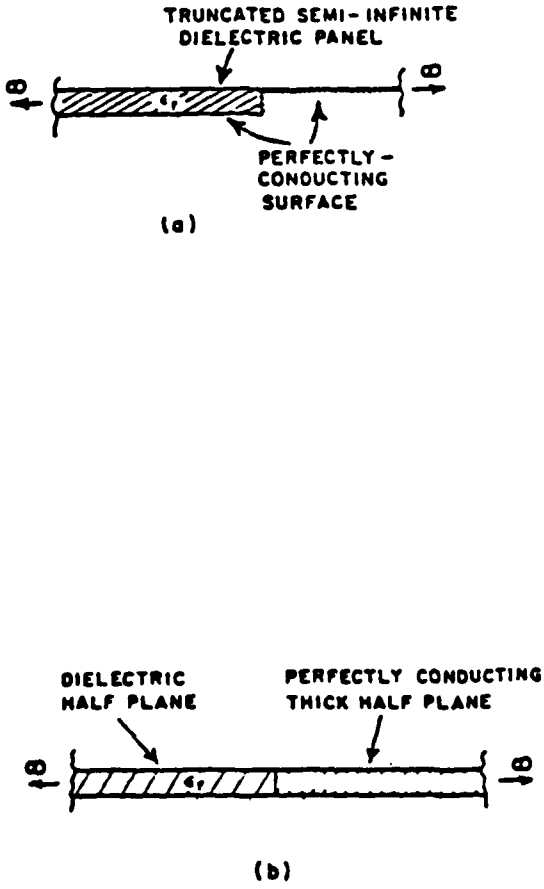

Figure B-1. Discontinuity formed by the junction of a dielectric and perfectly-conducting structure.

of the radiation of a single element or an array of electrically small microstrip patch antennas which are placed conformally on an electrically large perfectly-conducting smooth convex surface (such as the fuselage of an aircraft or a missile). The latter problem, as depicted in Figure B-2, requires a combination of low frequency techniques (for handling the electrically small microstrip patches) with the high frequency ray technique (for handling the electrically large convex surface).

Currently, work is in progress to obtain an efficient, hybrid GTD-MM solution to the problem of the diffraction by the structure shown in Figure B-1(a). The dielectric is made inhomogeneous near the junction of the dielectric conducting body in order to reduce the surface wave reflection from that junction. A computer program searches for the selection of dielectric material to accomplish this purpose. Some results of the surface wave reflection coefficient and the radiation pattern for the case where the dielectric is homogeneous are shown in Figures B-3 and B-4. Also shown in these figures are solutions of the same problem obtained by Pathak [1] using a Wiener-Hopf type technique. The agreement between the two methods is generally very good. One should note that the technique employed by Pathak in [1] is not feasible in dealing with the problem where the dielectric is inhomogeneous. The inhomogeneous dielectric problem is now being investigated using the hybrid GTD-MM technique. Both surface wave and plane wave incidences, TE and TM polarizations, when the boundary

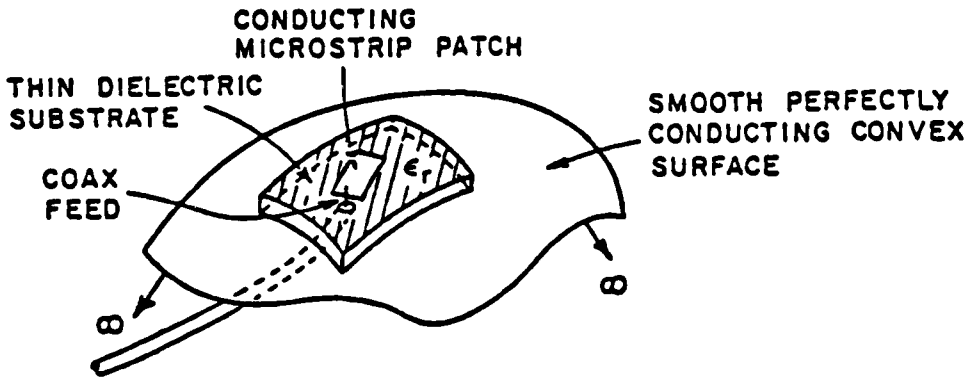

Figure B-2. Microstrip antenna element on a convex surface.

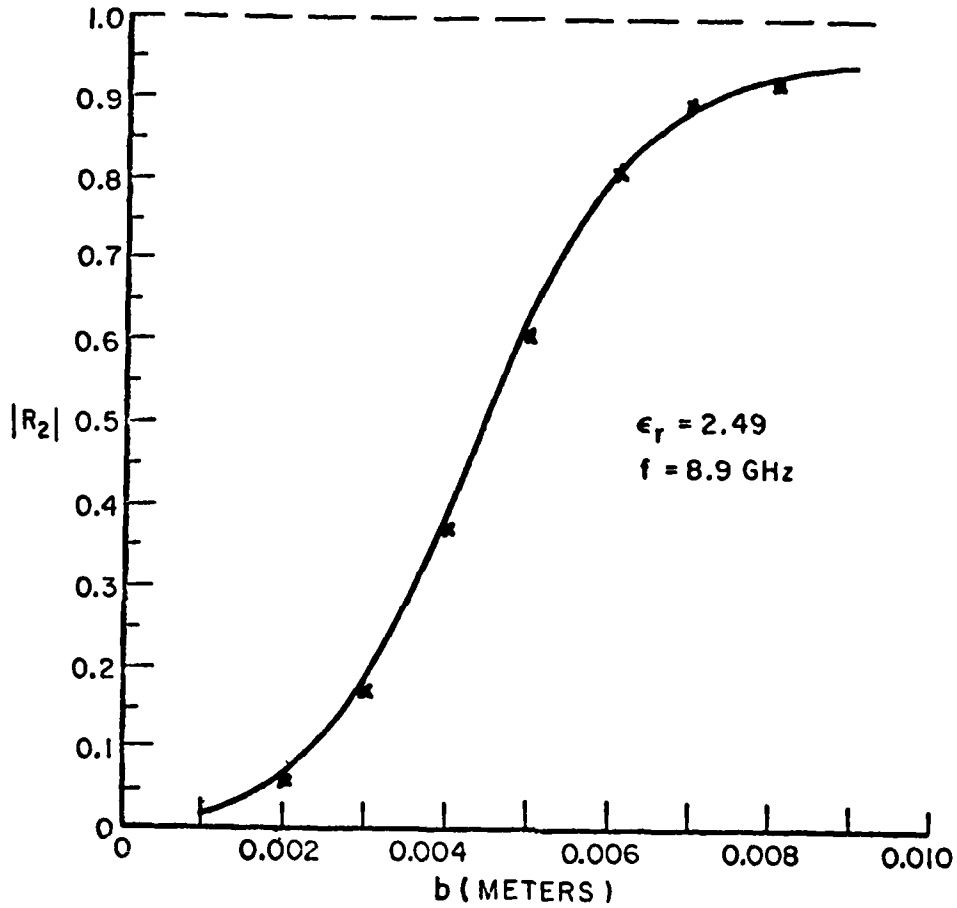

Figure B-3. Surface wave reflection coefficient as a function of the dielectric thickness. Solid curve is reproduced from reference [1].

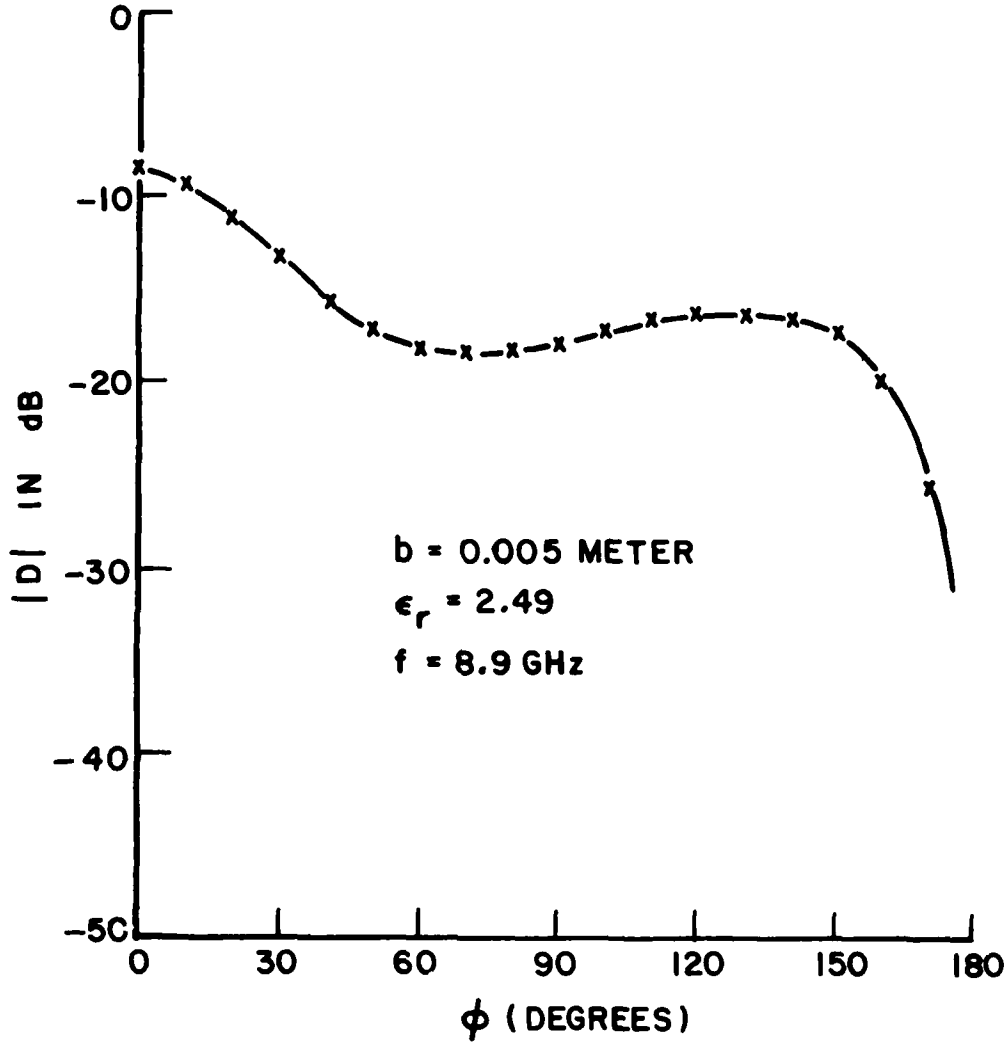

Figure B-4. Radiation pattern of the structure in Figure B-1(a) with surface wave incidence. Solid curve is reproduced from reference [1].

beneath the dielectric is either an electric conductor or a magnetic conductor, are considered. Combinations of these general solutions enable one to solve the problem posed in Figure B-1(b). These solutions will be reported and published in the future.

A hybrid GTD-MM solution to the problem of an exterior line source excitation of an aperture in a parallel plate wave guide as seen in Figure B-5 was also initiated during this past year. It is of interest to know the energy scattered from and penetrated through the aperture. A proper choice of special Green's functions in the integral equation formulation of this problem requires one to find only the unknown electric field in the aperture. The aperture field can be obtained using the moment method technique for small apertures and the hybrid technique for large apertures. An example of the aperture field is shown in Figure B-6 which was obtained using the moment method technique. Extension to the case of a very large aperture using hybrid technique will be evaluated in the future. The fields scattered by the aperture into the interior and exterior regions can be found easily once the aperture field is determined. An analyses of two related problems involving the EM diffraction by an aperture in a thick perfectly conducting screen, and by a groove in a planar conducting surface, respectively, which employed a combination of moment method and multiple scattering techniques, was mentioned in the last annual report [2]. A technical report and a paper dealing with these two related problems is currently in preparation; namely,

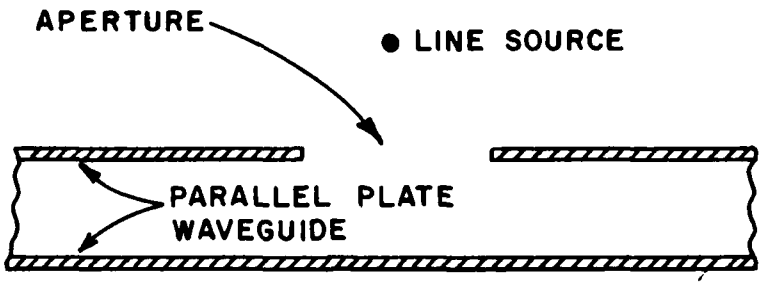

Figure B-5. Exterior line source excitation of a parallel plate waveguide through an aperture in the wall.

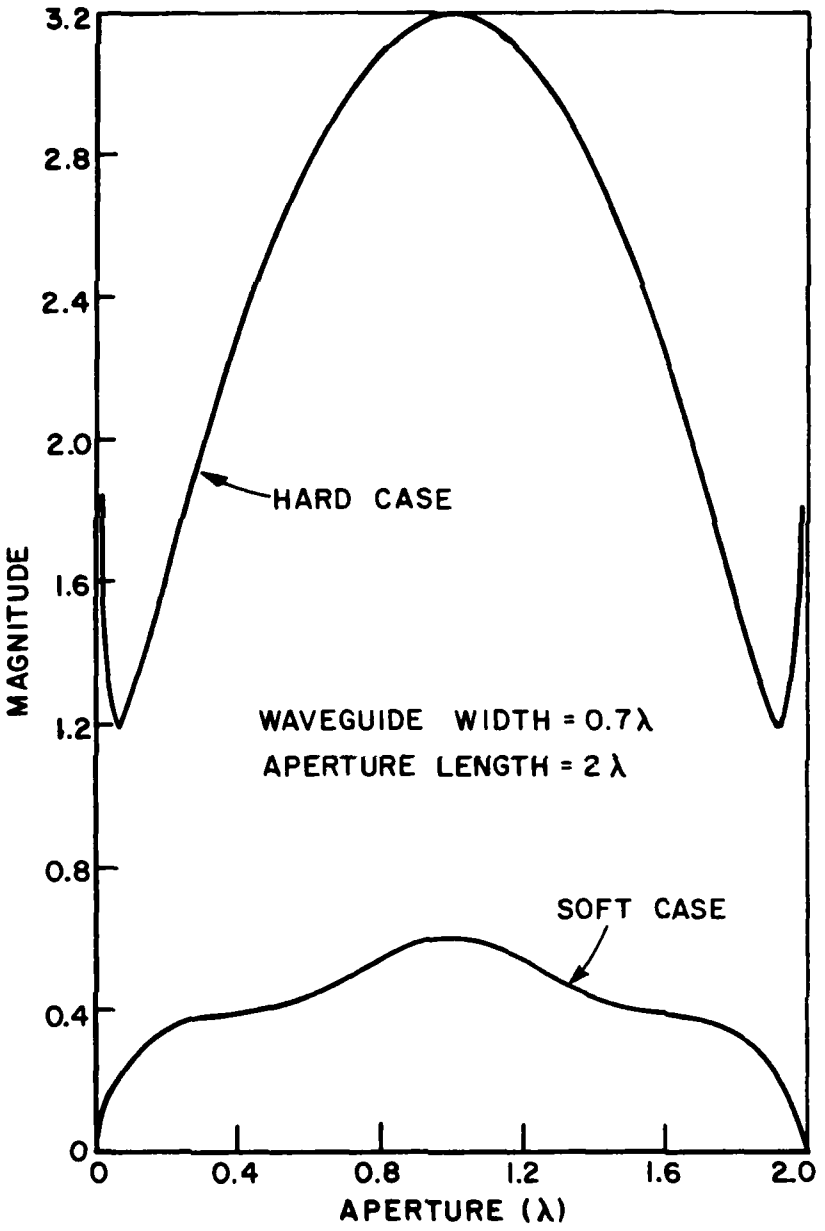

Figure B-6. Relative magnitude of the electric field across the aperture. The line source is at a distance 1λ above the center of the aperture.

"EM Scattering by Slits and Grooves in Thick Perfectly-Conducting Planar Surfaces", by R. Kautz, P.H. Pathak, and L. Peters, Jr.,

A third problem of interest involving the EM diffraction by a perfectly conducting half (circular) cylinder, which has also been investigated during the past year is illustrated in Figure B-7. The geometry chosen for this problem is one of the simplest examples of an edge in an otherwise smooth, perfectly conducting finite size convex body. A hybrid GTD-MM technique has been applied to analyze the scattering by this half-cylinder configuration. At the present time, only the hybrid GTD-MM analysis of the TE (or $\bar{H}$ parallel to the cylinder edge) case has been completed. A corresponding analysis of the TM (or $\bar{E}$ parallel to the cylinder edge) case is currently being pursued. This hybrid solution for the TE case is very efficient since, in general, only 8-12 unknowns are required to represent the induced surface current in the moment method procedure which employs the mixed (hybrid) basis representation for the current in terms of a few pulse basis functions for the current around the edges, and the uniform GTD type basis functions for the current elsewhere on the surface of the half cylinder. It is noted that the above number of unknowns stays the same in this hybrid GTD-MM approach even if the electrical size of the cylinder is increased; in contrast, the conventional MM approach always requires an increase in the number of unknowns with an increase in the

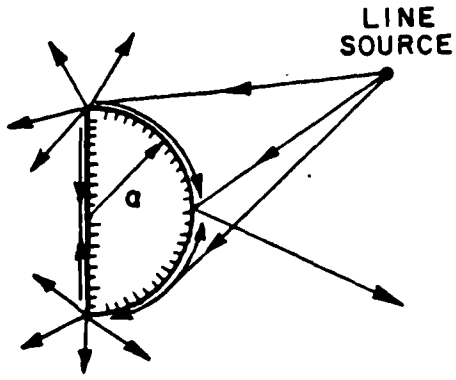

Figure B-7. Diffraction by a half cylinder of radius = a.

cylinder size. Some typical results for the TE radiation patterns of an electric current line source in the presence of the half cylinder of Figure B-7 that are based on the hybrid GTD-MM procedure are illustrated in Figures B-8 and B-9 which also show a comparison with the corresponding conventional MM solutions. For a cylinder whose perimeter is approximately 10λ (here λ=wavelength) in these figures, the number of unknowns (using a pulse basis set) in the conventional MM solution is 100; whereas, in the present hybrid GTD-MM solution, the number of unknowns in only 12. A paper describing this work is planned in the near future.

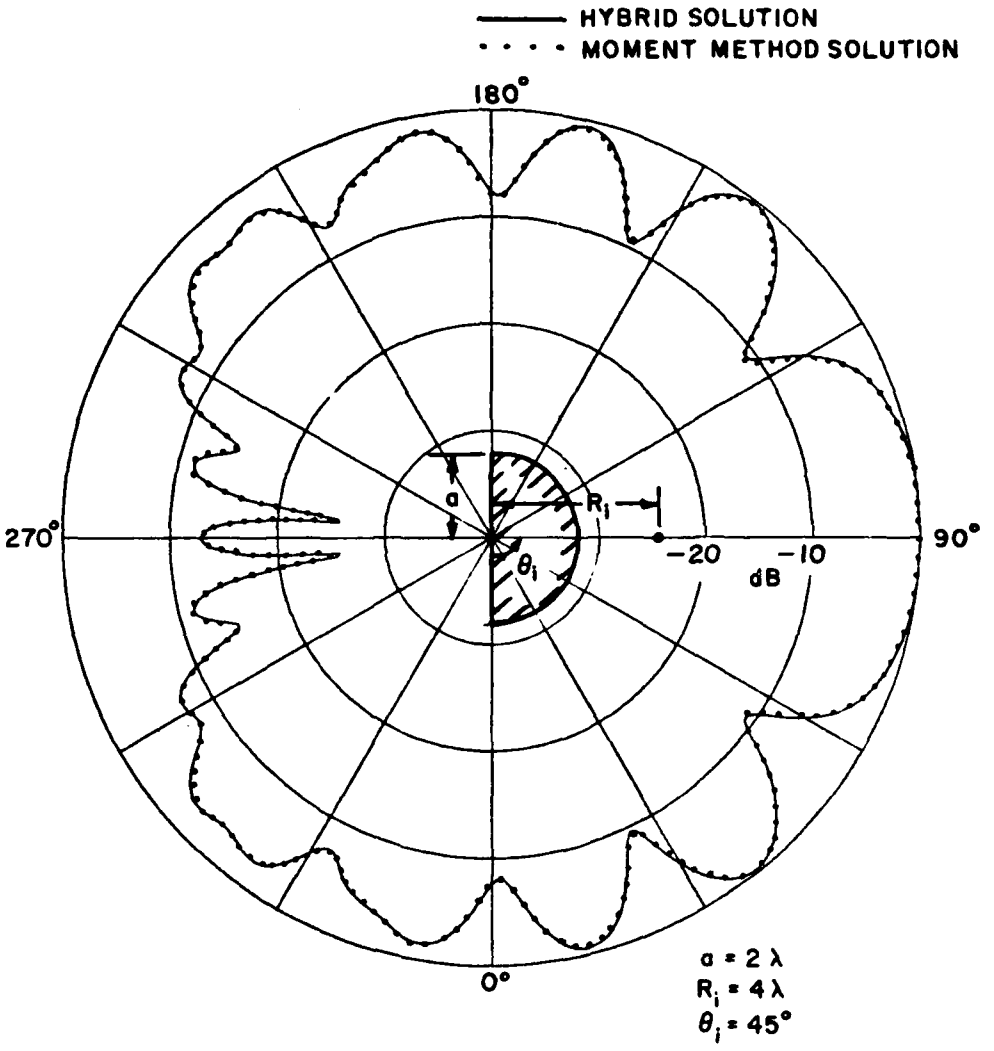

Figure 3-8. Pattern of an electric line source in the presence of a perfectly conducting half cylinder.

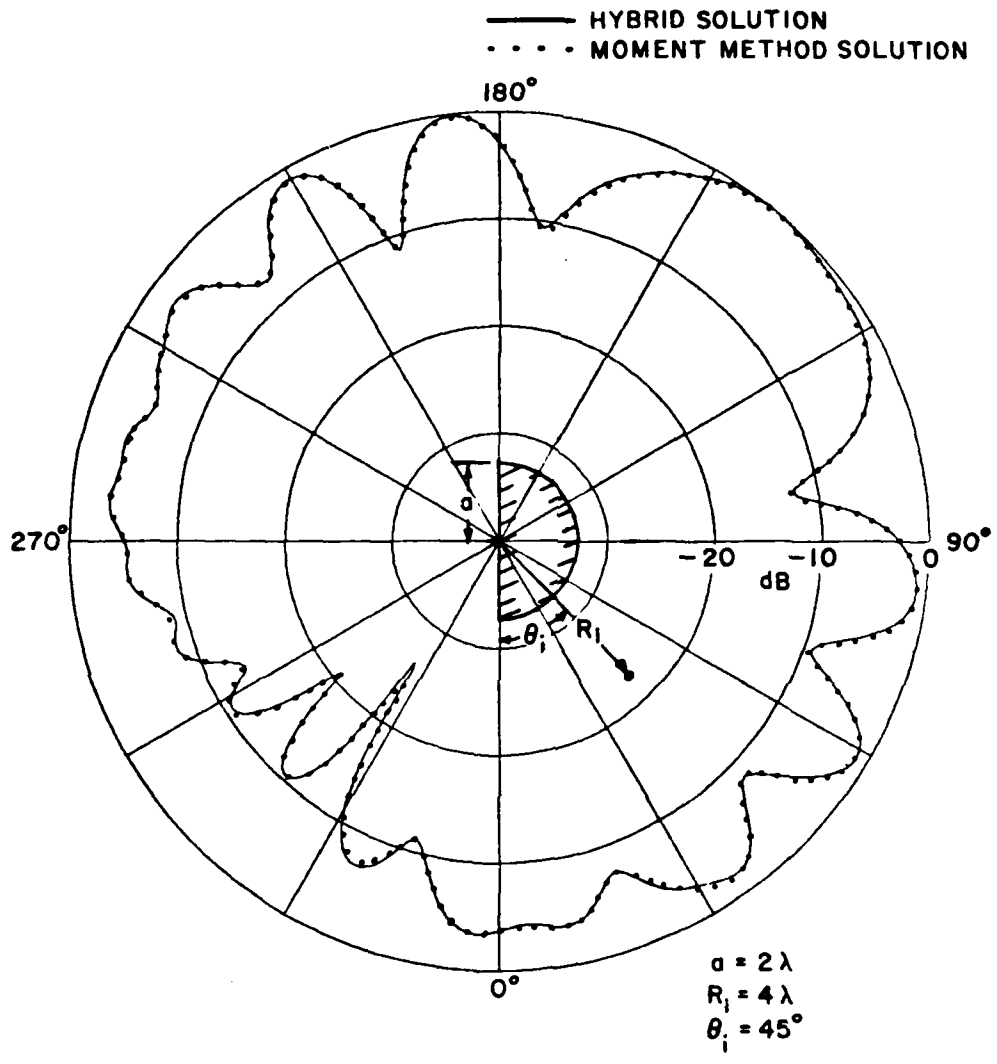

Figure B-9. Pattern of an electric line source in the presence of a perfectly conducting half cylinder.

The half cylinder configuration of Figure B-7 highlights the effects of edge excited surface rays. It is planned in the future phases of this study to numerically extract the uniform GTD diffraction coefficient for edge excited surface rays using the hybrid GTD-MM procedure. This work dealing with the diffraction by an edge in an otherwise smooth convex surface is a natural and proposed extension of the work reported in the previous years on the development of a hybrid GTD-MM solution, and an approximate uniform asymptotic solution to the problem of the diffraction by a perfectly conducting convex surface with a discontinuity in curvature. A paper dealing with the latter approximate uniform asymptotic solution is currently in preparation:

"Diffraction by a Perfectly Conducting Surface with a Discontinuity in Surface Curvature", by C.W. Chuang.

REFERENCES

[1] Pathak, P.H. and R.G. Kouyoumjian, "Surface Wave Diffraction by a Truncated Dielectric Slab Recessed in a Perfectly Conducting Surface", Radio Science, Vol. 14, p. 405-417, May-June 1979.

[2] "Joint Services Electronics Program", Fifth Annual Report 710816-12, December 1982, The Ohio State University ElectroScience Laboratory, Department of Electrical Engineering; prepared under Contract N00014-78-C-0049 for the Department of the Navy, Office of Naval Research, 800 Quincy Street, Arlington, Virginia 22217.

C. Integral Equation Studies

Researchers: Dr. E.H. Newman, Research Scientist (Phone (614) 422-4999)

M.R. Schrote, Graduate Research Associate

Introduction

The goal of our research is to perform basic work in the area of integral equation solutions of general or "arbitrarily" shaped structures. It is anticipated that based upon this work general purpose method of moments (MM) computer codes will be developed (although not under JSEP sponsorship) for the analysis of "arbitrary" structures. In the past, we have studied such basic problems as a perfectly conducting rectangular plate, the junction of a wire to a plate near the edge of the plate, the junction of several plates, and the polygonal plate [1-6]. Much of this basic work has already been implemented into general purpose MM computer codes [7]. The philosophy of these codes is to model the structure as an interconnection of wires and plates. For example, we have modeled the Concorde aircraft as an interconnection of 14 polygonal plates. This model was used to accurately predict the magnitude (RCS) and phase of the backscattering from the Concorde at a frequency where it's overall length was about 1.9 wavelengths [8,9]. One can easily envisage how the polygonal plates could be interconnected

to model other aircraft, ships, buildings, etc. Thus, the computer code is capable of modeling a very general structure. Antennas on the structure are modeled using thin-wires.

All of the above work has dealt with perfectly conducting plates. Thus, it was suitable only for the modeling of (essentially) perfectly conducting structures. However, recently there has been increasing interest in the use of non-metallic materials for the construction of aircraft. These non-metallic materials, often called composite materials, are used to modify the RCS of the aircraft, or to make the aircraft frame strong and yet lightweight. It is our future goal to be able to model a general structure composed of metallic and/or composite materials. While the modeling of the perfectly conducting surfaces is well advanced, the following steps are required to realize this goal:

1. Develop a model for an isolated material plate. A material plate is a thin planar three dimensional slab composed of some dielectric/ferrite material. Also, it can be a perfectly conducting plate coated on one or both sides by a dielectric/ferrite material. This can be used to model absorber coated plates.

2. Develop a model for the junction of a material and a perfectly conducting plate.

3. Extend the above solutions to the non-planar case.

4. Implement the above in the form of a general purpose computer code capable of treating an interconnection of wires, perfectly conducting plates, and material plates.

Step 1 is now essentially complete [20,21], and will be described in detail in the next section. This will include a description of the theoretical solution in terms of four coupled integral equations, the simplification of these equations using a surface impedance approximation, and the generation of numerical results using the method of moments. Steps 2 and 3 have been proposed for future JSEP research. Step 4 is in the area of applied research or development and must be done under support other than JSEP.

1. Theoretical Solution

a. Integral equation development

Figure C-1a shows the side view of a material plate with constitutive parameters (μ,ε), and of thickness t, immersed in free space, i.e., a homogeneous medium with constitutive parameters (μ_o,ε_o). The plate is excited by the known impressed currents $(\underline{J}_i,\underline{M}_i)$ which in free space radiate the incident fields $(\underline{E}_i,\underline{H}_i)$, and the unknown fields $(\underline{E},\underline{H})$ in the presence of the plate. Let S denote the surface enclosing the plate. Using the surface equivalence principle, Figure C-1a can be decomposed into the two cases shown in Figures C-1b,c [10]. In Case A, the constitutive parameters of all space are (μ_o,ε_o), the fields are

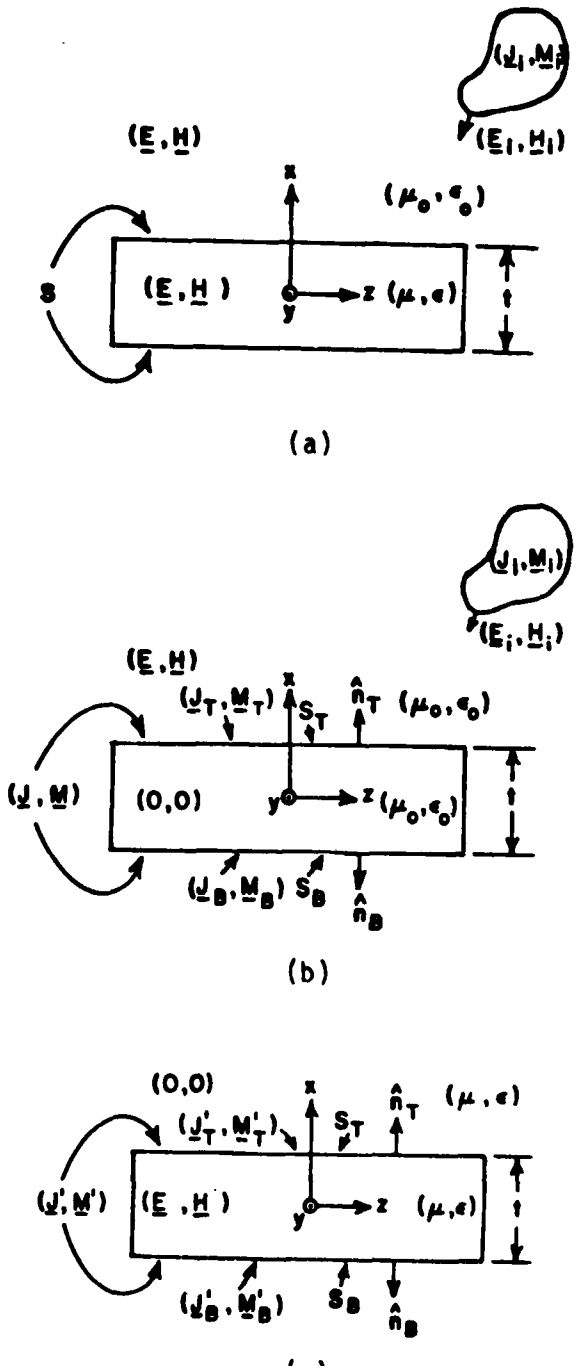

Figure C-1. (a) Side view of a material plate immersed in free space.
(b) Case A: Equivalent problem external to S.
(c) Case B: Equivalent problem internal to S.

zero inside the plate, the unknown fields ($\underline{E},\underline{H}$) exist outside the plate, and the surface currents ($\underline{J},\underline{M}$) flow on the surface S. The currents ($\underline{J},\underline{M}$) radiate the scattered fields ($\underline{E}_S,\underline{H}_S$) in free space. In Case B, the constitutive parameters of all space are (μ,ε), the fields are zero outside the plate, the unknown fields ($\underline{E},\underline{H}$) exist inside the plate, and the surface currents ($\underline{J}',\underline{M}'$) = ($-\underline{J},-\underline{M}$) flow on the surface S. We will consider that the plates are sufficiently thin so that the surface currents on the sides of the plate will be ignored. Note that use of the surface equivalence principle allows one to evaluate the fields either inside or outside a material body, although one must use the appropriate equivalent currents (i.e., Case A outside or Case B inside). Further, this statement is not changed by the use of an abc such as surface impedance relationships.

Referring to Figure C-1, define:

S_T = the top of surface S, i.e., that part of S at $x = t/2$

S_B = the bottom of surface S, i.e., that part of S at $x = -t/2$

$\underline{J}(x,y,z)$ = the electric current flowing on the closed surface S

$\underline{J}_T(y,z)$ = the top electric current, i.e., that part of $\underline{J}$ on S_T

$\underline{J}_B(y,z)$ = the bottom electric current, i.e., that part of $\underline{J}$ on S_B

$\underline{J}_S(y,z)$ = the sum electric current, i.e., a single surface current equal to the vector sum $\underline{J}_T + \underline{J}_B$ and arbitrarily considered to be on S_T

$\underline{J}_D(y,z)$ = the difference electric current, i.e., a single surface current equal to the vector difference $\underline{J}_T - \underline{J}_B$ and arbitrarily considered to be on S_T

$\underline{M}$, $\underline{M}_T$, $\underline{M}_B$, $\underline{M}_S$, and $\underline{M}_D$ have identical meanings, except that they refer to magnetic currents.

Now consider the problem of Figure C-1b. Since a null field exists interior to S, there will be zero reaction between the currents $(\underline{J},\underline{M})$ and $(\underline{J}_i,\underline{M}_i)$, and a test source interior to S. If the test source is electric with current density $\underline{J}_t$, this leads to the electric reaction integral equation (ERIE)

$$- \langle \underline{J}_t, (\underline{J},\underline{M}) \rangle = V^J \tag{C.1}$$

where

$$V^J = \langle \underline{J}_t, (\underline{J}_i,\underline{M}_i) \rangle \tag{C.2}$$

By definition [11], the reaction between sources a and b is

$$\langle a,b \rangle = \iint_b (\underline{E}_a \cdot \underline{J}_b - \underline{H}_a \cdot \underline{M}_b)\, ds = \langle b,a \rangle \tag{C.3}$$

where the integral is over the region occupied by the source b.

Figure C-2 shows the side view of the plate with an electric test source $\underline{J}_t$ in the interior. $\underline{J}_t$ is considered to be a surface current in the yz plane, and its fields in free space will be denoted $(\underline{E}^J_t, \underline{H}^J_t)$. The plate currents $(\underline{J},\underline{M})$ are explicitly shown as $(\underline{J}_T,\underline{M}_T)$ on S_T and $(\underline{J}_B,\underline{M}_B)$ on S_B. Using the linearity of the reaction operator, Equation (C.1) becomes

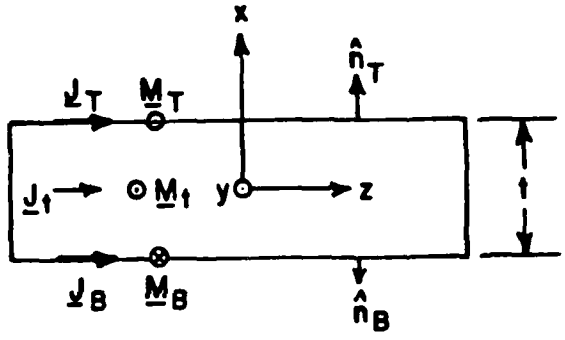

Figure C-2. Side view of material plate with an electric test source, $\underline{J}_t$, and a magnetic test source, $\underline{M}_t$, in the interior.

$$- \langle \underline{J}_t, (\underline{J}_T, \underline{M}_T) \rangle - \langle \underline{J}_t, (\underline{J}_B, \underline{M}_B) \rangle = V^J \quad , \quad \text{or} \tag{C.4}$$

$$- \int_{S_T} \int (\underline{E}^J_t \cdot \underline{J}_T - \underline{H}^J_t \cdot \underline{M}_T)\, ds - \int_{S_B} \int (\underline{E}^J_t \cdot \underline{J}_B - \underline{H}^J_t \cdot \underline{M}_B) ds = V^J \, , \tag{C.5}$$

Since the tangential electric and magnetic fields of $\underline{J}_t$ are even and odd functions of x, respectively

$$\underline{E}^J_t(S_T) \times \hat{n}_T = \underline{E}^J_t(S_B) \times \hat{n}_T \tag{C.6a}$$

$$\underline{H}^J_t(S_T) \times \hat{n}_T = -\underline{H}^J_t(S_B) \times \hat{n}_T \underset{\lim\, t \to o}{=} \underline{J}_t/2 \quad . \tag{C.6b}$$

Using the symmetry relations of Equations (C.6), we move the bottom currents, $(\underline{J}_B, \underline{M}_B)$, from S_B to S_T, and Equation (C.5) becomes

$$- \int_{S_T} \int [\underline{E}^J_t \cdot (\underline{J}_T + \underline{J}_B) - \underline{H}^J_t \cdot (\underline{M}_T - \underline{M}_B)]\, ds = V^J \quad , \quad \text{or} \tag{C.7}$$

$$- \langle \underline{J}_t, (\underline{J}_S, \underline{M}_D) \rangle = V^J. \tag{C.8}$$

Note that Equation (C.8) applies on the open surface S_T.

Next consider the case where the test source in Equation (C.3) is the magnetic current $\underline{M}_t$. This leads to the magnetic reaction integral equation (MRIE)

$$- \langle \underline{M}_t, (\underline{J}, \underline{M}) \rangle = V^M \tag{C.9}$$

where

$$V^M = \langle \underline{M}_t, (\underline{J}_i, \underline{M}_i) \rangle \ . \qquad (C.10)$$

Figure C-2 shows the side view of the plate with a magnetic test source $\underline{M}_t$ in the interior. $\underline{M}_t$ is considered to be a surface current in the yz plane, and its fields in free space will be denoted $(\underline{E}_t^M, \underline{H}_t^M)$. Again, using the linearity of the reaction operator, Equation (C.9) becomes

$$- \langle \underline{M}_t, (\underline{J}_T, \underline{M}_T) \rangle - \langle \underline{M}_t, (\underline{J}_B, \underline{M}_B) \rangle = V^M \ , \qquad (C.11)$$

or

$$- \int_{S_T} \int (\underline{E}_t^M \cdot \underline{J}_T - \underline{H}_t^M \cdot \underline{M}_T) ds - \int_{S_B} \int (\underline{E}_t^M \cdot \underline{J}_B - \underline{H}_t^M \cdot \underline{M}_B) ds = V^M \ . \qquad (C.12)$$

Since the tangential electric and magnetic fields of $\underline{M}_t$ are odd and even functions of x, respectively

$$\underline{E}_t^M(S_T) \times \hat{n}_T = - \underline{E}_t^M(S_B) \times \hat{n}_T \underset{\lim\, t \to o}{=} \underline{M}_t/2 \ . \qquad (C.13a)$$

$$\underline{H}_t^M(S_T) \times \hat{n}_T = \underline{H}_t^M(S_B) \times \hat{n}_T \ . \qquad (C.13b)$$

Using the symmetry relations of Equations (C.13), we again move $(\underline{J}_B, \underline{M}_B)$ from S_B to S_T, and Equation (C.12) becomes

$$- \iint_{S_T} [\underline{E}_t^M \cdot (\underline{J}_T - \underline{J}_B) - \underline{H}_t^M \cdot (\underline{M}_T + \underline{M}_B)] \, ds = V^M \ , \qquad (C.14)$$

or

$$- < \underline{M}_t, (\underline{J}_D, \underline{M}_S) > = V^M \quad , \tag{C.15}$$

valid on the open surface S_T.

Equations (C.8) and (C.15) constitute two of the four equations needed to solve for the four unknowns, $(\underline{J}_S, \underline{M}_S)$ and $(\underline{J}_D, \underline{M}_D)$. In obtaining these equations, we did not require that the plate thickness go to zero. The thickness does have to be sufficiently small that the side currents can be ignored. To obtain the remaining two equations, the zero reaction concept with test sources outside S is applied to the equivalent problem of Figure C-1c. An arbitrary test source $(\underline{J}_t, \underline{M}_t)$ exterior to S in Figure C-1c has zero reaction with the currents $(\underline{J}', \underline{M}') = (-\underline{J}, -\underline{M})$, or

$$<(\underline{J}_t, \underline{M}_t), (\underline{J}, \underline{M})> = 0. \tag{C.16}$$

Explicitly showing the integrations over the top and bottom surfaces, Equation (C.16) becomes

$$\iint_{S_T} (\underline{E}_t \cdot \underline{J}_T - \underline{H}_t \cdot \underline{M}_T) ds + \iint_{S_B} (\underline{E}_t \cdot \underline{J}_B - \underline{H}_t \cdot \underline{M}_B) ds = 0 \quad . \tag{C.17}$$

where $(\underline{E}_t, \underline{H}_t)$ are the fields of $(\underline{J}_t, \underline{M}_t)$ in the homogeneous medium (μ, ε). In practice, two independent equations can be obtained from Equation (C.16) by first placing $(\underline{J}_t, \underline{M}_t)$ in the plane $x = (t + \Delta t)/2$ and then in

AD-A140 434 JOINT SERVICES ELECTRONICS PROGRAM(U) OHIO STATE UNIV 2/3
COLUMBUS ELECTROSCIENCE LAB DEC 83 ESL-710816-15
N00014-78-C-0049

UNCLASSIFIED F/G 9/5 NL

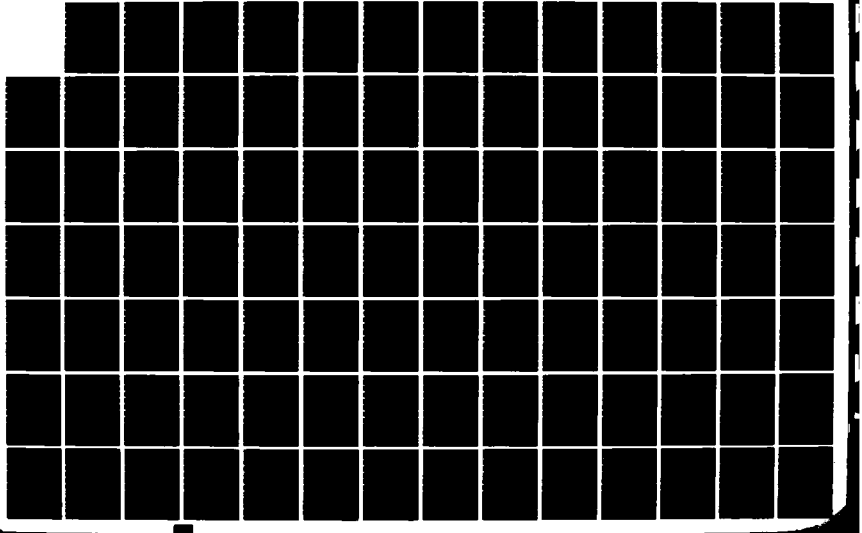

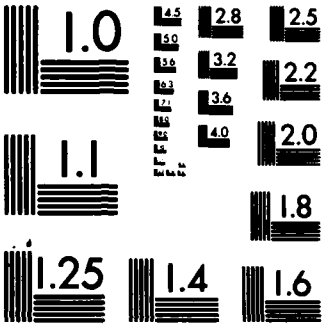

MICROCOPY RESOLUTION TEST CHART
NATIONAL BUREAU OF STANDARDS-1963-A

the plane $x = -(t+\Delta t)/2$ where Δt is a positive value. Thus, Equations (C.8), (C.15), and (C.16) twice constitute four coupled integral equations which could, in principal, be solved for $(\underline{J}_S, \underline{M}_S)$ and $(\underline{J}_D, \underline{M}_D)$. In order to properly account for plate thickness, one should convert the sum and difference currents to top and bottom currents prior to computing the scattered fields (interior or exterior to the plate). However, for thin plates and exterior field points whose x distance from the plate is large in comparison to plate thickness, one may compute the scattered fields from $(\underline{J}_S, \underline{M}_S)$ only.

2. Impedance Boundary Condition

In this section we will obtain the surface impedance relationships for a penetrable dielectric/ferrite plane sheet or slab. We will also obtain the surface impedance of an impenetrable perfect conductor backed on one or both sides by a dielectric/ferrite slab. This will be done by considering the simple one dimensional problem of a plane wave normally incident upon a dielectric/ferrite slab. Although the solution to this problem, in terms of plane wave reflections, appears in many texts on electromagnetic theory [12], we will investigate the solution using the surface equivalence principle and the reaction integral equations obtained in the previous section. For the case of the slab, Equation (C.16) has simple solutions from which we can deduce relationships between the equivalent electric and magnetic surface

currents, i.e., the slab surface impedance relationships. In the next section we will employ the approximation that these relationships (which are exact for the slab) apply also to the finite or three dimensional material plate. This will eliminate two of the four integral equations for the material plate.

Figure C-3a shows a plane wave of the form

$$\underline{E}_i = \hat{z}\, E_o\, e^{\gamma_o x} \quad , \tag{C.18a}$$

$$\underline{H}_i = \hat{y}\, E_o\, e^{\gamma_o x} / \eta_o \quad , \tag{C.18b}$$

where $\gamma_o = j\omega\sqrt{\mu_o \varepsilon_o}$ and $\eta_o = \sqrt{\frac{\mu_o}{\varepsilon_o}}$ incident upon a slab of thickness t and with parameters (μ,ε). The illuminated surface of the slab at $x = t/2$ will be referred to as S_T, the top surface. The surface at $x = -t/2$ will be referred to as S_B, the bottom surface. In direct analogy to Figure C-1, the equivalent currents will be constant sheets denoted $(J_T\hat{z}, M_T\hat{y})$ on S_T and $(J_B\hat{z}, -M_B\hat{y})$ on S_B. Referring to Figure C-1c and Equation (C.16), there will be zero reaction between a constant sheet current test source, located outside the slab, and the equivalent currents. If the test source is given by the electric current

$$\underline{J}_t = -2\hat{z} \quad . \tag{C.19}$$

and is located in the plane $x = x_t$ $(|x_t| > t/2)$, then its fields in the medium (μ,ε) are

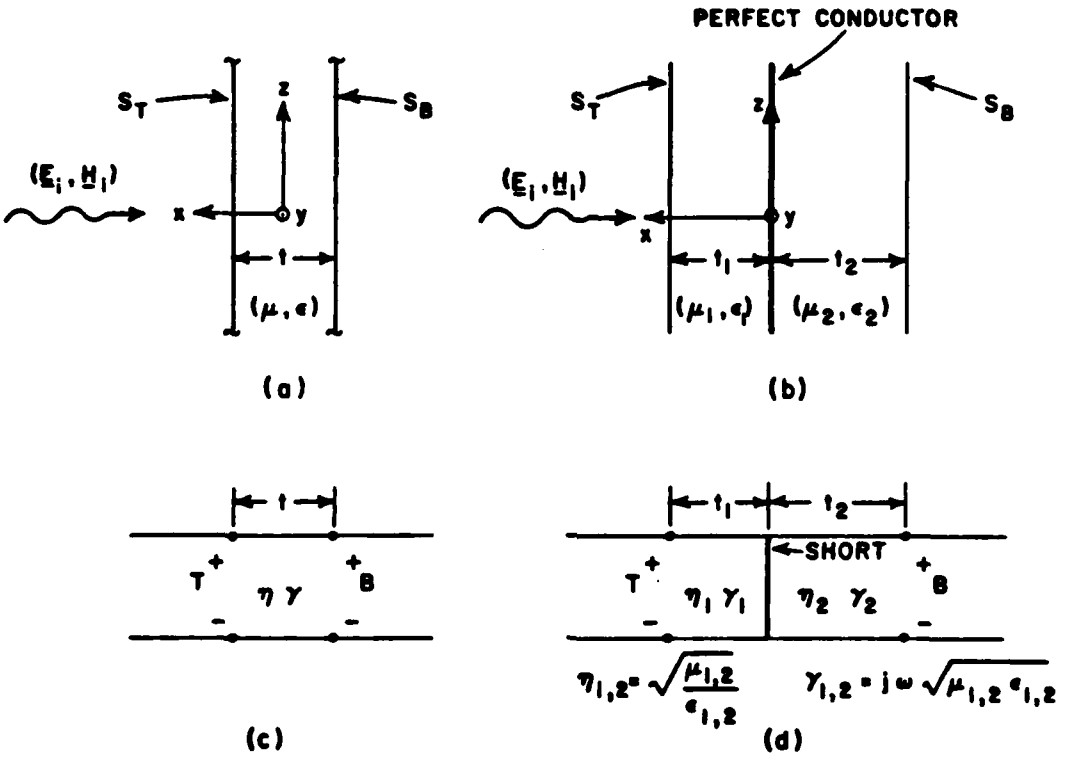

Figure C-3. (a) Side view of material slab immersed in free space,
(b) Side view of a coated, perfectly conducting sheet immersed in free space,
(c) Transmission line equivalent of (a), and
(d) Transmission line equivalent of (b).

$$\underline{E}_t = \hat{z}\, \eta\, e^{-\gamma|x-x_t|} \quad , \tag{C.20a}$$

$$\underline{H}_t = -\hat{y}\, \mathrm{sgn}\,(x-x_t)\, e^{-\gamma|x-x_t|} \quad , \tag{C.20b}$$

where $\eta = \frac{\mu}{\epsilon}$, $\gamma = j\omega\sqrt{\mu\epsilon}$, and sgn(x) = 1 if $x > 0$ and -1 if $x < 0$.

Inserting Equations (C.19) and (C.20) into Equation (C.16) yields

$$J_T \eta e^{-\gamma t/2} + J_B \eta e^{\gamma t/2} + M_T e^{-\gamma t/2} - M_B e^{\gamma t/2} = 0 \text{ for } x_t < -t/2 \ , \tag{C.21a}$$

$$J_T \eta e^{\gamma t/2} + J_B \eta e^{-\gamma t/2} - M_T e^{\gamma t/2} + M_B e^{-\gamma t/2} = 0 \text{ for } x_t > t/2 \ . \tag{C.21b}$$

Solving Equations (C.21) for M_T and M_B yields

$$M_T = Z_{TT} J_T + Z_{TB} J_B \quad , \tag{C.22a}$$

$$M_B = Z_{BT} J_T + Z_{BB} J_B \quad , \tag{C.22b}$$

where

$$Z_{TT} = Z_{BB} = \eta/\tanh\gamma t \quad , \tag{C.23a}$$

$$Z_{TB} = Z_{BT} = \eta/\sinh\gamma t \quad . \tag{C.23b}$$

These impedances are equal to the two port impedance parameters of the transmission line of length t, characteristic impedance η, and

propagation constant γ, shown in Figure C-3c. They are comparable to equations by Mitzner for an absorbing shell [25].

If the slab had been impenetrable, such as the perfectly conducting ground plane coated on one or both sides by a dielectric/ferrite slab of Figure C-3b, then the two port impedances would be those of the transmission line model of Figure C-3d. In this case we have $Z_{TB} = Z_{BT} = 0$, and

$$Z_{TT} = \eta_1 \tanh\gamma_1 t_1 \quad , \tag{C.24a}$$

$$Z_{BB} = \eta_2 \tanh\gamma_2 t_2 \quad . \tag{C.24b}$$

3. Surface Impedance Approximation

In the last section, two impedance boundary relationships (Equations (C.22)) for a one dimensional dielectric/ferrite slab were obtained. In this section, Equations (C.22) are used as an approximation for Equation (C.16). For a one dimensional slab at normal incidence these relationships are exact. For a three dimensional material plate they are not exact since:

(1) the incident wave may not have normal incidence,

(2) the edges and corners of the plate will modify the relationships.

Despite this, we will use the one dimensional slab surface impedance relationships for the three dimensional material plate. This is an application of what Senior [13] termed an approximate boundary condition (abc). As pointed out by Senior, there usually is no rigorous justification for the use of an abc. The justification is in their usefulness in predicting results obtained by measurements or by more rigorous techniques. Of course, the motivation for their use, as compared to more rigorous techniques, is that they simplify the analysis. It is possible that better results would be obtained by using a surface impedance which is dependent upon the angle of incidence, however, for simplicity this was not done here. Writing Equation (C.22) in terms of sum and difference currents gives

$$\underline{M}_S = Z_{SS}\underline{J}_S \times \hat{n}_T + Z_{SD}\underline{J}_D \times \hat{n}_T \quad , \tag{C.25a}$$

$$\underline{M}_D = Z_{DS}\underline{J}_S \times \hat{n}_T + Z_{DD}\underline{J}_D \times \hat{n}_T \quad , \tag{C.25b}$$

where

$$Z_{SS} = (Z_{TT} + Z_{TB} - Z_{BT} - Z_{BB})/2 \quad , \tag{C.26a}$$

$$Z_{SD} = (Z_{TT} - Z_{TB} - Z_{BT} + Z_{BB})/2 \quad , \tag{C.26b}$$

$$Z_{DS} = (Z_{TT} + Z_{TB} + Z_{BT} + Z_{BB})/2 \quad , \tag{C.26c}$$

$$Z_{DD} = (Z_{TT} - Z_{TB} + Z_{BT} - Z_{BB})/2 \quad . \tag{C.26d}$$

Combining Equations (C.8), (C.15), and (C.25) yields

$$- \langle \underline{J}_t, (\underline{J}_S, \underline{M}_D) \rangle = -\langle \underline{J}_t, (\underline{J}_S, Z_{DS}\underline{J}_S \times \hat{n}_T + Z_{DD}\underline{J}_D \times \hat{n}_T) \rangle = V^J \quad , \quad (C.27a)$$

$$- \langle \underline{M}_t, (\underline{J}_D, \underline{M}_S) \rangle = -\langle \underline{M}_t, (\underline{J}_D, Z_{SS}\underline{J}_S \times \hat{n}_T + Z_{SD}\underline{J}_D \times \hat{n}_T) \rangle = V^M \quad . \quad (C.27b)$$

Equations (C.27) represent two coupled integral equations on the open surface S_T which can be solved for the electric currents $\underline{J}_S$ and $\underline{J}_D$. Having solved for $\underline{J}_S$ and $\underline{J}_D$, the magnetic currents $\underline{M}_S$ and $\underline{M}_D$ can be found from Equation (C.25). We reemphasize that the $Z_{DS}\underline{J}_S \times \hat{n}_T + Z_{DD}\underline{J}_D \times \hat{n}_T$ and $Z_{SS}\underline{J}_S \times \hat{n}_T + Z_{SD}\underline{J}_D \times \hat{n}_T$ terms in Equation (C.27) are not electric currents, but rather are the magnetic currents, $\underline{M}_D$ and $\underline{M}_S$, respectively.

In the remaining part of this section, Equation (C.27) is examined for various special cases.

CASE 1 - PERFECTLY CONDUCTING PLATES

If the plate is a perfect conductor, then $Z_{SS} = Z_{DD} = Z_{DS} = Z_{SD} = 0$ and Equation (C.27) reduces to

$$-\langle \underline{J}_t, (\underline{J}_S, 0) \rangle = V^J \quad , \quad (C.28a)$$

$$-\langle \underline{M}_t, (\underline{J}_D, 0) \rangle = V^M \quad . \quad (C.28b)$$

Equation (C.28) was previously presented and solved by the authors [14].

CASE 2 - UNIFORM MATERIAL PLATE

If the plate is of uniform μ and ϵ, then from Equations (C.23) and (C.26), $Z_{SS} = Z_{DD} = 0$ and

$$Z_{SD} = Z_{TT} - Z_{TB} = \eta(\cosh\gamma t - 1)/\sinh\gamma t \quad , \tag{C.29a}$$

$$Z_{DS} = Z_{TT} + Z_{TB} = \eta(\cosh\gamma t + 1)/\sinh\gamma t \quad . \tag{C.29b}$$

In this case, Equation (C.27) reduces to

$$- \langle \underline{J}_t, (\underline{J}_S, \underline{M}_D) \rangle = -\langle \underline{J}_t, (\underline{J}_S, Z_{DS}\underline{J}_S \times \hat{n}_T) \rangle = V^J \quad , \tag{C.30a}$$

$$- \langle \underline{M}_t, (\underline{J}_D, \underline{M}_S) \rangle = -\langle \underline{M}_t, (\underline{J}_D, Z_{SD}\underline{J}_D \times \hat{n}_T) \rangle = V^M \quad . \tag{C.30b}$$

An important point is that the equations uncouple for this case. However, note that both equations must be solved to find $(\underline{J}_S, \underline{M}_S)$ which radiate the far-zone scattered field. In general, for any symmetric slab (i.e., $Z_{TT}=Z_{BB}$ and $Z_{TB}=Z_{BT}$) the equations uncouple.

CASE 3 - VERY THIN UNIFORM MATERIAL PLATE

Now consider Equation (C.30a) in the limit as the thickness γt goes to zero. By reciprocity, Equation (C.30a) can be written as

$$- \iint_t \underline{J}_t \cdot (\underline{E}(\underline{J}_S) + \underline{E}(\underline{M}_D) + \underline{E}_i)\, ds = 0 \quad . \tag{C.31}$$

where $\underline{E}(\underline{J}_S)$ and $\underline{E}(\underline{M}_D)$ are the free-space electric fields of $\underline{J}_S$ and $\underline{M}_D = Z_{DS}\,\underline{J}_S \times \hat{n}_T$, respectively, and the integral is over the surface of the arbitrary electric test source $\underline{J}_t$. Note that $\underline{J}_t$ is located in the interior of the closed surface S and is directed tangential to the broad surfaces of S.

Since Equation (C.31) must apply for an arbitrary $\underline{J}_t$, it is clear that

$$\underline{E}_{tan}(\underline{J}_S) + \underline{E}_{tan}(\underline{M}_D) = -\underline{E}_{i\ tan} \text{ interior to S.} \qquad \text{(C.32)}$$

As $\gamma t \to 0$, the tangential electric field of $\underline{M}_D$ will be essentially (see Equation (C.13a))

$$\underline{E}_{tan}(\underline{M}_D) = -\hat{n}_T \times \underline{M}_D/2 \quad . \qquad \text{(C.33)}$$

Also from Equation (C.29b).

$$\lim_{\gamma t \to 0} Z_{DS} = \frac{2\eta}{\gamma t} \quad . \qquad \text{(C.34)}$$

Combining Equations (C.25b), (C.32), (C.33), and (C.34) gives

$$-\underline{E}_{tan}(\underline{J}_S) + \frac{\eta}{\gamma t}\underline{J}_S = \underline{E}_{i\ tan} \quad . \qquad \text{(C.35)}$$

Equation (C.35) gives the current on a surface of sheet impedance $\eta/\gamma t$. It is equivalent to that used by Harrington to study thin dielectric shells [15] and by Senior to study resistive strips [16]. Note that

when treating impedance sheets, one simply adds the term $\frac{\eta}{\gamma t}\underline{J}_S$ to the equation for perfectly conducting surfaces. In a MM solution of Equation (C.35) this would result in an impedance matrix of the form [Z] + [ΔZ] where [Z] is the impedance matrix for the perfectly conducting surface, and a typical term of [ΔZ] would be

$$\Delta Z_{mn} = \frac{\eta}{\gamma\tau} \iint \underline{J}_m \cdot \underline{G}_n \; ds \quad . \tag{C.36}$$

Here $\underline{J}_m$ represents the m^{th} current expansion mode and $\underline{G}_n$ the n^{th} test mode or weighting function. Equation (C.36) can be evaluated in closed form for any of the usual choices for the modes. This permits the thin symmetric slab to be treated as a very simple modification of the perfect conductor. Note that $\Delta Z_{mn} = 0$ unless modes $\underline{J}_m$ and $\underline{G}_n$ overlap. Also, for extremely small γt, ΔZ_{mn} will be large, and this will result in small $\underline{J}_s$.

CASE 4 - COATED CONDUCTING PLATE

If the plate is a perfect conductor coated on one or both sides by a dielectric/ferrite, then from Equations (C.25) and (C.26)

$$Z_{SS} = Z_{DD} = (\eta_1 \tanh\gamma_1 t_1 - \eta_2 \tanh\gamma_2 t_2)/2 \quad . \tag{C.37a}$$

$$Z_{SD} = Z_{DS} = (\eta_1 \tanh\gamma_1 t_1 + \eta_2 \tanh\gamma_2 t_2)/2 \quad . \tag{C.37b}$$

and Equations (C.27) reduce to the coupled equations

$$- \langle \underline{J}_t, (\underline{J}_S, \underline{M}_D) \rangle = - \langle \underline{J}_t, (\underline{J}_S, Z_{SD} \underline{J}_S \times \hat{n}_T + Z_{SS} \underline{J}_D \times \hat{n}_T) \rangle = V^J \quad , \quad \text{(C.38a)}$$

$$- \langle \underline{M}_t, (\underline{J}_D, \underline{M}_S) \rangle = - \langle \underline{M}_t, (\underline{J}_D, Z_{SS} \underline{J}_S \times \hat{n}_T + Z_{SD} \underline{J}_D \times \hat{n}_T) \rangle = V^M \quad . \quad \text{(C.38b)}$$

4. Moment Method Solution

The current distributions on the material plates can be found by solving the integral equations of the previous section by the numerical technique known as the method of moments (MM) [18]. Here we will present the MM solution to Equations (C.27) which represent the most general case, rather than one of the special cases which follow. The solution is similar to that for perfectly conducting surfaces [1,2,7], and thus our description will be brief, emphasizing only those parts which are new.

The first step in the MM solution is to expand the unknown currents, $\underline{J}_S$ and $\underline{J}_D$ in a finite set of N basis functions:

$$\underline{J}_S = \sum_{n=1}^{N} I_{Sn} \underline{F}_n \quad . \quad \text{(C.39a)}$$

$$\underline{J}_D = \sum_{n=1}^{N} I_{Dn} \underline{F}_n \quad . \quad \text{(C.39b)}$$

Then using the abc's of Equations (C.25), $\underline{M}_S$ and $\underline{M}_D$ are the dependent unknowns

$$\underline{M}_S = \sum_{n=1}^{N} \left(Z_{SS}\, I_{Sn} + Z_{SD}\, I_{Dn}\right) \underline{F}_n \times \hat{n}_T \quad , \tag{C.40a}$$

$$\underline{M}_D = \sum_{n=1}^{N} \left(Z_{DS}\, I_{Sn} + Z_{DD}\, I_{Dn}\right) \underline{F}_n \times \hat{n}_T \quad . \tag{C.40b}$$

Choosing our test modes identical to the expansion modes (except that they are in the yz plane), Equations (C.27) reduce to the set of 2N simultaneous linear equations written in block matrix form as

$$\begin{bmatrix} [Z^{EE}] + Z_{DS}\,[Z^{EM}] & Z_{DD}\,[Z^{EM}] \\ Z_{SS}\,[Z^{MM}] & [Z^{ME}] + Z_{SD}\,[Z^{MM}] \end{bmatrix} \begin{bmatrix} I_S \\ I_D \end{bmatrix} = \begin{bmatrix} V^J \\ V^M \end{bmatrix} \quad , \tag{C.41}$$

where

$$Z_{mn}^{EE} = -\iint_n \underline{E}_m^J \cdot \underline{F}_n \, ds \quad , \tag{C.42a}$$

$$Z_{mn}^{EM} = -\iint_n \underline{H}_m^J \cdot \left(\underline{F}_n \times \hat{n}_T\right) ds \quad , \tag{C.42b}$$

$$Z_{mn}^{ME} = -\iint_n \underline{E}_m^M \cdot \underline{F}_n \, ds \quad , \tag{C.42c}$$

$$Z_{mn}^{MM} = \iint_n \underline{H}_m^M \cdot (\underline{F}_n \times \hat{n}_T)\, ds \quad , \tag{C.42d}$$

$$V_m^J = \iiint_v (\underline{J}_i \cdot \underline{E}_m^J - \underline{M}_i \cdot \underline{H}_m^J)\, dv \quad , \tag{C.42e}$$

$$V_m^M = \iiint_v (\underline{J}_i \cdot \underline{E}_m^M - \underline{M}_i \cdot \underline{H}_m^M)\, dv \quad . \tag{C.42f}$$

The integrations in Equations (C.42a-C.42d) are over the surface of the n^{th} expansion mode located on S_T. $(\underline{E}_m^J, \underline{H}_m^J)$ and $(\underline{E}_m^M, \underline{H}_m^M)$ are the free space fields of the m^{th} electric and magnetic test modes, respectively. Since the expansion and test modes used in this solution are identical (except for a shift of t/2), the method is essentially a Galerkin solution, and each of the matrices $[Z^{EE}]$ and $[Z^{MM}]$ are symmetric. Also $[Z^{EM}] = -[Z^{ME}]^T$.

A typical rectangular plate is shown in Figure C-4. Two orthgonal and overlapping sets of surface-patch modes cover the surface of the plate forming a two-dimensional vector surface density which could be used to represent $\underline{J}_S$, $\underline{J}_D$, $\underline{M}_S$, or $\underline{M}_D$. The normal components of $\underline{J}_S$ and $\underline{M}_D$ must vanish at a plate edge, however, the normal components of $\underline{J}_D$ and $\underline{M}_S$ do not. Thus, we include a series of edge modes, consisting of a single monopole with terminals at the plate edge. This allows for a non-zero normal component of current at the plate edge. The plate in Figure C-4 is made up of ten monopole edge modes and seven dipole interior modes. The monopole edge modes will be identically zero for $\underline{J}_S$ and $\underline{M}_D$, but not for $\underline{J}_D$ and $\underline{M}_S$.

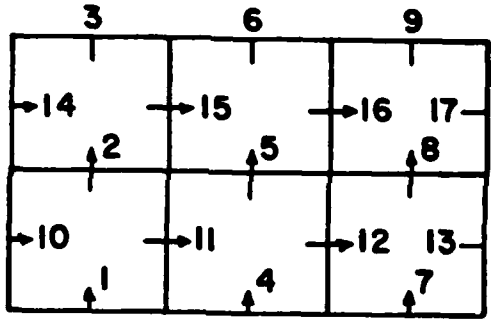

Figure C-4. Surface patch dipole mode layout for a flat plate.

5. Numerical Results

In this section we will present numerical results for electromagnetic scattering by material plates. Our results, computed using Equations (C.41) and (C.42) will be compared with measurements.

Figure C-5 shows the radar cross section (RCS) versus angle of incidence for a 0.813λ square by 0.051λ thick penetrable dielectric plate with relative dielectric constant, $\varepsilon_r = \varepsilon/\varepsilon_0 = 4$. Both TE and TM polarizations are shown and compared with measurements by Thal and Finger [18]. The agreement is seen to be good near broadside, however, it worsens as one approaches grazing. This is to be expected, since the surface impedance relationships were evaluated for a normally incident wave. Also shown in Figure C-5 is the RCS computed by the impedance sheet approximation of Equation (C.35). The sheet impedance approximation produces a less accurate result since it requires $|\gamma t| \ll 1$, while in this case $|\gamma t| = 0.64$. Our experience indicates that $|\gamma t|$ should be less than about 0.2 to use the impedance sheet approximation.

The insert in Figure C-6 shows a 1.5λ square perfectly conducting plate coated on one side by a narrow band dielectric/ferrite absorber with $\varepsilon_r = 7.8 - j1.6$, $\mu_r = 1.5 - j0.7$, and thickness 0.065λ. This is an example of an impenetrable plate with asymmetric surface impedance relationships. Figure C-6 shows the RCS of this plate evaluated with

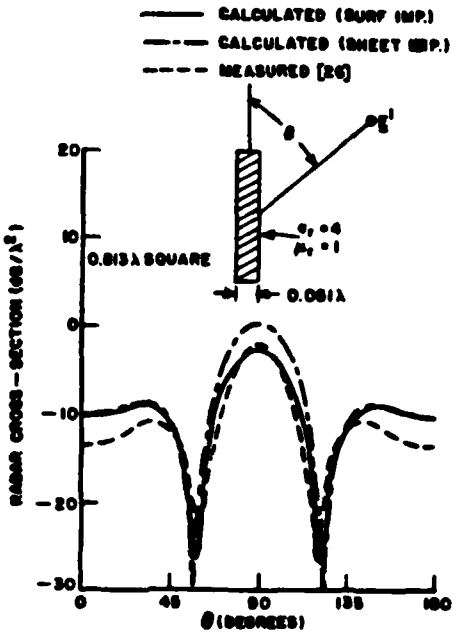

(a)

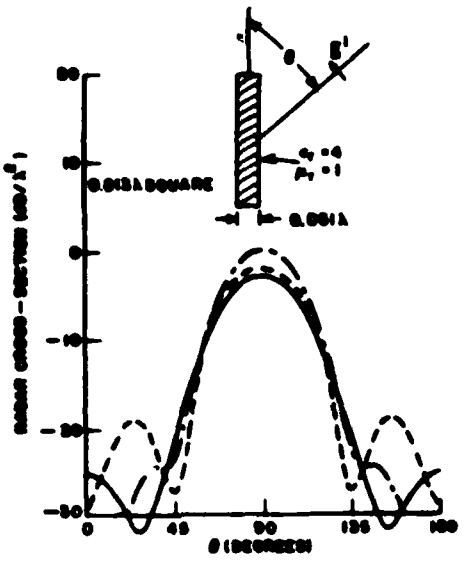

(b)

Figure C-5. (a) TE radar cross-section of a square dielectric plate.
(b) TM radar cross-section of a square dielectric plate.

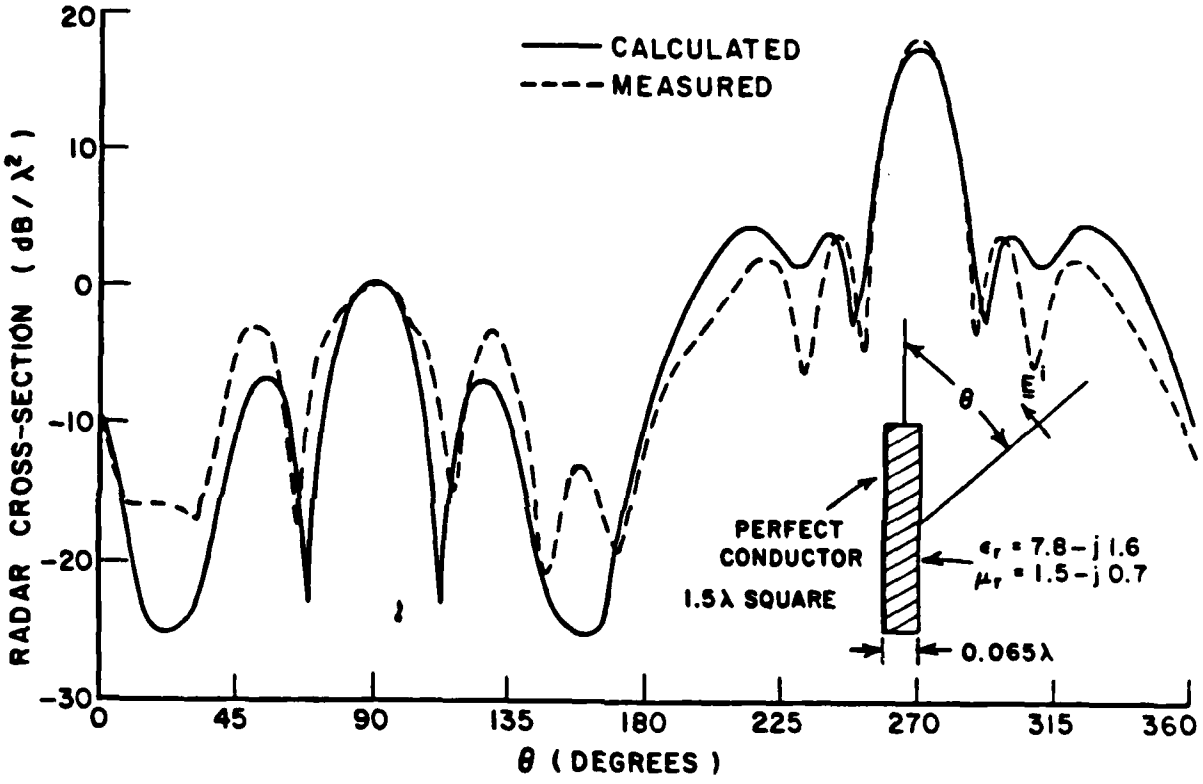

Figure C-6. Radar cross-section of a coated, perfectly conducting plate.

the surface impedance relationships of Equation (C.37), and compared with measurements. Note that the theory correctly predicts about a 20 dB drop in RCS when the incident field is broadside to the absorber, rather than the perfect conductor.

Figure C-7 shows the RCS at broadside for a fiberglass strip dipole of width 0.1λ, thickness 0.032λ, and $\varepsilon_r=4.8$ versus the dipole length L. Our compuration is slightly below the previous computations (based upon the more exact equivalent volume current representation) and measurements of Richmond [19]. Since the surface impedance approximation is felt to be most accurate away from corners and edges, the degree of error in Figure 9 is probably less than one would expect, considering that it is being applied to an extremely small plate.

Figure C-8 shows the RCS at broadside for an aluminum strip dipole of width 0.0056λ, conductivity 35 megamho/meter (i.e., skin depth $\delta = 1.03 \times 10^{-5}$) versus the dipole length L. Curves are shown for thicknesses of $t = \delta/1000$, $\delta/100$ and $\delta/10$, and δ. The agreement between our results and the more exact results of Richmond [19] is seen to be good, especially for the larger t values.

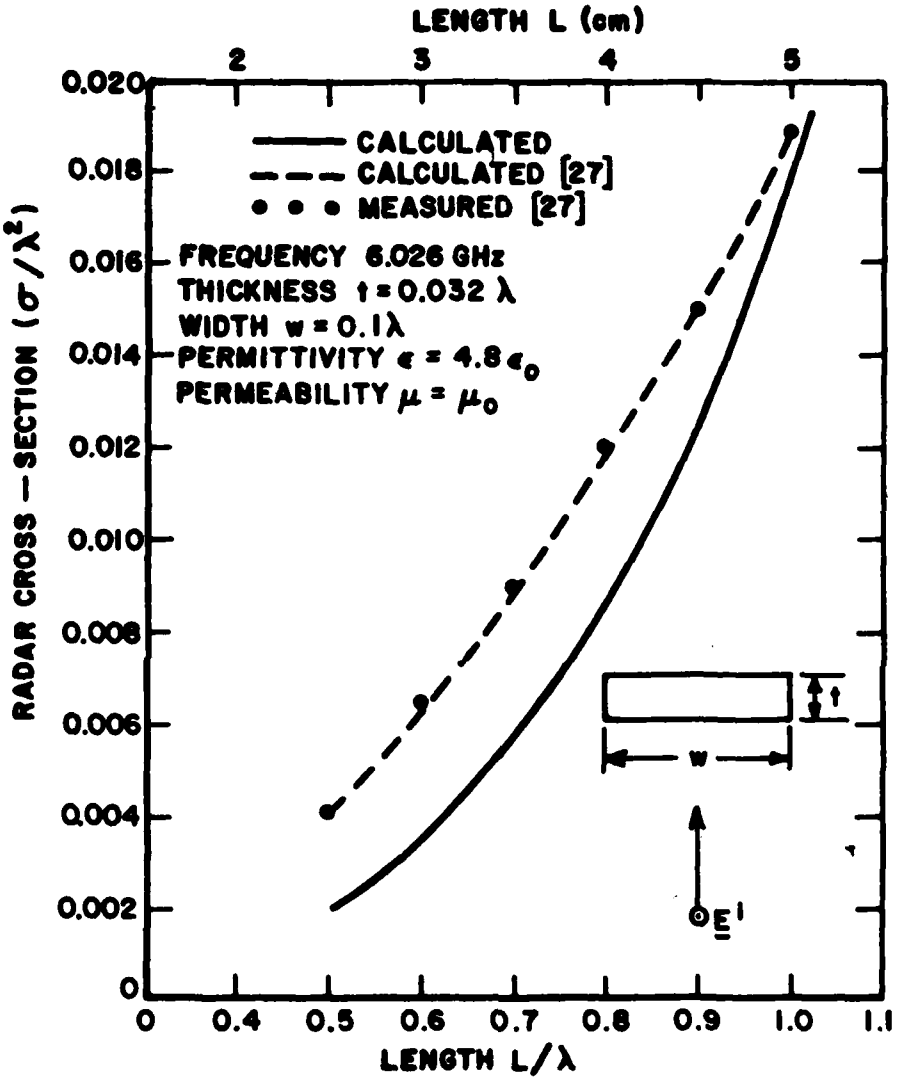

Figure C-7. Radar cross-section of a rectangular fiberglass strip.

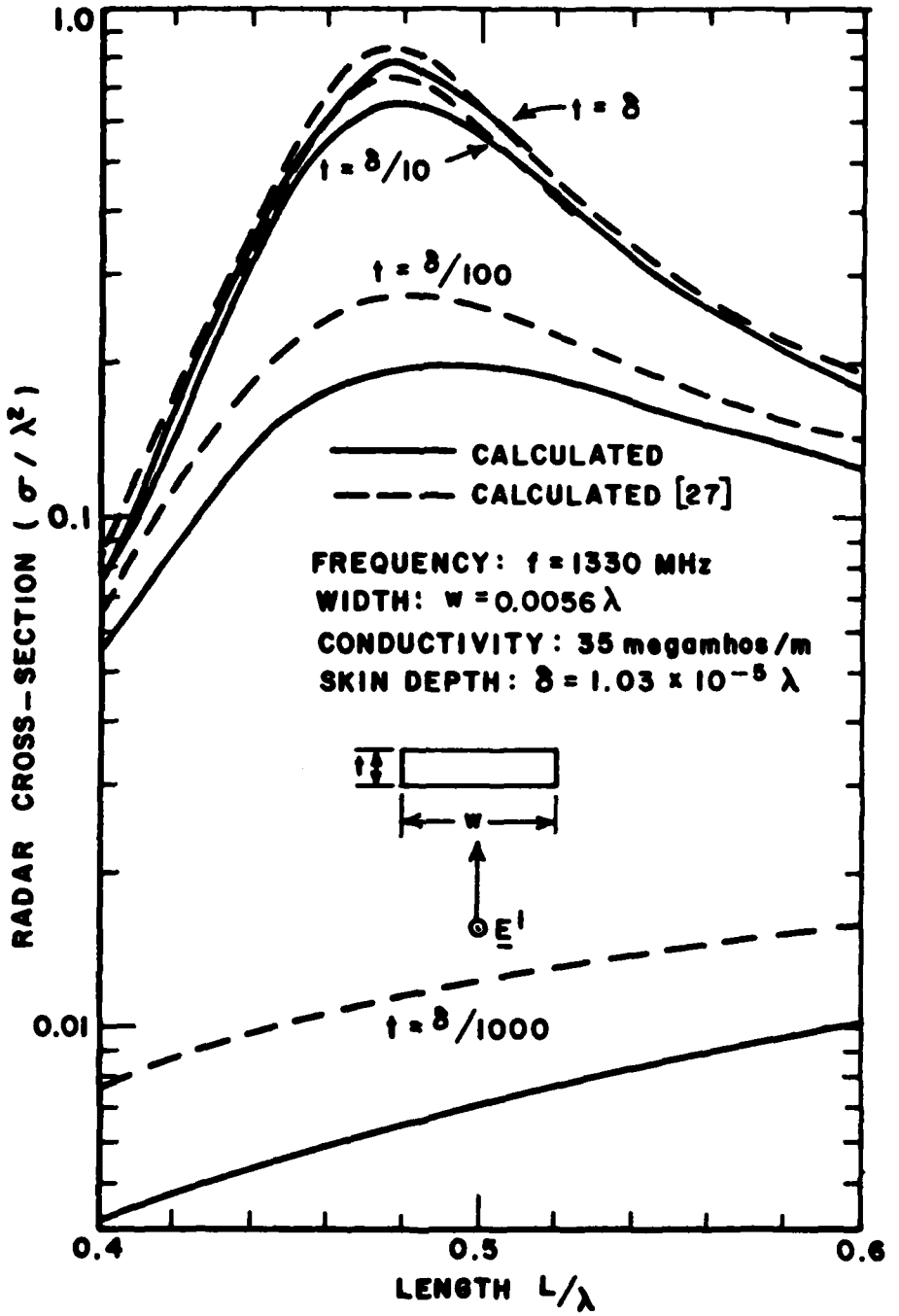

Figure C-8. Radar cross-section of rectangular aluminum strips.

6. Summary

An integral equation formulation for the electromagnetic scattering from a thin material plate has been presented. The material plate is viewed as an open surface, in order that the solution appear as an extension or modification of that for perfectly conducting plates. Solutions for the sum and difference electric and magnetic equivalent surface currents are obtained in the form of four coupled integral equations. By using the abc or surface impedance relationships two of the four integral equations are eliminated. The surface impedance relationships are shown to be the two-port impedance parameters of a simple transmission line model. By including the off-diagonal terms in the two-port impedance matrix, penetrable as well as impenetrable plates can be treated. Several special cases of the two coupled integral equations are investigated, and it is shown that for electrically very thin plates, the results simplify to a single equation equivalent to the impedance sheet approximations used by Harrington [15] and Senior [16]. The equations were solved by the method of moments, and accurate results were obtained. Future work in this area should include solutions for non-planar geometries, and the intersection of a perfectly-conducting and a material plate.

REFERENCES

[1] E.H. Newman and D.M. Pozar, "Electromagnetic Modeling of Composite Wire and Surface Geometries", IEEE Trans. on Antennas and Propagation, Vol. AP-26, No. 6, November 1978, pp. 784-89.

[2] E.H. Newman and D.M. Pozar, "Considerations for Efficient Wire/Surface Modeling", IEEE Trans. on Antennas and Propagation, Vol. AP-28, No. 1, January 1980, 121-125.

[3] D.M. Pozar and E.H. Newman, "Near Fields of a Vector Electric Line Source Near the Edge of a Wedge", Radio Science, Vol. 14, No. 3, May/June 1979.

[4] E.H. Newman and D.M. Pozar, "Analysis of a Monopole Mounted Near or at the Edge of a Half-Plane", IEEE Trans. on Antennas and Propagation, Vol. AP-29, May 1981, pp. 488-496.

[5] E.H. Newman and D.M. Pozar, "Analysis of a Monopole Mounted Near an Edge or a Vertex", IEEE Trans. on Antennas and Propagation, Vol. AP-30, May 1982, pp. 401-408.

[6] E.H. Newman and P. Tulyathan, "Moment Method Solution for Polygonal Plates", IEEE Trans. on Antennas and Propagation, Vol. AP-30, July 1982, pp. 588-593.

[7] E.H. Newman, "A User's Manual For: Electromagnetic Surface Patch Code (ESP)", Report 713402-1, July, 1981, The Ohio State University ElectroScience Laboratory, Department of Electrical Engineering; prepared under Contract DAAG29-81-K-0020 for the Department of the Army, U.S. Army Research Office, Research Triangle Park, North Carolina.

[8] E.H. Newman, P. Alexandropoulos and E.K. Walton, "Polygonal Plate Modeling of Realistic Structures", submitted for publication to IEEE Transactions on Antennas and Propagation.

[9] P. Alexandropoulos and E.H. Newman "A User's Manual for Electromagnetic Surface Patch (ESP) Code: Version II, Polygonal Plates and Wires", Technical Report 712692-3, September 1983, The Ohio State University ElectroScience Laboratory, Department of Electrical Engineering; prepared under Contract N00014-78-C-0049 for the Department of the Navy, Office of naval Research, Arlington, Virginia 22217.

[10] Y. Chang and R.F. Harrington, "A Surface Formulation for Characteristic Modes of Material Bodies", IEEE Trans. on Antennas and Propagation, Vol. AP-25, pp. 789-795, November 1977.

[11] V.H. Rumsey, "Reaction Concept in Electromagnetic Theory", Physical Review, Vol. 94, pp. 1483-1491, June 1954.

[12] J.A. Stratton, Electromagnetic Theory, McGraw-Hill, New York, pp. 511-513, 1941.

[13] T.B.A. Senior, "Approximate Boundary Conditions", IEEE Trans. of Antennas and Propagation, Vol. AP-29, pp. 826-829, September 1981.

[14] E.H. Newman and M.R. Schrote, "On the Current Distribution for Open Surfaces", IEEE Trans. on Antennas and Propagation, Vol. AP-31, May 1983.

[15] R.F. Harrington and J.R. Mautz, "An Impedance Sheet Approximation for Thin Dielectric Shells", IEEE Trans. on Antennas and Propagation, Vol. AP-23, pp. 531-534, July 1975.

[16] T.B.A. Senior, "Backscattering from Resistive Strips", IEEE Trans. on Antennas and Propagation, Vol. AP-27, pp. 808-813, November 1979.

[17] R.F. Harrington, Field Computations by Moment Methods, New York: MacMillan, 1968.

[18] H.L. Thal and J.F. Finger, "Scattering by Dielectric Containers", IEEE Trans. on Antennas and Propagation, Vol. AP-18, pp. 709-711, September 1970.

[19] J.H. Richmond, "Scattering by Dielectric and Conducting Dipoles with Circular and Rectangular Cross Sections", Report 3754-2, April 1974, The Ohio State University ElectroScience Laboratory, Department of Electrical Engineering; prepared under Contract No. N00140-74-C-6017 for the Naval Regional Procurement Office.

[20] E.H. Newman and M.R. Schrote, "An Open surface Integral Formulation for the Radiation and Scattering from a Material Plate", accepted for publication IEEE Transactions on Antennas and Propagation.

[21] M.R. Schrote, "An Open Surface Integral Formulation for Electromagnetic Scattering by a Material Plate", Ph.D. Dissertation, 1983, The Ohio State University, Department of Electrical Engineering.

D. Scattering by Absorber Geometries

Researchers: J.H. Richmond, Professor (Phone: (614) 422-7601)

The increased use of materials including absorbers on aerospace vehicles leads to requirements for more efficient analytic treatment of such configurations. One such analysis was developed under another project [1]. The expansion of this technique requires a substantial basic research program to support the application of these materials. Thus this research is to be expanded on the Joint Services Program. The original results presented in [1] are outlined in the following pages.

Accomplishments

1. Introduction

An efficient moment-method solution (with only three equations and three unknowns) was developed for plane-wave scattering by a thin lossy dielectric strip with infinite length. We expanded the field in the dielectric region as the sum of three plane waves: the forced wave and two traveling surface waves. Galerkin's method was applied to determine the amplitudes of these waves and finally, the far-zone scattered field was determined by considering the electric polarization currents radiating in free space. This work is reported in reference [1].

2. Scattering by Ferrite and Ferrite-Coated Cylinders and Strips

Background

Although Richmond [2,3] published the first moment-method solutions for scattering by dielectric cylinders with arbitrary cross-sectional shape in 1965, the technique has not yet been extended to ferrite cylinders. A dielectric cylinder is modeled with electric polarization currents, while a ferrite cylinder requires magnetic (as well as electric) polarization currents.

In 1973, Richmond [4] developed a user-oriented moment method for scattering by a perfectly conducting polygon cylinder. Later, Wang [5] extended the theory and computer program to include a thin dielectric coating on the polygon cylinder. While promising, Wang's results might be improved by including surface waves in the analysis.

In the area of RCS control, Professor Leon Peters has suggested that a thin ferrite coating may offer unique properties that cannot be duplicated with a thin lossy dielectric coating. This idea has been reinforced by the numerical results of Hill [6] for the propagation constant of a surface wave on a thin lossy ferrite coating.

To take advantage of these unique properties, we require an analysis of scattering by a thin lossy ferrite slab, or a conducting strip with a thin ferrite coating. An analysis for the lossless case has been developed recently by Burnside and Burgener [7] with the GTD format. Their results agree closely with moment method calculations

except for those situations where surface wave effects are dominant. The surface waves are not included in their analysis.

As discussed in an earlier section, Pathak and Rojas-Teran have applied the Wiener-Hopf technique to the thin dielectric half-plane. They have obtained excellent results, except for difficulties in the vicinity of grazing incidence.

Richmond [1] has developed an efficient moment-method solution (with only three equations and three unknowns) for plane-wave scattering by a thin lossy dielectric strip (see Figure D-1) with the incident electric field vector parallel with the edges of the strip as in Figure D-2. The electric field intensity in the dielectric region was expressed as the sum of three traveling waves as follows:

$$E_z(x,y) = C_1 e^{f_1 x} \cosh(g_1 y) + C_2 e^{fx} \cosh(gy) + C_3 e^{-fx} \cosh(gy) \ .$$

The first term represents the "forced wave", or the field induced in an infinitely-wide dielectric slab. The last two terms represent surface waves traveling in opposite directions across the thin dielectric strip. Galerkin's method is employed to determine the constants C_1, C_2 and C_3. Finally, the far-zone scattered field is calculated by considering the polarization currents radiating in free space. Figure D-3 illustrates the electric field distribution induced in a thin dielectric strip by a plane wave with grazing incidence. The results obtained with the new method (plane-wave expansion) show excellent agreement with those from the old method (pulse bases) which involved a system of 200 simultaneous linear equations.

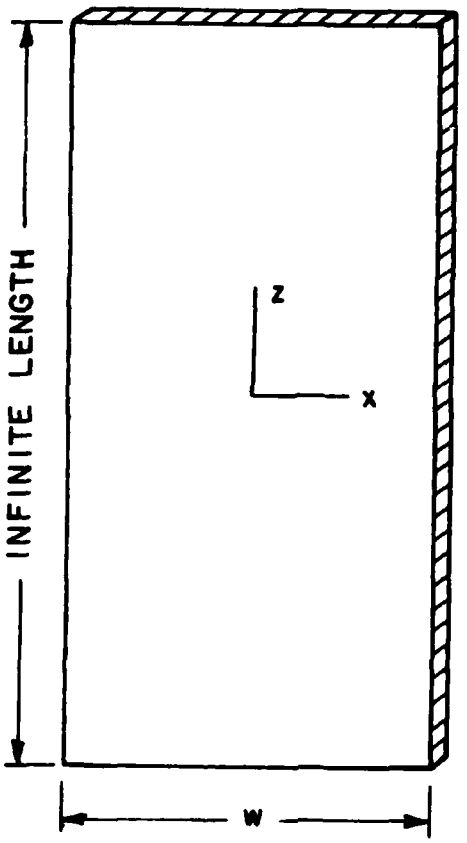

Figure D-1. A dielectric strip and the coordinate system.

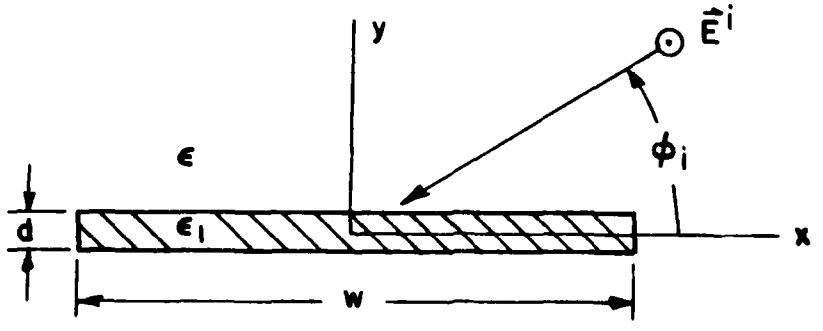

Figure D-2. Cross-sectional view of thin dielectric strip with incident plane wave.

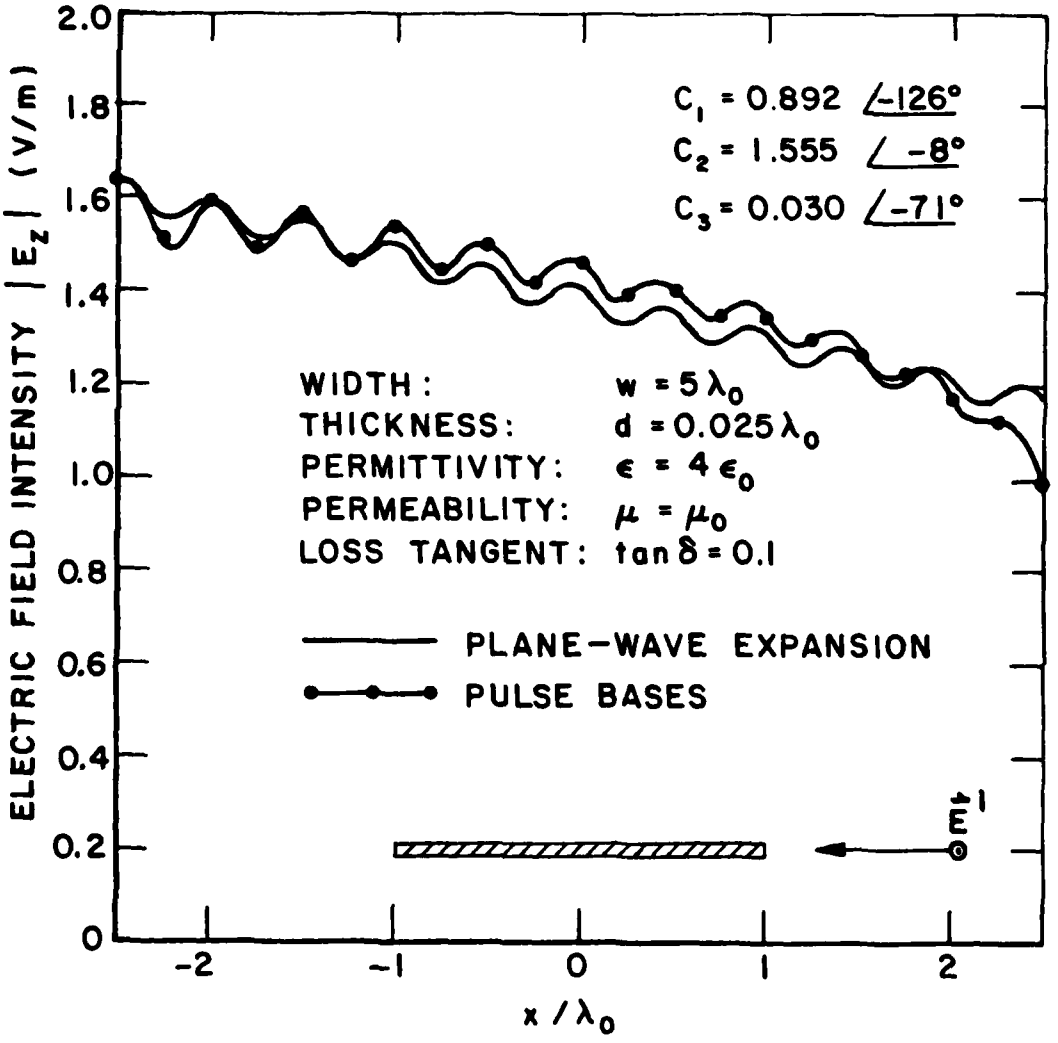

Figure D-3. Electric field distribution induced in thin dielectric strip by plane wave with grazing incidence.

Future Research

We propose to investigate scattering by thin dielectric strips with the aid of moment methods and plane wave basis functions. Having already demonstrated the technique with the electric field parallel to the edges of the strip, we propose to extend it to the following situations:

a. thin dielectric strip with the other polarization

b. thin ferrite strip

c. perfectly conducting strip with thin ferrite coating

d. perfectly conducting polygon cylinder with thin ferrite coating.

In each phase of this investigation, the results calculated by the new method will have to be tested against experimental measurements or independent calculations. Since measurements or independent data are not available in most cases, alternative formulations and programs will have to be developed for test purposes. This in itself will represent a substantial effort and a very useful product.

REFERENCES

[1] J.H. Richmond, "Scattering by Thin Dielectric Strips", Technical Report 711930-7, August 1983, The Ohio State University ElectroScience Laboratory, Department of Electrical Engineering; prepared under Grant NSG 1613 for the National Aeronautics and Space Administration, Langley Research Center, Hampton, Virginia.

[2] J.H. Richmond, "Scattering by a Dielectric Cylinder of Arbitrary Cross Section Shape", IEEE Trans. on Antennas and Propagation, Vol. AP-13, May 1965, pp. 334-341.

[3] J.H. Richmond, "TE-Wave Scattering by a Dielectric Cylinder of Arbitrary Cross-Section Shape", IEEE Transactions on Antennas and Propagation, Vol. AP-14, July 1966, pp. 460-464.

[4] J.H. Richmond, "An Integral-Equation Solution for TE Radiation and Scattering from Conducting Cylinders", Report 2902-7, October 1972, The Ohio State University ElectroScience Laboratory, Department of Electrical Engineering; prepared under Grant No. NGL 36-008-138 for National Aeronautics and Space Administration, Washington, D.C.

[5] N. Wang, "Reaction Formulation for Radiation and Scattering from Plates, Corner Reflectors and Dielectric-Coated Cylinders", Ph.D. Dissertation, The Ohio State University, Spring 1974.

[6] Roger A. Hill, "Propagation Characteristics of Parallel Polarized Surface Waves on a Grounded Lossy Dielectric Slab", Masters Thesis, Spring 1983, The Ohio State University, Columbus, Ohio.

[7] W.D. Burnside and K.W. Burgener, "High Frequency Scattering by a Thin Lossless Dielectric Slab", IEEE Transactions on Antennas and Propagation, Vol. AP-31, January 1983, pp. 104-110.

E. Time Domain Studies

Researchers: D.L. Moffatt, Associate Professor (Phone: (614) 422-5749)

E.M. Kennaugh, Professor Emeritus (Deceased)

Chun-Yue Lai, Graduate Research Associate

Ted C. Lee, Graduate Research Associate

Introduction

The optimum exploitation of the interaction of electromagnetic waves and material objects can only be achieved with a clear understanding of how the physical properties of the object (size, shape and composition) in situ are related to scattered or radiated fields. For whatever purpose, e.g., target identification, radar cross section control, specific radiation waveforms, etc., a basic understanding of the electromagnetic interactions is vital. Our research has shown that a time domain approach provides ideal insight into how such an understanding can be realized. Increasingly, solutions to radiation or scattering problems are sought over broad bandwidths. The canonical response waveforms (response waveforms to impulse, step or ramp excitation) are ideally suited for this purpose because the response to an arbitrary excitation is simply obtained using convolution.

Much of our recent research has stressed the complex natural resonances of a scatterer or radiator, that is, those complex frequencies which ellicit singularities in the transfer function relating excitation and response in a linear system. For distributed parameter systems such as electromagnetic scatterers and radiators, the response to an aperiodic excitation consists of, first, a forced response as the wavefront moves across the body and then a free or natural response as the wavefront moves beyond the body. For fixed time-independent residues, only the free response can be described in terms of the natural oscillation frequencies of the object.

The general goals of our research include:

1) Prediction of scattered and radiated waveforms from objects of increasing complexity for point or plane wave electromagnetic sources with arbitrary waveforms.

2) Investigation of target-dependent excitation waveforms and/or signal processing algorithms to identify and optimize electromagnetic response from specific targets.

3) Determination of the effects of system bandwidth and noise on recommended techniques for detection and identification of radar targets.

A very real measure of the significance of the basic research performed on a program is the transfer of the developed techniques and methods to other less basic programs. The extraction of the complex natural resonances of a target from measured multifrequency scattering data using rational function approximants and the recognition of a target using such resonances in prediction-correlation processing (both concepts developed on this program) are now being extensively tested on another program.* This other program has resulted in a unique new broadband compact range reflectivity measurement facility capable of rapidly measuring the complex polarization scattering matrix of model targets over a 12:1 band (present) with planned extensions to 30:1 band (future) and possibly a 100:1 band (ultimately). This other program (ESL Project 714190) has as one major goal the establishment of prediction-correlation target recognition statistics using complex natural resonances and a realistic data base. Accordingly, no future research on routine extraction of complex natural resonances from measured scattering data nor on application of prediction-correlation processing for target recognition is anticipated on this program. Our research is summarized in the following paragraphs. Written publications and oral presentations are listed at the end of this section. We stress here the fact that we have been extremely active in disseminating our results to the research community.

---

*Project 714190, Contract # N00014-82-K-0037 between The Ohio State University Research Foundation and the Department of the Navy, Office of Naval Research, Arlington, Virginia.

Accomplishments

1. Complex Natural Resonances and Geometrical Procedures

The K-pulse provides a means of relating surface waves on a structure to the complex natural resonances of the structure [1]. For solid structures such as spheres, prolate spheroids, circular and elliptical cylinders, etc., the method has been found to be limited only by the geometrical theory of diffraction (GTD) estimate of the attenuation and phase shift of surface rays on the structure [1,2]. That is, the first one or two lowest frequency (natural oscillations) natural resonances predicted are incorrect because the estimates are asymptotic. Higher frequency "pole" estimates are excellent for spheres and circular cylinders and good to adequate for other classical geometries. Therefore, for sufficiently simple solid target geometries a method for obtaining estimates of the complex natural resonances has been delineated. The method itself (circumferential paths) also refutes the idea that the complex natural resonances are simply a mathematical tool and unrelated to the target's physical properties.

For wire structures, results were somewhat less satisfactory except for cases where the wire was very thin (length to diameter ratios (L/D) greater than 1000)[2]. It has been found that for "fatter" wires, improved estimates of the attenuation and excess phase shift of current on the wire are now available [3]. For a straight wire, these formulas yield pole locations with improved estimates of the damping but somewhat

poorer estimates of the oscillation frequencies. By properly combining the new and old analytical estimates of attenuation and phase shift, good estimates of the pole locations can now be obtained for both "fat" and "thin" wires. These results are presently being used to modify the analytical estimates of the pole locations of bent wires, curved wire segments, loops and other wire geometries [2]. The delayed technical report [4] on these procedures is now being modified and the report should be available by early 1984.

Related questions concern the frequency-dependent current reflection, transmission and radiation characteristics at wire junctions and the radiative coupling at end points of the wires. The improved estimate of current attenuation and excess phase shift will permit a brief reeximination of these parameters but it is not intended to further delay the technical report on these topics.

2. Complex Natural Resonances Via Rational Function Approximants

A definitive report on the use of rational function approximants to extract complex natural resonances of a target from measured multiple frequency scattering data is in process*[5]. It has been found that a combination of filtering, windowing, averaging and judicious selection of test frequencies (resonance region) permits a consistent set of

---

*The processing methods developed were completed on this contract. Application of the methods and techniques to actual measured scattering data was done on the related contract (ESL Project 714190) mentioned earlier. Target recognition algorithms are being studied on the latter contract.

complex natural resonances (poles) to be extracted from measured scattering data. There are, however, several limitations. These limitations and some initial conclusions are listed below:

a) The measured data must have an integrated signal to noise ratio of at least 15.0 dB before consistent poles can be extracted. This assumes that the noise is additive. Multiplicative noise remains a moot question.

b) The limitation in a) suggests that in most situations the scattering data for estimating poles must be taken in a controlled environment. This means that target recognition algorithms should not use direct extraction of poles *from* full scale data. Fortunately, prediction-correlation target recognition does not extract poles directly and is therefore unaffected by this limitation.

c) The extracted pole set for a target, while clearly consistent, does not display precise excitation invariance. Therefore, as a practical matter a geometrically complex target will, for target recognition purposes, have to be considered as several targets, with a set of averaged poles related to a given span of aspects and/or polarizations.

d) The report in process also uses GTD estimates to obtain the creeping wave poles for a thin circular disk geometry. From the results, the K-pulse and response waveform for edge-on incidence for the disk are presented.

No further studies of processing techniques for extracting complex natural resonances from measured scattering or radiation data are anticipated on this contract. We shall, however, continue to explore geometrical and asymptotic procedures, particularly with regard to future K-pulse studies.

3. Transient Current Density Waveforms on a Conducting Sphere

A technical report presenting the transient current waveforms induced on a conducting sphere when illuminated by a plane electromagnetic wave with impulsive time dependence has been published [6]. On the illuminated side of the sphere, the inadequacies of the physical optics approximation in both the E and H planes are illustrated and a simple correction form is suggested. On the shadowed side of the sphere, the changing form of the current density waveforms is discussed and demonstrated. This report demonstrates that first order corrections of the physical optics backscatter approximation are possible even for an object which does not have a depolarized scattering component. This report, with some additional references to research on time domain scattering and radiation performed at the ElectroScience Laboratory, will also be published in a book of NATO Conference Proceedings [7].

4. Cavity Structures

Research on the electromagnetic scattering from finite and open circular waveguide structures is continuing. The ultimate goal is a realistic modeling of the intake and exhaust cavities of jet engine configurations. At the moment, particular emphasis is on the complex natural resonances of such structures and on the K-pulses to be constructed from such complex natural resonances. It should be emphasized that some portions of the research on cavity scattering have been done on other projects.*

While completely consistent results for all aspects of the problem have not yet been obtained, some preliminary results have proved publishable. A paper [8] which demonstrates a technique for using rational function approximations to combine low frequency and high frequency scattering estimates has been accepted for publication by WAVE MOTION. In this case, the low frequency results come from the Wiener-Hopf solution for an open circular waveguide [9] and the high frequency estimates from the asymptotic unified theory of diffraction (UTD) [10]. The targets in this case are finite circular waveguides with various internal (transverse to guide axis) loads. The rational function approximations permit a smooth spanning and transition of the

---

*Project 714190, Contract # N00014-82-K-0037 between The Ohio State University Research Foundation and the Department of the Navy, Office of Naval Research, Arlington, Virginia and project 712661, Contract # F19628-80-C-0056 between The Ohio State University Research Foundation and the Department of the Air Force, Electronic Systems Division, Air Force Systems Command, Hanscom Air Force Base, Massachusetts.

spectral range between the lowest cut off frequency for the waveguide (TE_{11} mode) and a higher frequency where the UTD results are apparently valid. Another publication [11] stresses a rational function approximant for extracting complex natural resonances from measured or calculated multiple frequency scattering data. Included here also are estimates of certain of the complex natural resonances of finite and open circular waveguides.

The problem of a finite circular waveguide loaded with a shorted conical structure is currently being studied using a method of moments program for rotationally symmetric scatterers. At present, a portion of the scattered field spectrum is being generated and the poles extracted using a rational function fit approximation. A numerical search procedure will ultimately be added. The new compact range reflectivity facility mentioned in the introduction will materially aid in providing verification data for new cavity scattering results obtained during the next interim.

5. K-pulse Studies

The K-pulse waveform as intepreted in the time domain is a unique waveform of minimal duration which, as input to a specified linear system (scatterer or radiator) produces response waveforms of finite duration at all points of interest. Derivations of the input waveform would also possess this property, thus uniqueness requires that the highest order discontinuity be of minimal order as well. It must be recognized that while it would appear that any linear combination of

derivatives of finite orders would appear to satisfy the minimal duration test, this process also would introduce new zeros. The further condition that the K-pulse transform zeros match only the system poles must be impressed. The K-pulse for a distributed parameter system can be similarly modified to be the K-pulse for this distributed parameter system and a specified lumped content system without further lengthening.

In a recent paper [12], Pearson purports to show that while the singularity expansion is an ill-suited means for modeling a scatterer's response to a time-limited excitation (since it cannot be made practically useful through truncation), one is mistaken to conclude that it is incorrect or incomplete through this fact. We disagree with this conclusion primarily because of his simplified definition for the Laplace transform of a K-pulse. It is unlikely that this disagreement will be resolved in the near future. We note, however, that two papers [13,14] to appear in the near future both demonstrate that there is a nonzero region in the space-time domain where the scattered field cannot be expressed in terms of natural-mode contributions only and where the conventional SEM representation does not hold. One must recognize however, that this result is for a linearly polarized electromagnetic pulse of finite duration incident on a homogeneous or inhomogeneous lossy dielectric slab. Thus, here the target is neither finite nor perfectly conducting.

The question raised by Kennaugh [1] regarding the completeness of the SEM representation has no bearing on the future usefulness of the K-pulse. It remains a unique and powerful tool in identification and imaging and also appears to be useful in antenna studies.* We have only recently resumed research on the K-pulse as unpublished notes and memorandums by Professor Kennaugh became available. First priority is being given to completion of the report "K-pulse for Transmission Lines".

Recent Publications Under Time Domain Studies

D.L. Moffatt, C-Y Lai and T.C. Lee, "Time Domain Electromagnetic Scattering by Open-Ended Circular Waveguide and Related Structure", accepted for publication in WAVE MOTION, October, 1983.

D.L. Moffatt, J.D. Young, A.A. Ksienski, E. Lin and C. Rhoads, "Transient Response Characteristics in Identification and Imaging" in Microwave Imaging Techniques edited by C.K. Chan and T.L. Lim, a series on "Benchmark Papers in Electrical Engineering and Computer Science", edited by John B. Thomas, Hutchinson Ross Publishing Company, Stroudsburg, Pennsylvania, 1984.

---

*See JSEP proposal, Time Domain Studies, for 1983-1984, pp. 77-90.

D.L. Moffatt and T.C. Lee, "Time-Dependent Radar Target Signatures, Synthesis and Detection of Electromagnetic Authenticity Features", in Proceedings of NATO Advanced Research Workshop on Inverse Methods in Electromagnetic Imaging, edited by W.M. Boerner, D. Reidel Publishing Company, Dordrecht, Holland, 1984.

E.M. Kennaugh and D.L. Moffatt, "Transient Current Density Waveforms on a Spherical Scatterer", in Proceedings of NATO Advanced Research Workshop on Inverse Methods in Electromagnetic Imaging, edited by W.M. Boerner, D. Reidel Publishing Company, Dordrecht, Holland, 1984.

T.W. Johnson and D.L. Moffatt, "Electromagnetic Scattering by an Open Circular Waveguide", Radio Science, Vol. 17, No. 6, pp. 1547-1556, November-December, 1982.

D.L. Moffatt and C.M. Rhoads, "Radar Identification of Naval Vessels", IEEE Transactions on Aerospace and Electronic Systems, Vol. AES-18, No. 2, March 1982.

E.M. Kennaugh and D.L. Moffatt, Comments on "Impulse Response of a Conducting Sphere Based on Singularity Expansion Method", Proceedings of the IEEE, Vol. 70, No. 3, March 1982.

L.C. Chan, D.L. Moffatt, and L. Peters, Jr., "Subsurface Radar Target Imaging Estimates", IEEE Trans. on Antennas and Propagation, Vol. AP-29, No. 2, March 1981.

E.M. Kennaugh, "Polarization Dependence of RCS - a Geometrical Interpretation", IEEE Trans. on Antennas and Propagation, Vol. AP-29, No. 2, March 1981.

L.C. Chan, D.L. Moffatt, and L. Peters, Jr., "Improved Performance of a Subsurface Radar Target Identification System Through Antenna Design", IEEE Trans. on Antennas and Propagation, Vol. AP-29, No. 2, March 1981. Invited.

E.M. Kennaugh, "Opening Remarks", IEEE Transactions on Antennas Propagation, Vol. AP-29, No. 2, March 1981.

D.L. Moffatt, J.D. Young, A.A. Ksienski, H.C. Lin, and C.M. Rhoads, "Transient Response Characteristics in Identification and Imaging", IEEE Trans. on Antennas and Propagation, Vol. AP-29, No. 2, March 1981, Invited.

E.M. Kennaugh, "The K-pulse Concept", IEEE Trans. on Antennas and Propagation, Vol. AP-29, No. 2, March 1981.

D.L. Moffatt, "Ramp Response Radar Imagery Spectral Content", IEEE Trans. on Antennas and Propagation, Vol. AP-29, No. 2, March 1981.

D.B. Hodge, "Scattering by Circular Metallic Disc", IEEE Transactions on Antennas and Propagation, Vol. AP-28, No. 5, September 1980.

L.C. Chan, D.L. Moffatt, and L. Peters, Jr., "Estimation of the Complex Natural Resonances of a Class of Subsurface Targets", in Acoustical, Electromagnetic and Elastic Wave Scattering - Focus on the T-matrix Approach, edited by V.K. and V.V. Varadan, Pergamon Press, 1980.

L.C. Chan, D.L. Moffatt, and L. Peters, Jr., "A Characterization of Subsurface Radar Targets", Proc. IEEE, Vol. 17, No. 7, July 1979.

Recent Oral Presentations Under Time Domain Studies

D.L. Moffatt and T.C. Lee, "Time-Dependent Radar Target Signatures Synthesis and Detection of Electromagntics Authenticity Features", presented at NATO Advanced Research Workshop on Inverse Methods in Electromagnetic Imaging, Bad Windsheim, Federal Republic of Germany, September 1983. Invited.

D.L. Moffatt, "Contributions by Professor E.M. Kennaugh to High Resolution Broadband Radar Polarimetry", presented at the Second Workshop on Polarimetric Radar Technology, Huntsville, Alabama, May 1983. Invited.

D.L. Moffatt, N. Wang, C.Y. Lai and T.C. Lee, "Special Response Waveforms - Cavity and Related Structures", presented at "Workshop on Research Techniques in Wave Propagation and Scattering", The Ohio State University, October 18-October 21, 1982. Invited.

D.L. Moffatt, "Time Domain Electromagnetics - An Elementary Review", presented to the IEEE Local Chapter on Antennas and Propagation at Kharagpur, India on March 24, 1983. Invited.

E.M. Kennaugh and D.L. Moffatt, "Improved Response Waveforms for the Circular Disk", presented at the 1982 Joint International IEEE/ APS Symposium and National Radio Science Meeting, Albuquerque, New Mexico, May 1982.

D.L. Moffatt and Chun-Yue Lai, "Electromagnetic Scattering by Loaded Open Circular Waveguides", National Radio Science Meeting, University of Colorado, January 1982.

D.L. Moffatt and J.G. Bagby, "Approximate Characteristic Equations for Simple Structures", National Radio Science Meeting, University of Colorado, January 1982.

E.M. Kennaugh, "Canonical Electromagnetic Response Waveforms and Their Estimation", International Union of Radio Science, XXth General Assembly, Washington, D.C., August 1981.

T.W. Johnson and D.L. Moffatt, "Electromagnetic Scattering by Open Circular Waveguides", National Radio Science Meeting, Los Angeles, California, June 1981.

E.M. Kennaugh, "Prediction of Cavity and Natural Resonance Frequencies by GTD", International IEEE AP-S/USNC Symposium, Quebec, Canada, June 1980.

E.M. Kennaugh, "Resonances of Thin-Walled Penetrable Scatterers", International IEEE AP-S/USNC Symposium, Quebec, Canada, June 1980.

D.L. Moffatt and K.A. Shubert, "Pulse Response Waveforms of Aircraft", National Radio Science Meeting, Seattle, Washington, June 1979.

D.L. Moffatt and C.M. Rhoads, "An Update on Naval Vessel Identification", National Radio Science Meeting, Seattle, Washington, June 1979.

D.L. Moffatt, "A Chronological History of Radar Target Imagery at The Ohio State University", National Radio Science Meeting, Seattle, Washington, June 1979.

Recent Technical Reports Under Time Domain Studies

Joint Services Electronics Program Annual Report 710816-1, December 1978.

"The Calculation of Far Field Scattering by a Circular Metallic Disk", Report 710816-2, D.B. Hodge, February 1979.

"Electromagnetic Scattering by a Metallic Disk", Report 710816-3, D.P. Mithouard and D.B. Hodge, September 1979. Thesis.

Joint Services Electronics Program Annual Report 710816-6, December 1979.

"Electromagnetic Scattering by Open Circular Waveguides", Report 710816-9, T.W. Johnson and D.L. Moffatt, December 1980. Dissertation.

Joint Services Electronics Program Third Annual Report 710816-10, December 1980.

Joint Services Electronics Program Fourth Annaul Report 710816-11, December 1981.

"Transient Current Density Waveforms on a Spherical Scatterer", Report 710816-13, E.M. Kennaugh and D.L. Moffatt, October 1983.

Technical Reports in Preparation Under Time Domain Studies

E.M. Kennaugh, D.L. Moffatt and N. Wang, "K-pulse for Transmission Lines".

D.L. Moffatt, J.G. Bagby, and H.T. Kim, "A Geometrical Approach to Characteristic Equations".

T.C. Lee and D.L. Moffatt, "Approximate Methods for Obtaining the Complex Natural Electromagnetic Oscillations of an Object".

Ph.D. Dissertations Under time Domain Studies

T.C. Lee, 1983

T.W. Johnson, 1980

L.C. Chan, 1978

M.Sc. Thesis Under Time Domain Studies

J.G. Bagby, 1981.

REFERENCES

[1] Kennaugh, E.M., "The K-pulse Concept", IEEE Trans. on Antennas and Propagation, Vol. AP-29, No. 2, March 1981.

[2] Bagby, J.G., "Natural Electromagnetic Oscillations: A Geometrical Theory", M.Sc. Thesis, The Oho State University, August 1981.

[3] Hoorfar, A. and David C. Chang, "Analytical Determination of the Transient Response of a Thin-Wire Antenna Based Upon an SEM Representation", IEEE Trans. on Antennas and Propatation, Vol. AP-30, No. 6, November 1982.

[4] Moffatt, D.L., J.G. Bagby and H.T. Kim, "A Geometrical Approach to Characteristic Equations", Technical Report in preparation.

[5] Lee, T.C., "Approximate Methods for Obtaining the Complex Natural Electromagnetic Oscillations of an Object", Technical Report in preparation.

[6] Kennaugh, E.M. and D.L. Moffatt, "Transient Current Density Waveforms on a Perfectly Conducting Sphere", Technical Report 710816-13, October 1983, The Ohio State University ElectroScience Laboratory, Department of Electrical Engineering; prepared under contract N000114-78-C-0049 for the Department of the Navy, Office of Naval Research, Arlington, Virginia.

[7] Kennaugh, E.M. and D.L. Moffatt, "Transient Current Density Waveforms on a Perfectly Conducting Sphere", in Proceedings of NATO Advanced Research Workshop on Inverse Methods in Electromagnetic Imaging, Edited by W.M. Boerner, D. Reidel Publishing Company, Dordrecht, Holland, 1983.

[8] Moffatt, D.L., C-Y. Lai and T.C. Lee, "Time Domain Electromagnetic Scattering by Open-Ended Circular Waveguide and Related Structure", accepted for publication in WAVE MOTION, October 1983.

[9] Johnson, T.W. and D.L. Moffatt, "Electromagnetic Scattering by an Open Circular Waveguide", Radio Science, Vol. 17, No. 6, pp. 1547-1556, November-December, 1982.

[10] Huang, C.C., P.H. Pathak, C-Y. Lai and D.L. Moffatt, "Analysis of Electromagnetic Backscattering from an Inlet Cavity Configuration, Final Report 712661-4, October 1982, The Ohio State University ElectroScience Laboratory, Department of Electrical Engineering; prepared under Contract F19628-80-C-0056 for the Department of the Army, Electronic Systems Command (AFSC), Hanscom Air Force Base.

[11] Moffatt, D.L. and T.C. Lee, "Time-Dependent Radar Target Signatures, Synthesis and Detection of Electromagnetic Authenticity Features", in Proceedings of NATO Advanced Research Workshop on Inverse Methods in Electromagnetic Imaging, Edited by W.M. Boerner, D. Reidel Publishing Company, Dordrecht, Holland, 1983.

[12] Pearson, L. Wilson, "Present Thinking on the Use of the Singularity Expansion in Electromagnetic Scattering Computation", WAVE MOTION, 5 (1983), pp. 355-368.

[13] Tijhuis, Anton G. and Hans Blok, "SEM Approach to the Transient Scattering by an Inhomogeneous, Lossy Dielectric Slab; Part 1: The Homogeneous Case", WAVE MOTION 6 (1984).

[14] Tijhuis, Anton G. and Hans Blok, "SEM Approach to the Transient Scattering by an Inhomogeneous, Lossy Dielectric Slab; Part 2: The Inhomogeneous Case", to appear in WAVE MOTION.

F. Transient Signature Measurements of Radar Targets for Inverse Scattering Research

Researchers: J.D. Young, Research Scientist (Phone: (614) 422-6657)
E.K. Walton, Senior Research Associate
W. Leeper, Graduate Research Associate

Introduction

The objective of the effort is to assemble "complete" complex scattering cross section data on several canonical targets. The data are complete in the following respects:

1. Both amplitude and phase of the backscattered return are measured.
2. The data cover a 96:1 bandwidth.
3. The results are actual backscatter, i.e., precisely at 0° bistatic angle.
4. The backscatter is measured for three polarizations: vertical-vertical, horizontal-horizontal, vertical-horizontal.
5. The measurements were made at aspects of every 15° from 0° - 180°.
6. The vertical-horizontal (cross) polarized measurements were made at aspects out of the principal planes.

The complete target signature data for canonical targets is much more valuable when they are interpreted and scattering mechanisms are identified. The impulse response signature is being used as the vehicle for this study.

This section describes progress in several aspects of this study. The experimental system has been significantly improved, and its configuration is reviewed. New data have been collected, particularly on the ellipsoid and disk targets, and a few illustrative signatures are presented. The study of interpretation of scattering mechanisms is represented by a brief discussion of the ellipsoid features. Finally, a study of optimum approaches to sampling the signature data in frequency and aspect angle is summarized.

1. Measurement System

The system which has been used to acquire the data is shown in Figure F-1. This differs from the block diagram of prior measurement systems primarily in the use of a Scientific Atlanta compact antenna range reflector to obtain far-zone radar data for targets up to four feet in extent. To the manufacturers knowledge, this is the first system in the world to use their reflector for acquiring transient response signature data.

The system has been described in two oral papers [1,2] and a written paper which has been submitted to IEEE/APS [3]. The performance of this facility is an advance in the state of the art, and it is being directly copied by several other organizations. A portion of the

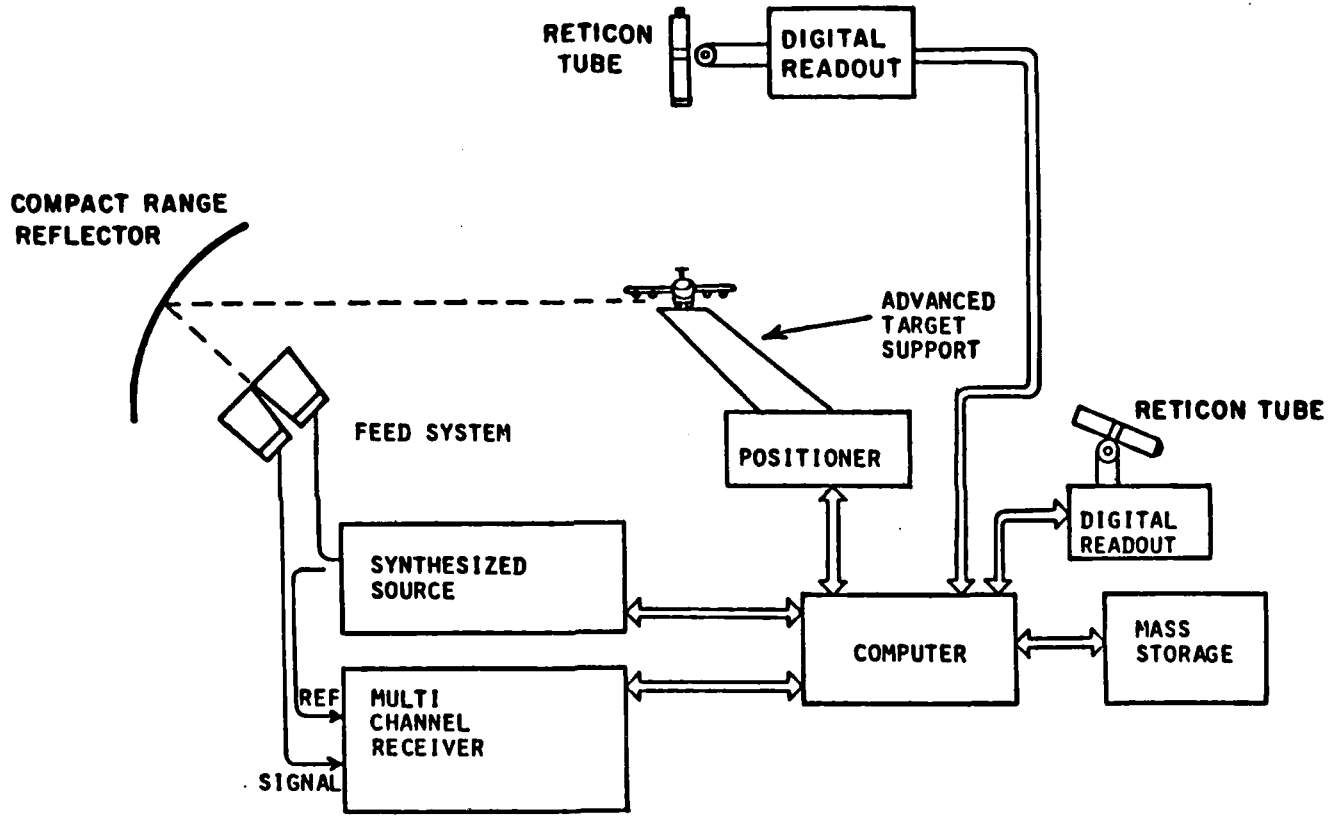

Figure F-1. Diagram of proposed advance target measurement.

signature effort was devoted to improvement of this range, with the result that at the close of this effort the system had an effective noise floor of approximately -50 dBsm from 1 to 12 GHz, and - 70 dBsm in the range of 8 to 12 GHz. Other JSEP research areas have contributed concepts which are being applied to enlarge the "sweet spot" area of this range and extend its usable frequency range to a final goal of 1 to 100 GHz.

For the new system, a comparison of measured and theoretical sphere response signatures covering a 48:1 frequency band are shown in Figures F-2 and F-3.

2. Target Signature Measurements

The two targets which received the most attention during the year were the 4:2:1 ellipsoid and the circular disk. The coverage of the frequency, polarization, and aspect angle coverage of the ellipsoid is particularly complete. It is summarized in Table F-1. The data base on the ellipsoid has been supplied to two other organizations at the present time, and is available to others. A report specifying the data base format for the data which are supplied on a floppy disk has been written [4].

A reference frame for discussion of aspect angle data on the ellipsoid is shown in Figure F-4. Figures F-5a through F-5d show approximate impulse response signatures for the ellipsoid at several look angles. Figure F-6a through F-6e shows cross-polarized impulse

TABLE F-1

DATA BASE SPECIFICATIONS FOR ELLIPSOID SCATTERING SIGNATURE MEASUREMENTS

(a)

1.5 ELLIPSOID

TILT	POL.	FLAT	EDGE-UP	TIP-UP
0°	V	2-12*	2-12*	2-12*
0°	H	2-12*	2-12*	2-12*
0°	X		1-12	
30°	X	1-12*	1-12*	
45°	V	1-4.5	1-6.3	
		4-12	6-12	
45°	H	1-4.5	1-4.5	
		4-12	4-12	
45°	X	1-12*	1-12*	
60°	X	1-12*	1-12*	

(b)

12.0 INCH ELLIPSOID

0°	H	6-6.3	
		6-12	
30°	V	6-12	
45°	V	1.0-6.3	1.3-6.3
		6-12	6-12
45°	H	1-6.3	1-6.3
		6-12	6-12
45°	X	1-6.3	1-6.3
		1-12*	6-12

NOTE:

1. All measurements at 15° aspect intervals.
2. TILT is the elevation of the major axis from horizontal.
3. FLAT means with the 2 axis horizontal.
4. EDGE-UP means with the 1 axis horizontal.
5. TIP-UP means with the 4 axis vertical.

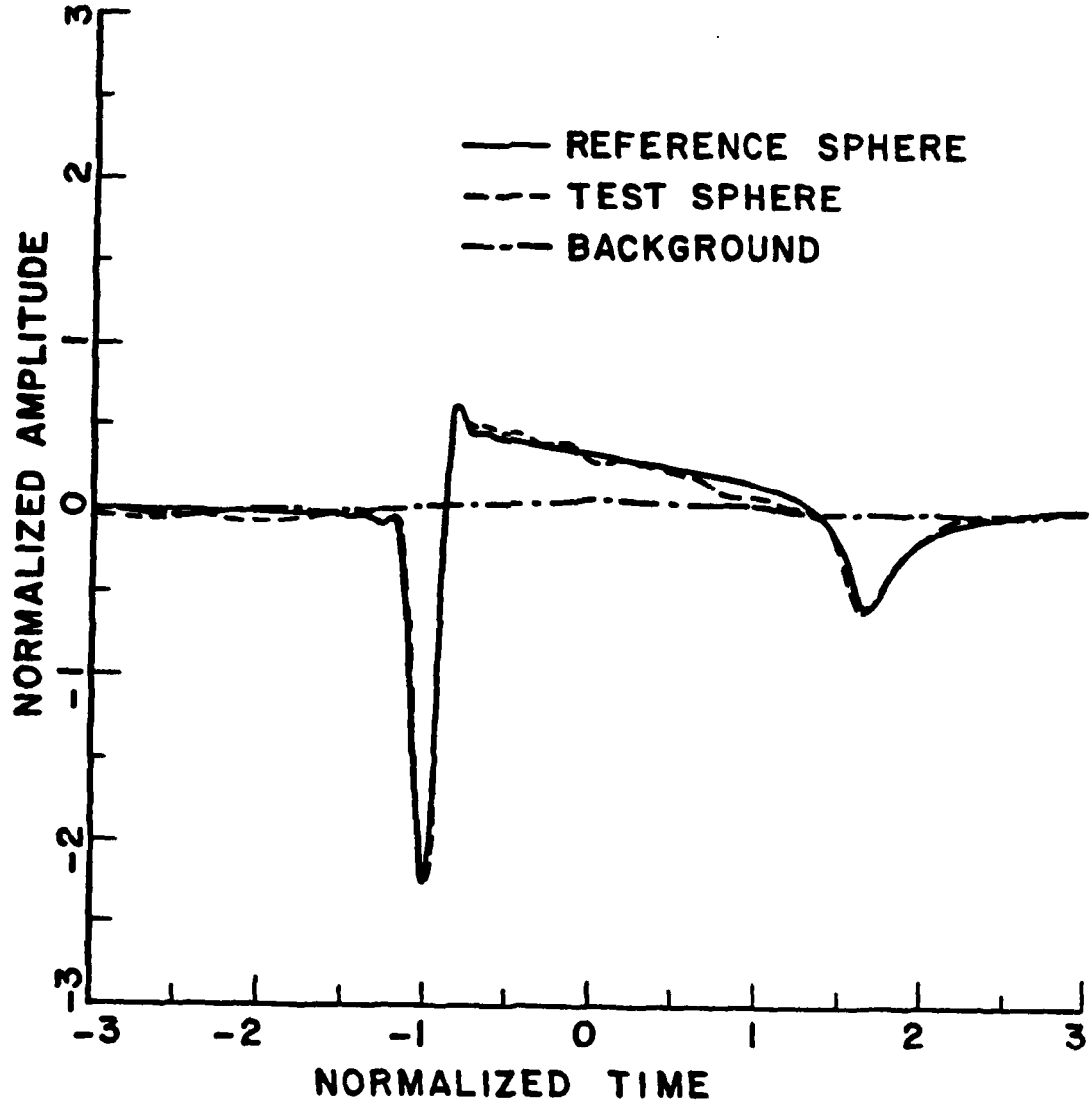

Figure F-2. Calibrated waveforms.
a. sphere
b. second sphere
c. background.

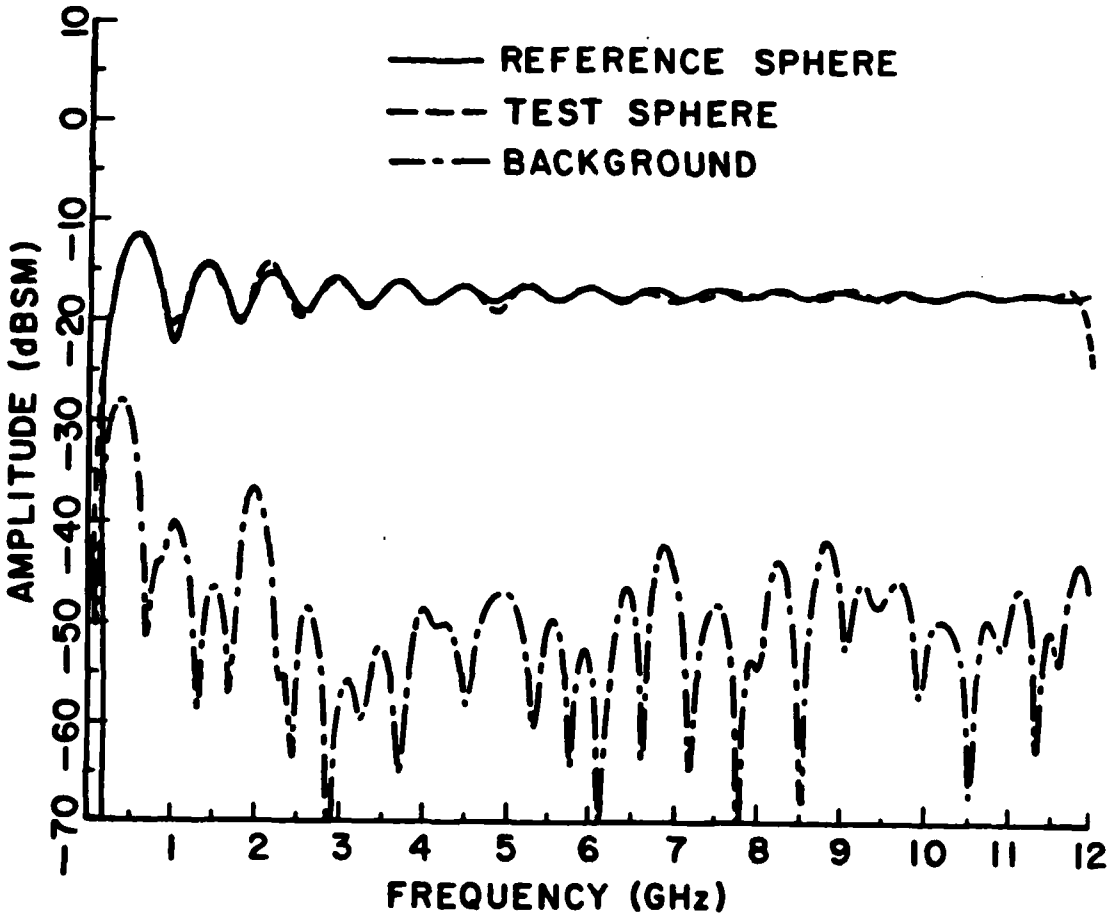

Figure F-3. Frequency domain waveforms.
a. sphere
b. second sphere
c. background.

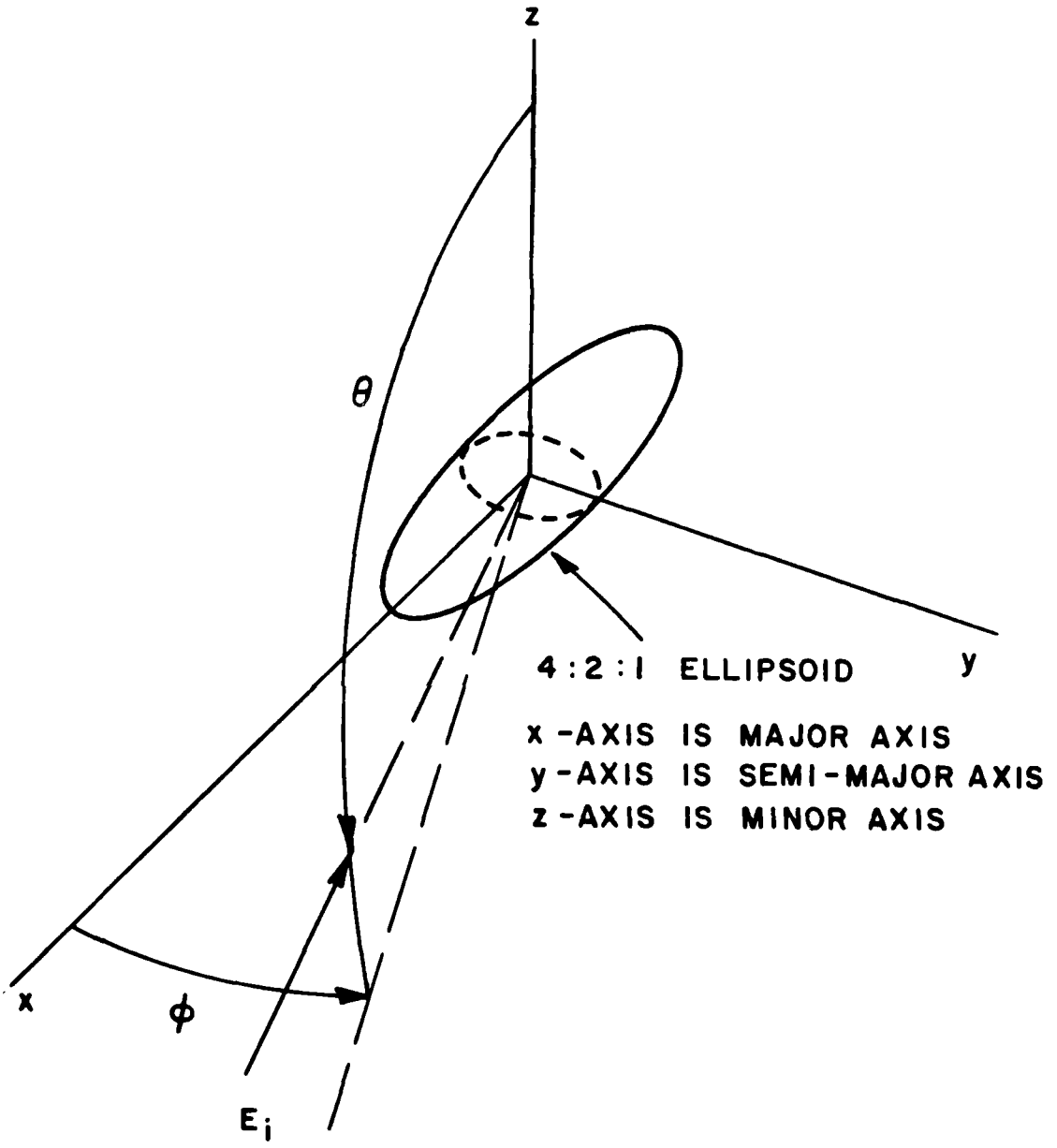

Figure F-4. Reference frame for ellipsoid meas rements.

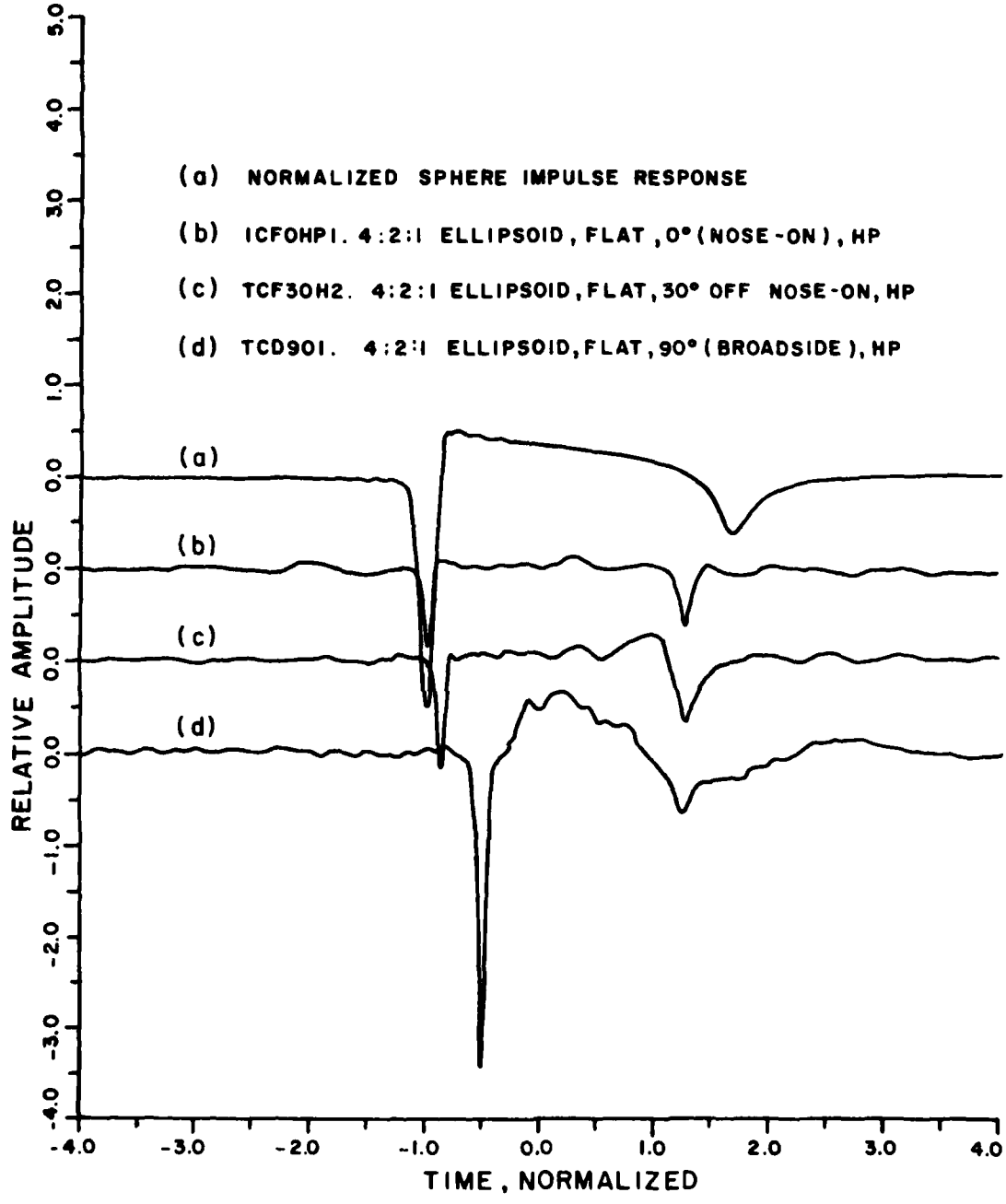

Figure F-5. Impulse response waveforms for 4:2:1 ellipsoid, compared to the sphere impulse response.

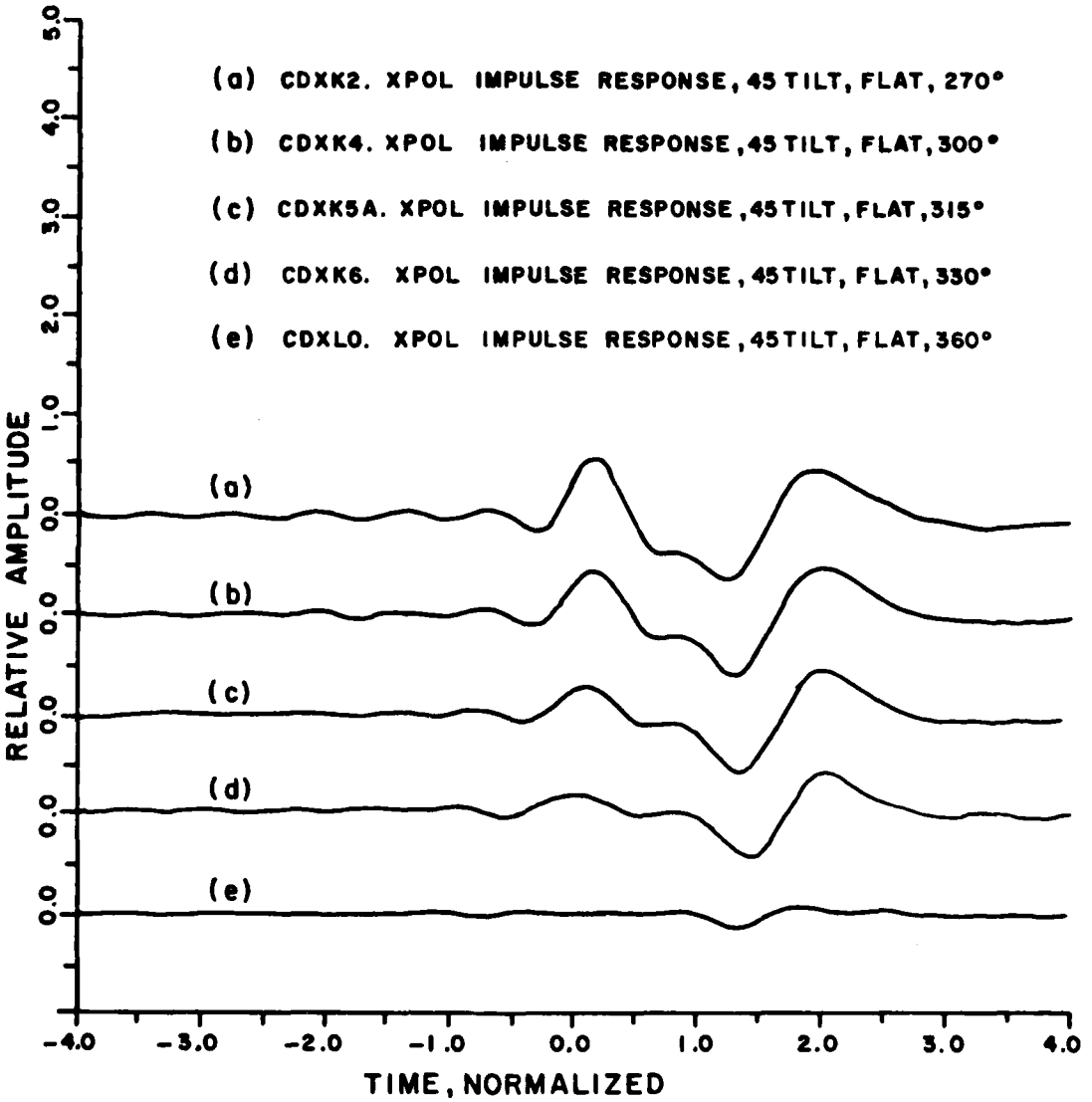

Figure F-6. Cross-polarized impulse response vs aspect angle for a 4:2:1 ellipsoid (10:1 bandlimited approximation).

response signatures for the ellipsoid. These data have been discussed in a separate report [5], and will be submitted for publication.

A pair of impulse response signatures for the circular disk at look angles shown on the figures are shown in Figures F-7 and F-8. These data are being used by Professor Moffatt and colleagues in his JSEP studies in order to clarify and assess the differences in the predicted signatures of the circular disk arrived at by different analytical techniques.

3. Interpretation of Scattering Mechanisms from Impulse Signatures

Following up on last year's JSEP studies in this area, reports and papers refining and interpreting the sphere-capped cylinder and spheroid data have been presented and submitted for publication [6,7,8]. The results show, in particular, how easily UTD mechanisms can be understood in the time domain, and how the scattering mechanisms are clearly separable in a time-history point of view.

The same techniques may be applied to the signatures of Figure F-5. For the nose-on ellipsoid case, the specular reflection off the nose and the creeping wave around the rear of the target are identifiable, and their amplitude and position are related correctly to basically similar returns from a sphere. As the ellipsoid is rotated in azimuth, the specular term grows as the local radius of the specular point increases, and the time delay between the specular return and the creeping wave decreases proportional to the projection of the target along the

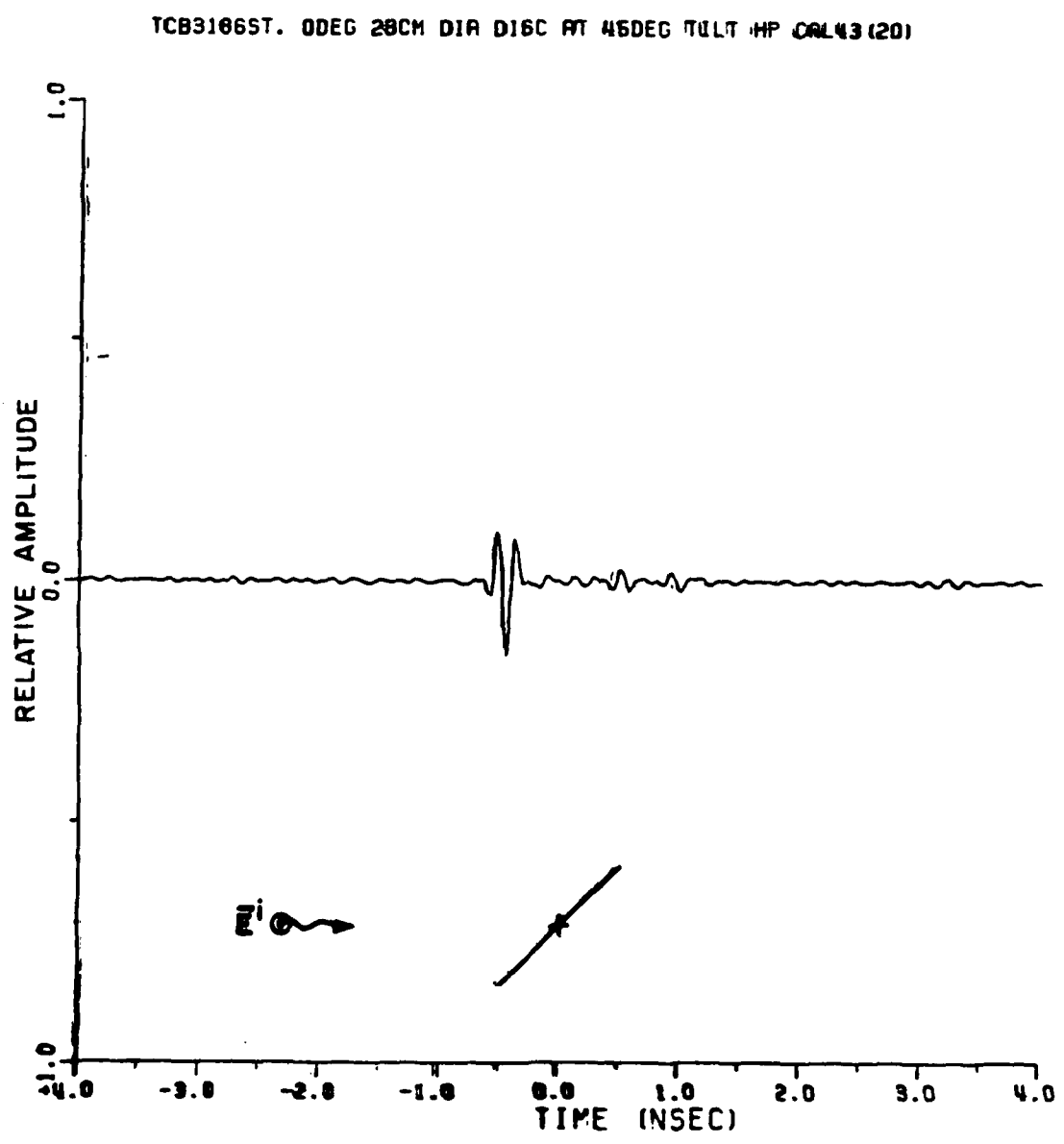

Figure F-7. Impulse response of a conducting disk, 45° from normal incidence, horizontal polarization.

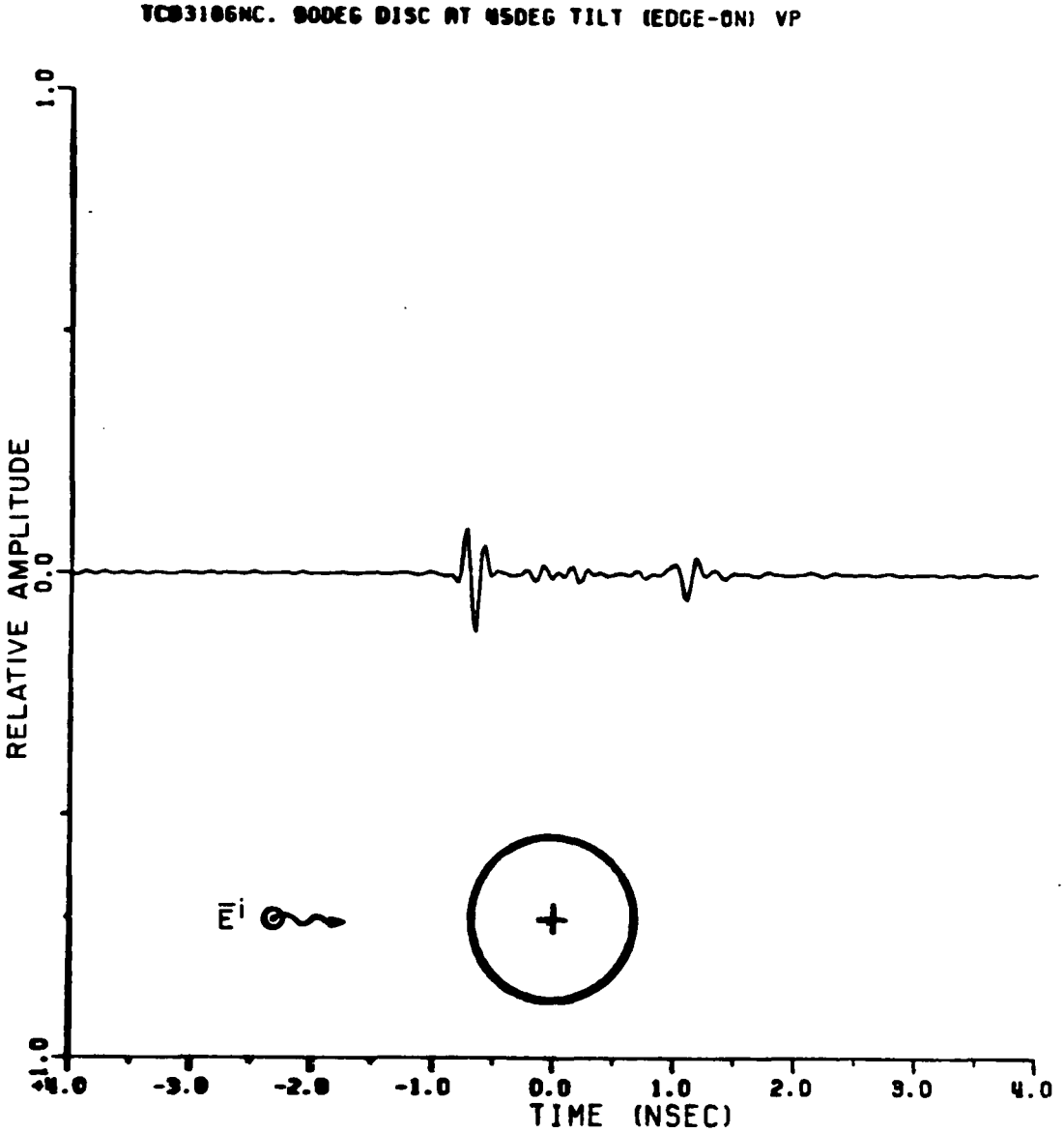

Figure F-8. Impulse response of a conducting disk, 90° from normal incidence, polarization at 45° to surface.

line-of-sight. At broadside, the time of arrival and character of the creeping wave term is significantly different for hh and vv polarizations, as is expected due to the different paths of the creeping wave propagation around the body.

4. Optimum Sampling of a Scattering Signature in Aspect Angle and Frequency

Acquiring comprehensive target scattering signature data is equivalent to sampling its scattering properties in aspect angle and frequency. The accuracy of the data is improved and cost of data acquisition reduced if optimal sampling is done. The following paragraphs summarize present progress on a study in this area.

This discussion will explore applications of the N-dimensional sampling theorem to invese scattering. More specifically, the application is on the reconstruction of the impulse response [9] of a target using one-dimensional sampling theorem.

In theory, an impulsive electric field is sent to the target at a given aspect angle. The measurement of the back scattered echo is referred to as the impulse response of the target at that particular aspect angle. Another approach to obtain the impulse response is similar to deconvolution: dividing the complex frequency response spectrum of the target by its input signal frequency spectrum; then the result is inverse Fourier Transformed to give the impulse response. In mathematical terms:

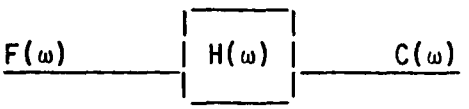

Let i) $f(t)$ be the input in time,

$F(\omega)$ be its Fourier transformed pair,

ii) $H(t)$ be the impulse response of the target,

$H(\omega)$ be its Fourier transformed pair,

iii) $C(t)$ be the output in time (i.e., the scattering)

$C(\omega)$ be its Fourier transformed pair,

then by the convolution theorem in Fourier transform,

$$C(\omega) = F(\omega)\, H(\omega)$$

$$\therefore H(\omega) = \frac{C(\omega)}{F(\omega)} \quad .$$

Next, Fourier transform $H(\omega) \rightarrow h(t) = \frac{1}{2a} \int_{-\infty}^{\infty} \frac{C(\omega)}{F(\omega)} e^{j\omega t} d\omega$

= impulse response of the target.

According to Kennaugh and Moffatt [10], the impulse response will decay exponentially for large values of t-r/c, where

t = time

r = distance between observation point and the origin

c = speed of light.

Therefore, one can define a settling time when the impulse response has its amplitude embedded in noise. For all practical purposes, the

settling time will be the end of the impulse response, though the impulse response may linger on for infinite time in reality. Defining the end of the impulse response is another way of saying that the impulse response is time limited. From the sampling theorem [11]:

> A time limited signal can be reproduced from its discrete frequency values, if it is sampled over the complete frequency domain using the Nyquist rate. As a consequence, the impulse response may be reproduced by measuring its frequency response values at the Nyquist sampling frequencies.

Next, the use of an N-dimensional sampling theorem is considered. Any physical object is finite in dimensions. If it is located in a rectangular coordinate system $(\bar{X};\ X_1,\ X_2,\ X_3)$, then it can be said to have limited dimensions in the $\bar{X}$ coordinates. Namely, the object is confined in:

$$X_1^a < X_1 < X_1^b$$

$$X_2^a < X_2 < X_2^b$$

$$X_3^a < X_3 < X_3^b$$

where $X_1^a,\ X_2^a,\ X_3^a,\ X_1^b,\ X_2^b,\ X_3^b$ are some real constants.

Now, consider the impulse response of such an object. An impulsive magnetic field $\bar{H}^i$ incident on the body will set up current $(\bar{J})$ on the surface. As a result, $\bar{J} = \hat{n} \times \bar{H}^i$ will start generating a scattered

field in all directions. After $\bar{H}^i$ has washed over the target, the current created and its scattered field will start to exponentially decay. Therefore, at one aspect angle, the start of the target response is defined by the initial time (T_i); the time (T_f) denotes the beginning of the exponential decay.

Let X be the length of the object at an aspect angle

Δt be the time difference between the critical and final time at that angle

C be the speed of light

$$\Delta t = T_f - T_i .$$

Then,

$$2X = C[\Delta t]$$

$$= C(T_f - T_i) \quad .$$

Putting the concepts together, the confinement of an object in space at one angle is equivalent to time limiting of its impulse response.

While there is only one sampling theorem, there are different forms of the theorem, depending on how the time limited or frequency limited signal is assumed to repeat itself. In the 3-D sense, this relates to whether the target is confined by a unit of sphere, parallelpiped, ellipsoid, etc., and as assumption on whether the unit is repeated in the 3-dimensional space.

Since the target is of arbitrary shape already, one would not want to complicate the problem by assuming an arbitrarily shaped unit to confine the target. The logical approach would be to confine the object by either a sphere or parallelpiped. A decision rule may be derived after the efficiency has been defined.

The following formula is a modified version of the original formula defined by Peterson and Middleton [12]

Given:

$$\eta_s = \frac{\text{Conservative estimate of the volume of the object}}{\text{Volume of the smallest sphere enclosing the object}}$$

= efficiency using the sphere.

$$\eta_p = \frac{\text{Conservative estimate of the volume of the object}}{\text{Volume of the smallest perallelpiped enclosing the object}}$$

= efficiency using the parallelpiped.

Rule: If $\eta_s > \eta_p$, then use spherical confinement

If $\eta_p > \eta_s$, then use parallelpiped confinement.

N-dimensional sampling theorem (from Petersen and Middleton [12]):

A function $f(\bar{x})$ whose Fourier transform $F(\bar{\omega})$ vanishes over all but a finite portion of wave-number space can be everywhere reproduced from its sampled values taken over a lattice of points $\{\ell_1\bar{V}_1 + \ell_2\bar{V}_2 + \ldots + \ell_N\bar{V}_N\}$; $\ell_1,\ell_2,\ldots\ell_N = 0, \pm1, \pm2,\ldots$ provided that the vectors $\{\bar{v}_j\}$ are small enough to ensure non-overlapping of the spectrum $F(\bar{\omega})$ with its images on a periodic lattice defined by the vectors $\{\bar{u}_k\}$, with $\bar{v}_j \cdot \bar{u}_k = 2\pi\sigma jk$.

One can measure and reproduce the original 8-space signal. The procedure for reconstruction is

1. Sample the frequency response at the sampling lattice
2. Interpolate the sampled points
3. Fourier transform the frequency response to obtain the original signal.

Consider the non-overlapping condition in the N-dimensional sampling theorem. The requirement is 'non-overlapping' of the spectrum $F(\omega)$ with its images on a periodic lattice. In other words, the periodic lattice is not uniquely defined, e.g., an arbitrary guard band can be put around the spectrum $F(\overline{\omega})$, thus changing the periodic lattice. Furthermore, the periodicity defined by $\{\overline{u}_k\}$ is arbitrary. Figure F-9 shows a 2-D spectrum with different periodicity. However, an efficient sampling lattice may be defined. From Petersen and Middleton [12]: "An efficient sampling lattice is one which uses a minimum number of sampling points to achieve exact reproduction of a wave-number limited function". In other words, the closest pack of the spectrum and its images without overlapping will enable efficient sampling.

With the ease of calculation in mind, the following periodicity of the spectrum and its images are defined as in Figure F-10. From Petersen and Middleton:

$$F(\overline{\omega}) = \sum_{[\ell]} F(\overline{u}[\ell])G(\overline{\omega}-\overline{u}[\ell])$$

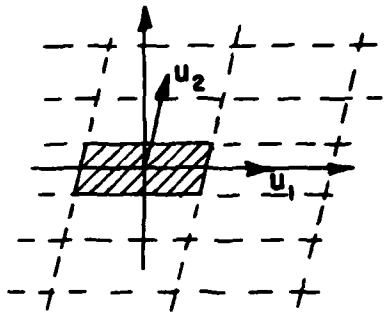

(a) ONE TYPE OF PERIODICITY

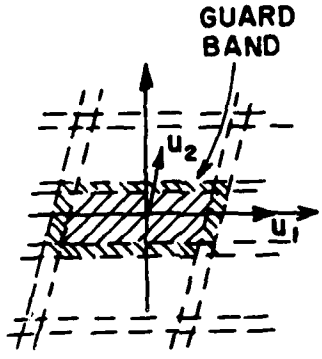

(b) SAME AS (a) WITH GUARD BAND

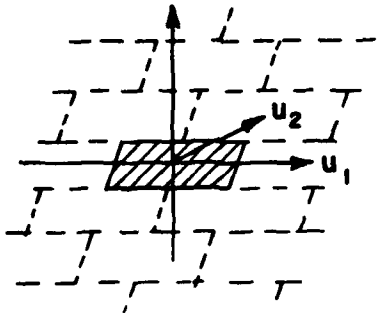

(c) PERIODICITY

Figure F-9. 2-D spectra.
(a) One type of periodicity.
(b) Same as (a) with guard band.
(c) Periodicity different from (a).

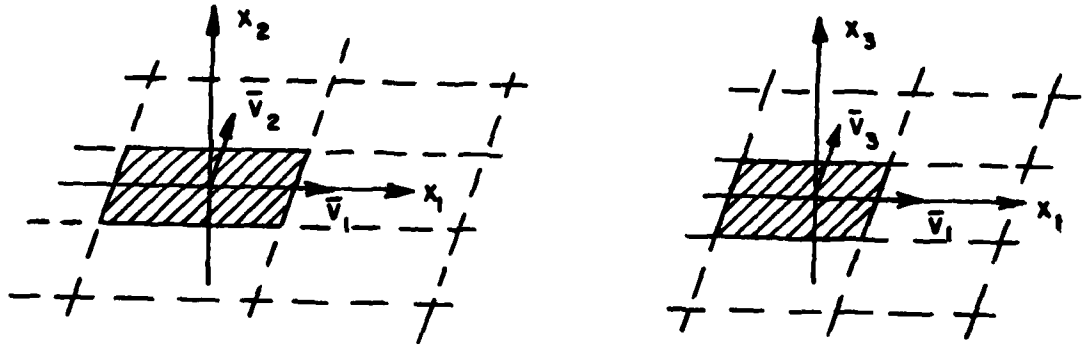

Figure F-10. Spatial spectrum periodicity as defined in the analysis by Middleton [12].

where

$$[\ell] = \ell_1, \ell_2, \ell_3 \quad \text{where } \ell_1, \ell_2, \ell_3 = 0, \pm 1, \pm 2\ldots$$

$$\bar{u}[\ell] = \bar{u}_1\ell_1 + \bar{u}_2\ell_2 + \bar{u}_3\ell_3 \quad .$$

For the parallelpiped:

$$G(\bar{\omega}) = \prod_{k=1}^{3} \frac{\sin 1/2\ \bar{v}_k \cdot \bar{\omega}}{1/2\ \bar{v}_k \cdot \bar{\omega}} = \text{Reconstruction Function}$$

and

$\bar{v}_1$, $\bar{v}_2$, $\bar{v}_3$ are defining the enclosure with $\bar{u}_k \cdot \bar{v}_j = 2\pi\sigma_{kj}$ and

$$\sigma_{kj} = \begin{bmatrix} 1 & \text{if } k=j \\ 0 & \text{if } k\neq j \end{bmatrix} \quad .$$

For the sphere or isotropic cell, the following configuration (Figure F-11) is adopted using the concept of closest packing of spheres defined by Coxeter.

<u>For 2-Dimensional case</u>: [12]

$$\bar{v}_1 = \begin{bmatrix} \sqrt{3}/2 \\ -1/2 \end{bmatrix} R \qquad \bar{v}_2 \begin{bmatrix} 0 \\ 1 \end{bmatrix} R$$

where R is the radius of the isotropic cell

$$\bar{u}_1 = \begin{bmatrix} 2/\sqrt{3} \\ 0 \end{bmatrix} \frac{1}{R} \qquad \bar{u}_2 \begin{bmatrix} 1/\sqrt{3} \\ 1 \end{bmatrix} \frac{1}{R}$$

and

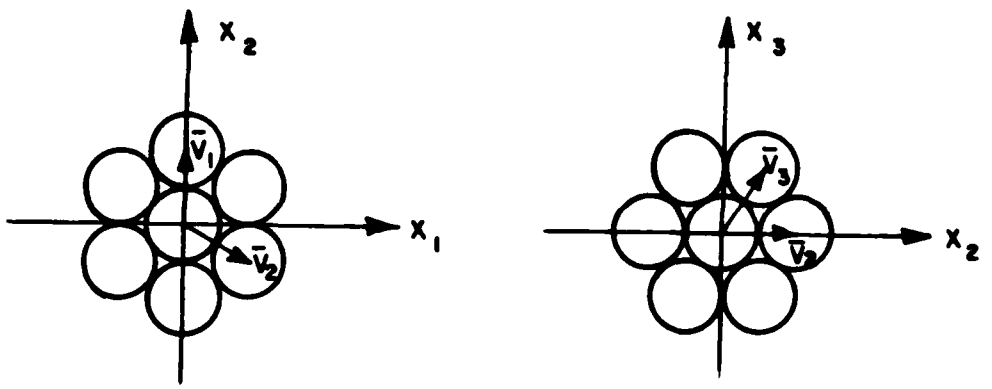

Figure F-11. Isometric spherical shell 2-D spectrum sampling as defined by Coxeter [16].

$$G(\bar{\omega}) = \frac{1}{(R)^2\omega_1(\omega_1^2-3\omega_2^2)} \times$$

$$\begin{bmatrix} 2\omega_1\cos(R\omega_1/\sqrt{3})\cos(R_1\omega_2) - 2\omega_1\cos(2R\omega_1/\sqrt{3}) \\ -2\sqrt{3}\,[\sin(R_1\omega_1/\sqrt{3})][\sin(R\omega_2)](\omega_2) \end{bmatrix} *$$

For 3-Dimensional case:

$$\bar{v}_1 = \begin{bmatrix} 1/\sqrt{2} \\ 1/\sqrt{2} \\ 0 \end{bmatrix} R \quad \bar{v}_2 = \begin{bmatrix} 1/\sqrt{2} \\ 0 \\ 1/\sqrt{2} \end{bmatrix} R \quad \bar{v}_3 = \begin{bmatrix} 1/\sqrt{2} \\ -1/\sqrt{2} \\ 0 \end{bmatrix} R$$

$$\bar{u}_1 = \begin{bmatrix} 1/\sqrt{2} \\ 1/\sqrt{2} \\ 1/\sqrt{2} \end{bmatrix} \frac{1}{R} \quad \bar{u}_2 = \begin{bmatrix} 0 \\ 0 \\ 1/\sqrt{2} \end{bmatrix} \frac{1}{R} \quad \bar{u}_3 = \begin{bmatrix} 1/\sqrt{2} \\ -1/\sqrt{2} \\ 1/\sqrt{2} \end{bmatrix} \frac{1}{R}$$

and

---

*There is a ω_2 factor missing in the third term of this expression in Reference [12].

$$G(\bar{\omega}) = \frac{1}{2(R/\sqrt{2})^3\,[\omega_1^4+\omega_2^4+\omega_3^4 - 2(\omega_1^2+\omega_2^2+\omega_1^2\omega_3^2 + \omega_2^2\omega_3^2)]} \times$$

$$\begin{bmatrix} -2\omega_1\sin(\sqrt{2}R\omega_1) - 2\omega_2\sin(\sqrt{2}R\omega_2) - 2\omega_3\sin(\sqrt{2}R\omega_3) \\ +(\omega_1+\omega_2+\omega_3)\sin R/\sqrt{2}(\omega_1+\omega_2+\omega_3) \\ +(\omega_1-\omega_2+\omega_3)\sin R/\sqrt{2}(\omega_1-\omega_2+\omega_3) \\ +(\omega 1-\omega_2-\omega_3)\sin R/\sqrt{2}(\omega_1-\omega_2-\omega_3) \\ +(\omega_1+\omega_2-\omega_3)\sin R/\sqrt{2}(\omega_1+\omega_2-\omega_3) \end{bmatrix} .$$

Implementation

Depending on the shape of the object, the object may be confined in a sphere or a parallelpiped such that the isotropic or parallelpiped form of the sampling theorem [12] may be employed respectively and effectively. But, in general, most objects can easily be fitted into a rectangular box; therefore, there is no advantage to go to the more general case of parallelpiped confinement. Nevertheless, programs are developed for both the isotropic and parallelpiped sampling.

Thus far, the development in the area has been in computer programming. After specifying isotropic or parallelpiped sampling, a file containing sampling angles and radii in the 2-D frequency domain will be output. Binary search is employed to arrange the angles in ascending order. The output file is then used to make actual measurement or storage selection.

Since the isotropic or parallelpiped sampled data are governed by the sampling theorem, they are sufficient to define the object in the 2-D frequency domain plane. Furthermore, the sampling theorem may be viewed as an interpolation formula. Interpolation to get the 1 aspect angle swept over a frequency band data (which after Fourier transform can provide the impulse response of that aspect angle) and interpolation to get the RCS measurement for a particular frequency inside the swept frequency band are available. The interpolation into 2-D rectangular coordinates in the frequency domain is possible, but as pointed out in the Mensa, et al. paper [14], it is very time consuming. The natural approach to obtain 2-D impulse response of the object will be to confine the object in a square box and take samples at the sampling points, thus filling the 2-D frequency plane. The rectangular grid frequency domain data may then be transformed into the time domain.

Since the FFT program was written to operate on rectangular coordinates and not on polar coordinates, the isotropic sampled points required a different approach to obtain the 2-D time response. A 2-D Fourier transform operating on polar coordinated points is required. In the Mensa, et al paper [14], they reduced the double integral into a single integral involving convolution using polar coordinates. Using a packaged subroutine FFT three times, the 2-D time domain waveform was constructed for each frequency ring. A similar approach was used successfully here.

5. Frequency Domain Decomposition of Scattering Mechanisms Via the Time Domain

It has long been recognized that the high frequency scattering from a body can be considered as a superposition of local scattering mechanisms. The mechanisms can be categorized and the common ones are reflection and edge, corner, tip and surface diffractions. Most of these mechanisms can be calculated accurately in the high frequency regime based upon asymptotic solutions. However, as the wavelength of the incident field becomes comparable to and smaller than the size of the body, these asymptotic solutions gracefully fail. A new approach to obtain the numerical bistatic values of these mechanisms for frequencies in the resonant region of the scatterer can be obtained through a time domain approach.

The time domain approach is simply to gate out, from the impulse representation of the scatterer, as much of the desired mechanism as possible without including any significant amount of any other mechanism. The gate is nothing more than a window concept that is common in communication applications where only a finite record of data is available for processing. The window symmetrically weights the desired portion of the time response by a factor that is unity at its center and smoothly goes to zero at its endpoints. The window portion of the time response is then numerically Fast Fourier Transformed (FFT) to obtain the frequency domain representation of the scattering mechanism. The original time domain representation of the scatterer may

be obtained directly through a time domain solution, time domain measurements, an eigenfunction solution or wideband frequency measurements. In any event, the original time domain scattering response is an approximation to the true impulse response.

This technique has been successfully employed on canonical shapes where the eigenfunction solution is readily available, i.e., the sphere and the infinitely long circular and elliptic cylinders. Here, the band limited impulse response was obtained by applying the FFT to unwindowed, lowpass frequency domain information. The results are excellent throughout most of the data record available. The endpoints of the processed record become distorted due to the standard limitations with data windowing. The extent of this distortion is small and located in the Rayleigh region and high frequency PO region of the scatterer where other techniques are available to predict the scattering.

An example of the results for this technique are shown in Figures F-12 through F-16. They pertain to the far field monostatic scattering due to an incident magnetic plane wave field polarized parallel to the cylinder axis from a perfectly conducting circular cylinder with a three inch radius. Comparisons of the reflected field obtained by a Luneberg-Kline expansion, subtracting the creeping wave field from the eigenfunction solution and the time domain approach are shown in Figure F-12. A comparison of the creeping wave field as predicted by GTD and the time domain approach is shown in Figure F-13. A comparison of

scattered field based upon an eigenfunction solution and that based upon the sum of the the reflected and creeping wave fields as predicted by the time domain approach is shown in Figure F-14. The previously mentioned end effects are illustrated in these figures. The approximate time response for the reflection and creeping wave mechanisms are shown in Figure F-15. These were obtained by appropriately windowing the frequency domain representations for the mechanisms and applying the FFT to them. A comparison between the directly transformed eigenfunction solution and the sum of the two mechanisms shown in Figure F-15 is shown in Figure F-16. The small disagreement in late time is attributed to the finite length of the time window.

The main benefit from this approach is the determination of scattering mechanisms in the resonant region of a body.

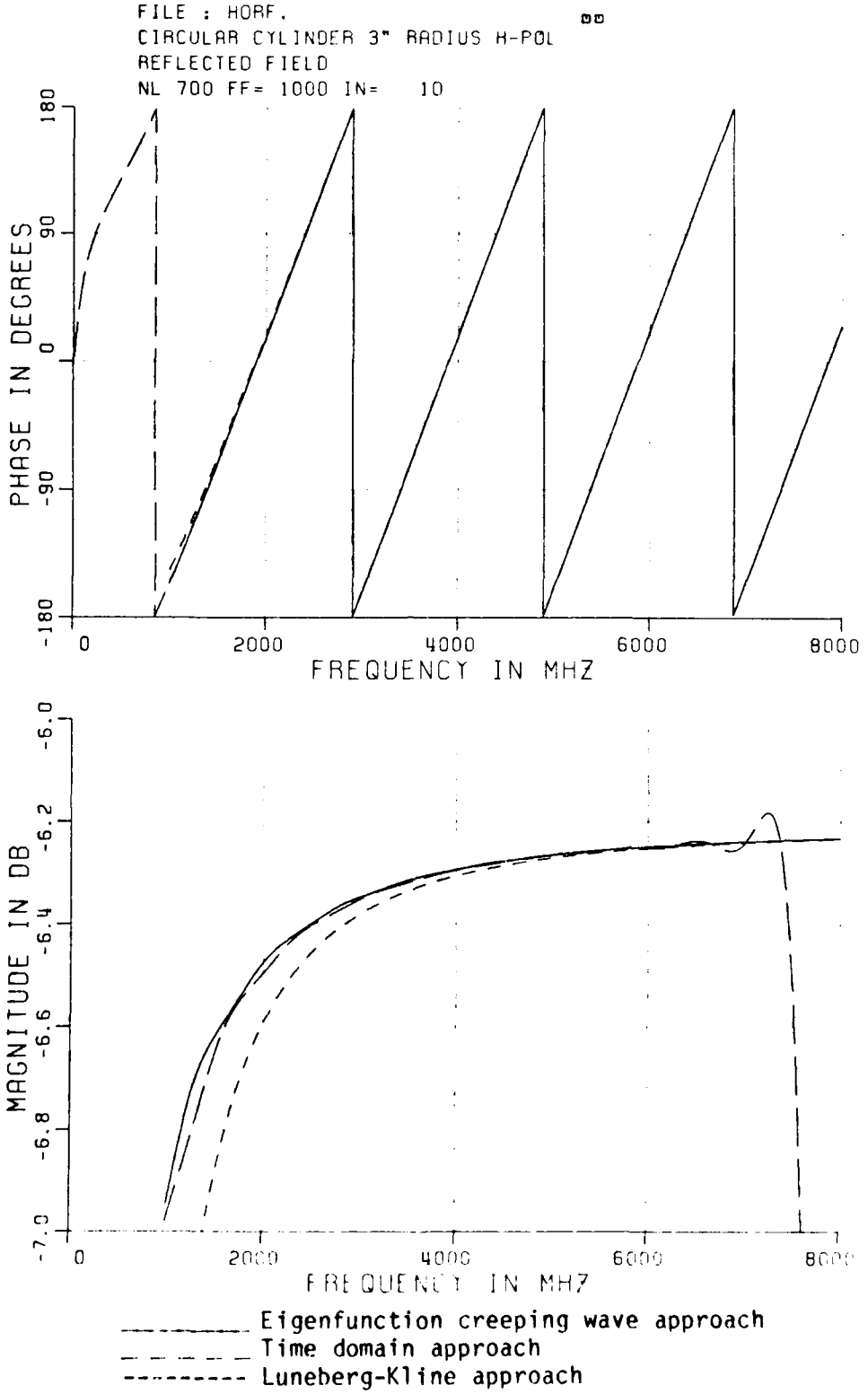

Figure F-12. Reflected field comparison.

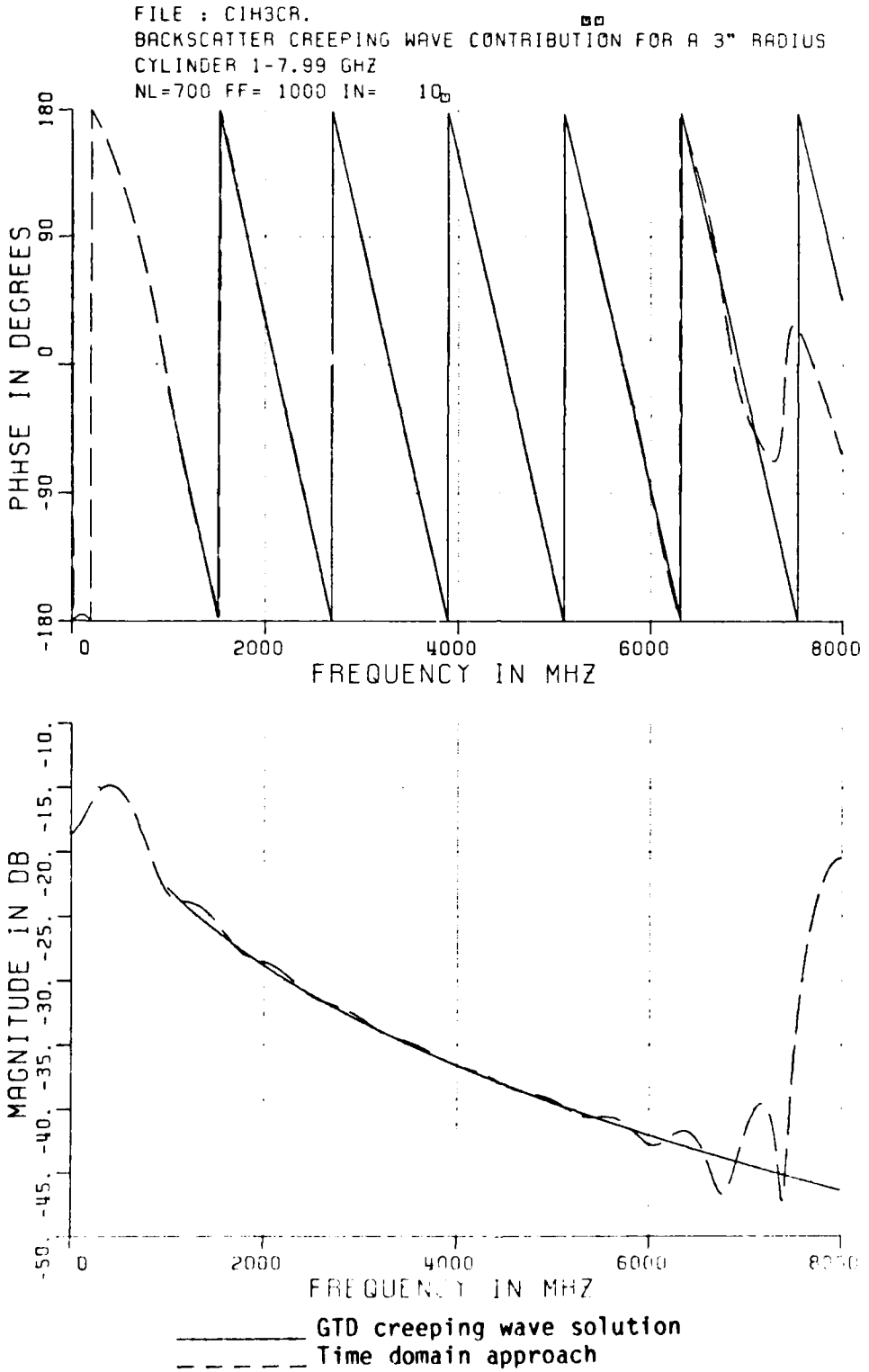

Figure F-13. Creeping wave field comparison.

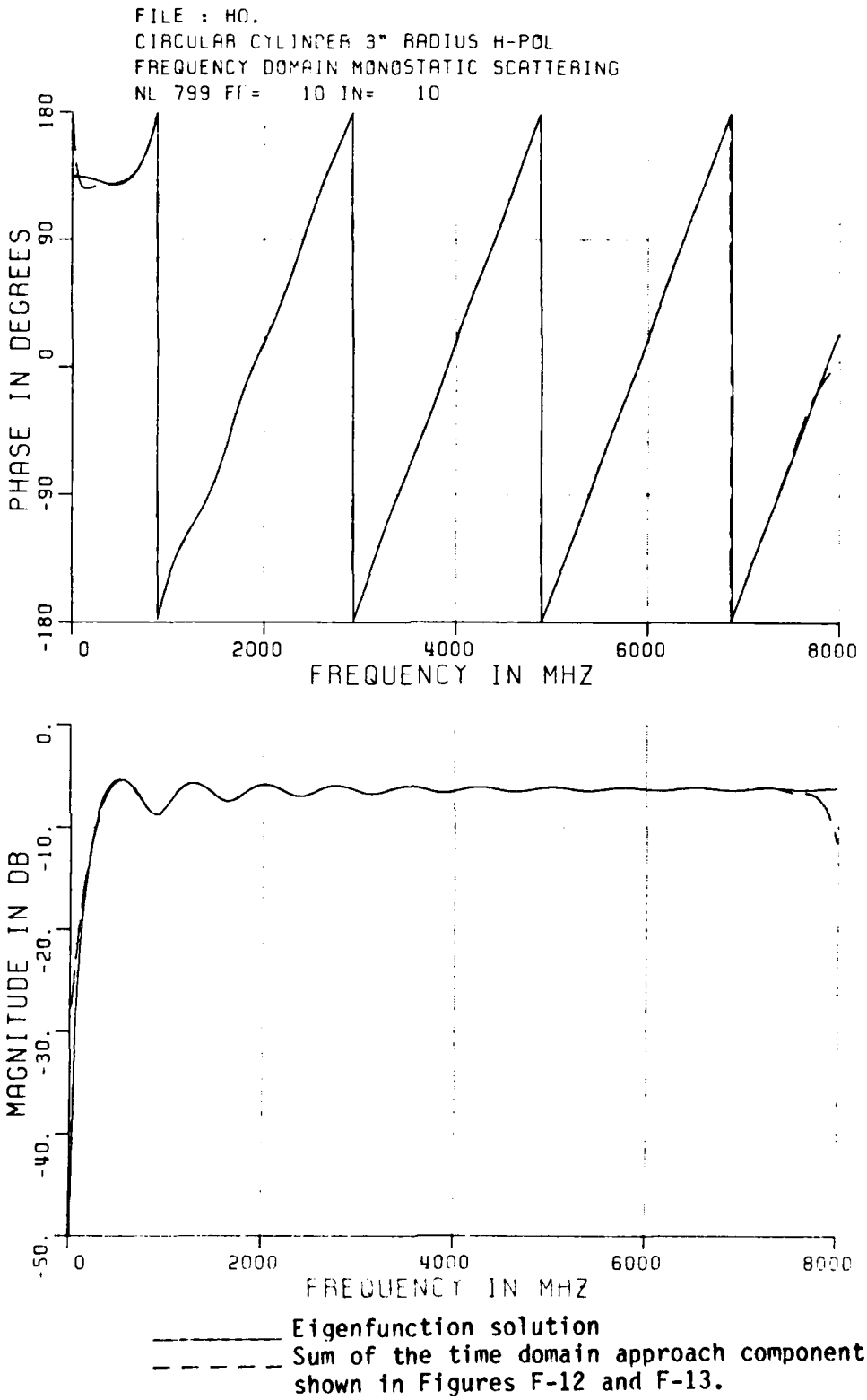

Figure F-14. Frequency domain scattering spectrum comparison.

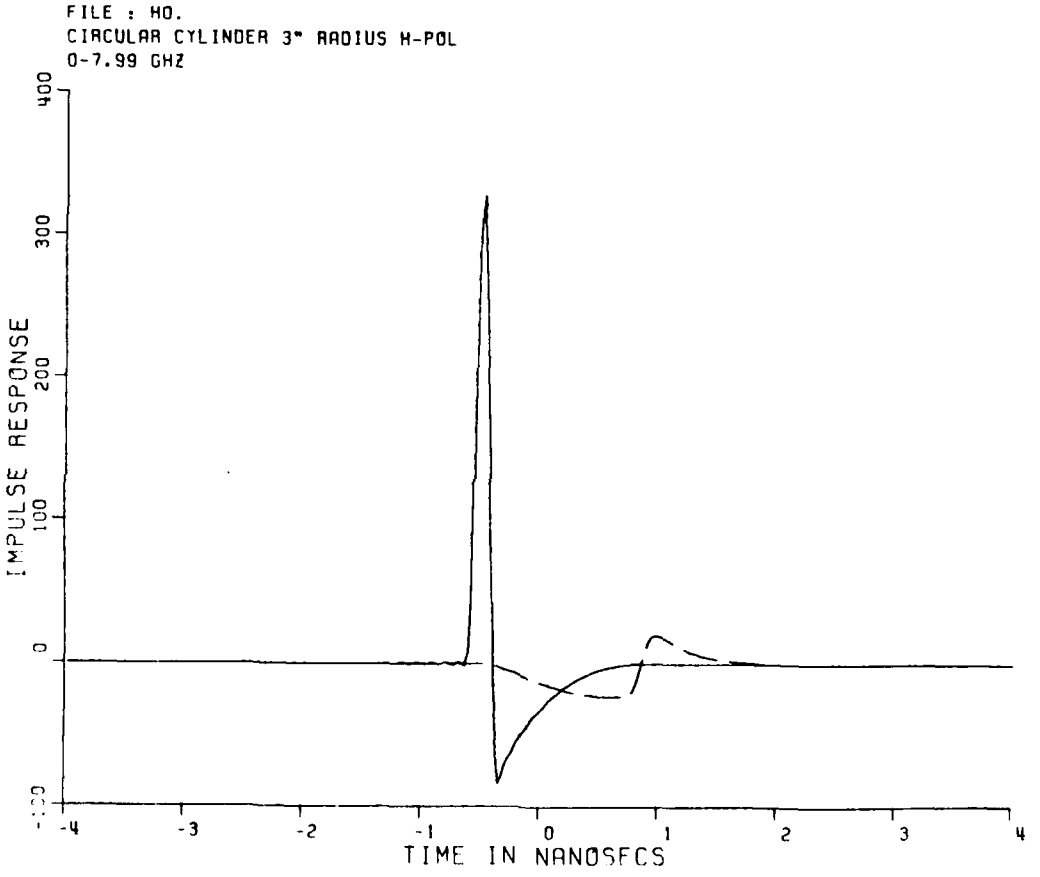

_____ Reflected field
_ _ _ _ _ Creeping wave field

Figure F-15. Time domain illustration of scattering mechanism.

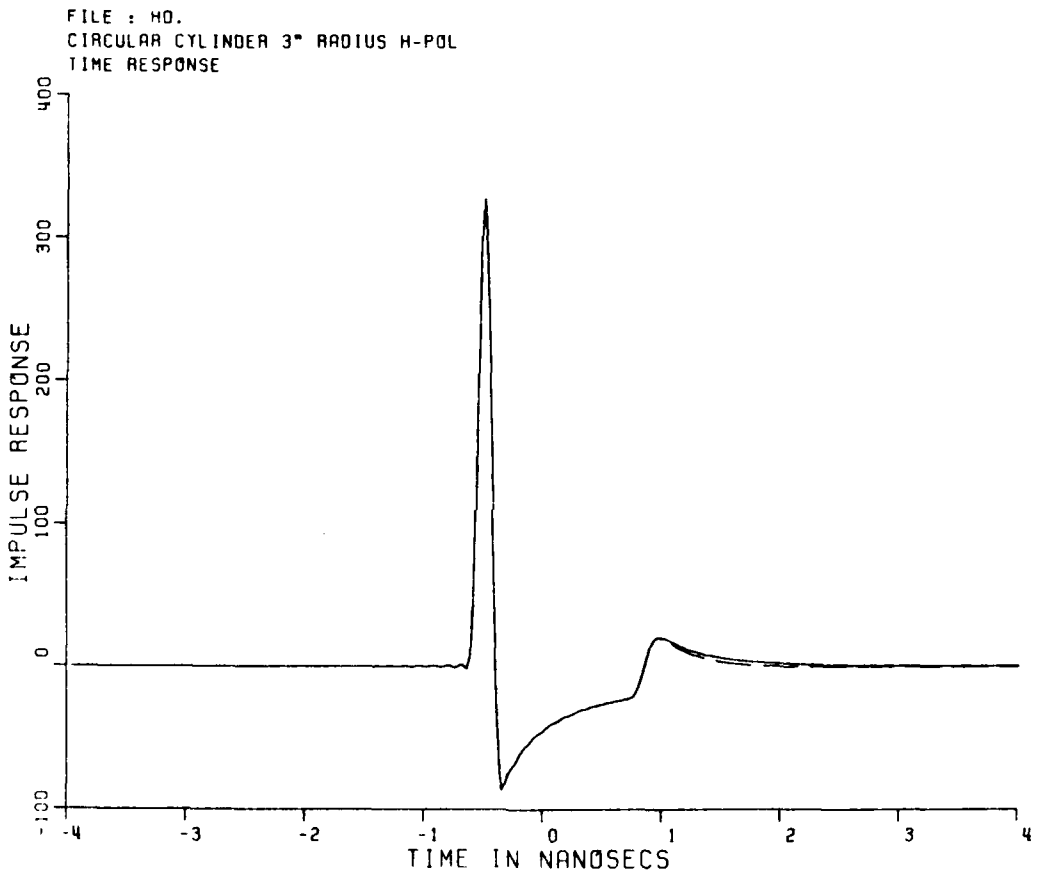

_____ Directly from the eigenfunction solution
_ _ _ _ _ Sum of the time domain components shown in Figure F-15.

Figure F-16. Time domain impulse comparison.

REFERENCES

[1] Young, J.D. and E.K. Walton, "Resonance Region Backscattered Signatures from a Conducting Ellipsoid", IEEE International Symposium Digest, Antennas and Propagation, May 23-26, 1983, Houston, Texas.

[2] Walton, E.K. and J.D. Young, "The Ohio State University Compact Radar Cross-Section Measurement Range", Proceedings of the Antenna Measurement Techniques Association, September 27-29, 1983, Annapolis, Maryland.

[3] Young, J.D. and E.K. Walton, "The Ohio State University Compact Radar Cross-Section Measurement Range", submitted to IEEE Transactions, AP-S, September 1983.

[4] Chen, J.S. and E.K. Walton, "The Ohio State University NCTR Data Base File Structure", Report 714190-1, October 1982, The Ohio State University ElectroScience Laboratory, Department of Electrical Engineering; prepared under Contract No. N00014-83-K-0037 for the Department of the Navy, Office of Naval Research.

[5] "Resonant Region NCTR Research", Annual Report 714190-5, February 1984, The Ohio State University ElectroScience Laboratory, Department of Electrical Engineering; prepared under Contract No. N00014-83-K-0037 for the Department of the Navy, Office of Naval Research.

[6] Leeper, W.J. and J.D. Young, "Identification of Scattering Mechanisms from Measured Impulse Response Signatures of Simple Conducting Objects", IEEE International Symposium Digest, Antennas and Propagation, May 23-26, Houston Texas.

[7] Leeper, W.J., "Identification of Scattering Mechanisms from Measured Impulse Response Signatures of Several Conducting Objects", Technical Report 712693-1, February 1984, The Ohio State University ElectroScience Laboratory, Department of Electrical Engineering; prepared under Contract No. N00014-78-C-0049 for the Department of the Navy, Office of Naval Research.

[8] Leeper, W.J. and J.D. Young, "Impulse Response Waveform Characteristics of Scattering Centers on a Sphere-Capped Cylinder", submitted to IEEE Trans. AP-S, February, 1984.

[9] Kennaugh, E.M. and R.L. Cosgriff, "The Use of Impulse Response in Electromagnetic Scattering Problems", 1958 IRE National Convention Record, Part 1, P. 72-77.

[10] Kennaugh, E.M. and D.L. Moffatt, "Transient and Impulse Response Approximation", IEEE Proceedings, August 1965, pp. 893-901.

[11] Papoulis, A., Fourier Integral and Its Application, New York, McGraw Hill (1962).

[12] Petersen, D.P. and D. Middleton, "Sampling and Reconstruction of Wave-Number Limited Functions in N-dimensional Euclidean Spaces", Information and Control 5, pp. 279-323, 1962.

[13] Coxeter, H.S.M., "Extreme Forms", Canadian Journal of Mathematics (3), 1951, pp. 391-441.

[14] Mensa, Halevy and Wade, "Coherent Doppler Tomography for Microwave Imaging", IEEE Proceedings, Vol. 71, No. 2 February, 1983.

APPENDIX I

PROJECT TITLES AND ABSTRACTS

Project 784652 An Advanced Prototype System for Locating and Mapping Underground Obstacles

The objective of this program is to develop a portable video pulse radar system for locating and mapping underground objects to a depth of 10-15 feet. The emphasis is on improving signal processing techniques and optimizing system performance to improve target resolution.

Project 710816 Block Funded Support for Electromagnetic Research

This is research in the area of electromagnetic radiation and scattering including: (1) extension of the Geometric Theory of Diffraction (GTD) for convex surfaces, edges, vertices and time domain solutions; (2) the GTD combined with the Method of Moments (MM); (3) extension of the MM codes utilizing polygon surface current patches and wire-patch attachment modes; (4) transient electromagnetic phenomena including target identification, radar imagery, K-pulse techniques and scattering from a thin, circular disk; and (5) improving the free space scattering range at The Ohio State University ElectroScience Laboratory to obtain accurate polarization matrix information on selected reference targets.

Project 710964 Analysis of Ariborne Antenna Patterns

The objectives of this program are to: (1) improve the aircraft model for far field pattern computations by considering a more realistic vertical stabilizer; (2) study various ways to model more general antenna types such as a monopole in the presence of directors; (3) examine various flat plate simulation codes; and (4) compare various calculated results with measurements supplied by NASA (Langley).

Project 711930 Radar Cross Section Studies

The objective is to establish the GTD techniques required to treat the scattering of missiles and to develop experimental techniques to obtain the scattered fields.

Project 712242 Formulate Quasi-Optical Techniques for Antennas at UHF

The goal of this program is to increase the electromagnetic effectiveness of Navy ships by developing low cost, integrated, systematic EM design procedures.

Project 712257 Application of Optical Computing Techniques to Jet Engine Control

This program involves the following tasks: (1) survey and document control requirements for jet engines using information supplied by sponsor; (2) survey and document the field of optical computing as applied to jet engine controls; (3) generate a report listing the various schemes and comparing them for speed, information processing capability, and ability to withstand the necessary environmental conditions; and (4) make recommendations as to the scheme most likely to satisfy the requirments stated in (1).

Project 712861 Coal Pile Electromagnetic Sensing Research

This project involves a research program in electromagnetic subsurface remote sensing as applied to accurate estimation of the quantity of coal in a large coal pile. This problem is important to inventory control at coal fired generating stations in the electric power industry. Coal quantity depends on both density and volume of the pile, and means for remote sensing of both of these parameters is sought.

Project 713169 EO Device Signature Reduction

This is a classified program.

Project 713176 Xenon Probe Laser for Atmospheric Studies

The objective is to construct and test a versatile laser, rugged enough for field operation and tunable to various lines in the 2-11.3 μm range, for use as an atmospheric probe laser.

Project 713206 Advanced RCS Reduction

This is a classified program.

Project 713302 Design of Dual Band Antennas

The Navy frequently has need for antennas which will operate at more than one band of frequencies. This project addresses the design of a dual band reflector antenna utilizing a dichroic surface design that is based on extensive experience at the ElectroScience Laboratory with transparent metallic surfaces.

Project 713402 Microstrip Analysis Techniques

This study extends the state of the art in microstrip analysis techniques by considering mutual coupling between microstrip antennas on a flat strip and on a cylinder.

Project 713533 Engineering Calculations for Communications Satellite Systems Planning

The objective of this program is to enhance the computational capability of NASA/Lewis Research Center for calculating the performance of proposed communications satellite systems. In particular, the effort addresses the potential interference between services sharing a common frequency band.

Project 529623 Terrascan Improvement

The objective is the development of an improved Terrascan unit for the location of buried pipes. Two areas are being addressed: 1) improvement of the sensor head (antenna) and 2) improvements in the ease of operation of the unit and its adaptability to a wide range of soil conditions.

Project 713656 Study of Meteorological Factors in Earth Satellite Propagation

The objectives of this program are to 1) conduct gain degradation measurements on Comstar D/4 28.56 Ghz synchronous satellite beacon and 2) conduct path diversity measurements using two 28 Ghz radiometers separated by approximately 12 Km.

Project 713712 Antenna and Radome Analysis and Design

The objective of this study is to analyze the performance of a design candidate antenna with a tunnel. Computer models are to be developed for the scan plane so that worst case performance can be predicted.

Project 312688 Geophysical Research

The objective of this program is to determine the state-of-the-art in underground exploration using electromagnetic techniques and define a program for an electromagnetic exploration system (EMES).

Project 713768 A Theoretical and Experimental Study of a Potential Mobile System for Evaluating Electrical Parameters of the Earth

The objective of this study is to evaluate a novel approach for rapidly estimating the electrical parameters of the earth over a broad frequency band.

Project 713774 The Effects of Atmospheric Water Vapor on Infrared Propagation

The objective of this program is to make measurements of the absorption of infrared radiation by pure and pressure-broadened water vapor samples at several different frequencies using a frequency-doubled CO_2 laser. Results of these measurements are to be incorporated into an analysis of continuum absorption as wings of strong absorption lines.

Project 714100 Navigation System Simulation

The objective of this program is to evaluate the simulation and performance of the GPS/JTIDS Adaptive Multifunction Array antenna design.

Project 714119 Support Services of Electromagnetic Design of RAM/RAS and Non-Specular Scattering

This is a classified program.

Project 714190 Resonant Structure NCTR

The objective of this research project is to measure the complex polarization scattering matrix of resonant structures.

AD-A140 434 JOINT SERVICES ELECTRONICS PROGRAM(U) OHIO STATE UNIV 3/3
COLUMBUS ELECTROSCIENCE LAB DEC 83 ESL-710816-15
N00014-78-C-0049

UNCLASSIFIED F/G 9/5 NL

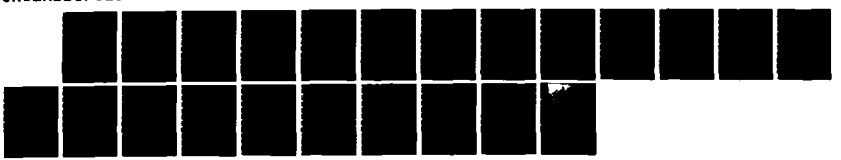

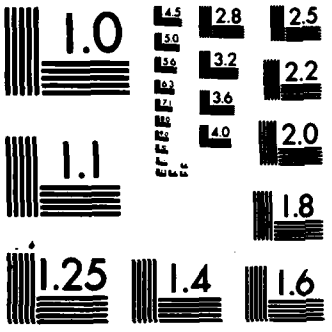

MICROCOPY RESOLUTION TEST CHART
NATIONAL BUREAU OF STANDARDS-1963-A

Project 713774 The Effects of Atmospheric Water Vapor on Infrared Propagation

The objective of this program is to make measurements of the absorption of infrared radiation by pure and pressure-broadened water vapor samples at several different frequencies using a frequency-doubled CO_2 laser. Results of these measurements are to be incorporated into an analysis of continuum absorption as wings of strong absorption lines.

Project 714100 Navigation System Simulation

The objective of this program is to evaluate the simulation and performance of the GPS/JTIDS Adaptive Multifunction Array antenna design.

Project 714119 Support Services of Electromagnetic Design of RAM/RAS and Non-Specular Scattering

This is a classified program.

Project 714190 Resonant Structure NCTR

The objective of this research project is to measure the complex polarization scattering matrix of resonant structures.

Project 714258 Advanced SATCOM ECCM Techniques

This is a classified project.

Project 714349 Radar Cross Section of Aircraft/Avionics Systems

This is a classified project.

Project 714381 Electromagnetic Reradiation Theoretical Prediction for Complex Building Structures

The purpose of this research project is to develop building models with sufficient structural detail to allow prediction of phase and gain patterns for rooftop-mounted antenna systems against any specified HF Signal.

Project 714414 Construction of Vehicle Tracking - Phase II

This project provides for the construction of a ground-based optical tracking system. This system will use three Reticon digital line scanning cameras to track a number of light sources moving over a portion of the Vehicle Dynamics Area of the Transportation Research Center of Ohio.

Project 714428 Radar Cross-Section (RCS) Controls

This project seeks to develop design parameters for slotted metallic radomes and RCS control of OSR antenna assembly.

Project 714505 Advanced Adaptive Antenna Techniques

The objective of this research program is to study the effect of frequency hopping on the performance of an adaptive array and the performance of the Frost algorithm with multiple constraints for use in communications systems.

Project 312145 DBS Antenna Measurements

The purpose of this program is to measure the performance of candidate antennas for DBS application.

Project 714614 Radar Cross Section Studies

A bistatic near- and far-field solution will be developed using the Uniform Geometrical Theory of Dliffraction (UTD) method for the scattering from airborne targets. Specifically, basic shapes such as finite flat plates, cylinders, ellipsoids, and cone frustrums will be analyzed separately and in combination with one another to provide an efficient approximate model for scattering bodies.

Project 714861 On-Aircraft Antennas

The objective is to develop the theory and the practical analysis techniques necessary to predict the performance of line array of stacked yagi antennas embedded in the leading edge of the wing of an aircraft. The method used to predict these antenna patterns shall be to adapt the aircraft antenna pattern prediction programs developed by the Ohio State University together with the geometrical theory of diffraction and related work also developed at the Ohio State University.

Project 714921 Computation of the Performance of an Element Antenna Array Mounted on an Aircraft

The potential communication capability provided by an array of antenna elements (5 monopoles) mounted on an aircraft in the presence of interference was assessed. The study involved the computation of the radiation pattern of each of the monopoles in situ, i.e., mounted as specified and the combined performance of the array operating in an adaptive mode. The Geometrical Theory of Diffraction was used to compute the radiation patterns of individual monopoles. The Least Mean Square and Power Inversion algorithms were used to study the performance of the array in adaptive modes.

Project 714946 Radar Cross Section Studies

This is a classified project.

Project 715010 Stereological Computer-Assisted Fluorometry: Development of Techniques for Analysis of Biological Material

This project involved the design of a prototype device to use optical fibers to transmit data on cell samples into a digital computer for statistical processing.

Project 715147 Basic Electromagnetic Scattering Studies

The research is directed toward the further development of the analytic and numerical techniques for generating the scattered fields of prototype aircraft configurations.

Project 715267 Mathematical Models to Predict the Near Field and Far Field RF Characteristics of Realistic Jet Intakes

This research project is concerned with an analysis of the scattering by circular and rectangular inlet shapes in the near field when the excitation is a plane wave. These inlets are terminated by an impedance surface within at some distance from the open end.

Project 715305 Design of Support Structure for Low RCS Targets

This program developed and constructed a low cross-section target support pedestal for radar cross-section measurements.

Project 715346 Design and Calculate Four Panels

This is a classified project.

Project 715354 Metallic Radome Design and Test

This is a classified project.

Project 715370 Research in Transient Response Scattering of Antennas

This program is investigating the impulse time domain response scattering of several antennas. Compact range measurements were obtained covering frequencies from 1 to 18 GHz. The process is being developed for use as a standard antenna diagnostic tool.

Project 715498 Support of the NASA Propagation Studies and Measurement Program - Meteorological Factors in Earth-Satellite Propagation

Two experiments are being performed on the effects of precipitation on satellite communications near 30 GHz. The first evaluates the improvement due to diversity reception on the ground by means of two radiometers which have been calibrated against the Comstar D4 satellite beacon at 28.6 GHz. The second is evaluating the gain degradation of a large paraboloid due to angle-of-arrival scintillations of the beacon signal. Future experiments are being planned for available and planned communications satellites.

Project 715559 Research on Analysis of Large Aperture Reflector Antennas

The objective is to aid NASA's effort to advance the technology of large space antenna systems. Available electromagnetic analyses and computer codes will be extended to provide the capabilities to predict the performance of large deployable reflector antennas with mesh surfaces.

Project 715582 Advanced Radar Cross Section Reduction

This is a classified project.

Project 715600 Laser Radar Cross Section and Optical Augmentation Descriminants

The laser radar cross section of a group of targets was measured on the ElectroScience Laboratory optical range at wavelengths in the near-IR and visible.

Project 715616 Development of a Theoretical Model for Ported Coaxial Cable Embedded at a Uniform Depth in a Lossy Half-Space

The guided radar uses a long coaxial cable with a periodic array of slots in the outer conductor, buried in the earth at a depth of a few inches. When an intruder walks over the cable, this induces a reflected wave traveling in the cable toward the detector. We are using moment methods and computer simulation to investigate the target coupling and the effects of planar and cylindrical layering in the earth.

Project 715655 Advanced Topics in Adaptive Arrays

Professor Compton, on sabbatical to NRL, is exploring mutual interests between OSU and NRL in the technical area of Adaptive Antenna Processing Systems.

Project 715723 Analysis of the Scattering from an Inlet Geometry with Lossy Walls

This project is concerned with a study of the effects on the scattering by an inlet geometry when the inner walls of the inlet duct are made lossy.

Project 715728 Small Array Phase Study

The purpose of this study is to investigate the relative phase between elements of a small array. Theoretical computations, based upon the method of moments, are performed to determine the effects of mutual coupling and interactions with the array support structure on the elements phases. Also, an experimental facility is being developed to permit the accurate measurement of the relative phase of the array elements.

Project 715731 Radar Cross Section (RCS) Prediction Code Modification

The analytical methodology will be developed necessary to predict the contributions of certain electromagnetic phenomena to the RCS of vehicles. Specifically, the contribution to the RCS of components partially shadowed by other components on the vehicle will be analyzed and measurements will be performed to validate the model.

APPENDIX II

ELECTROSCIENCE LABORATORY SPONSORING AGENCIES

OHIO STATE UNIVERSITY - ELECTROSCIENCE LABORATORY — ACTIVE PROJECTS DURING OCTOBER 1982 - OCTOBER 1983

PROJECT ENGINEER	PROJECT NUMBER	SPONSOR	CONTRACT OR GRANT NUMBER	STARTING DATE	ENDING DATE	AWARD AMOUNT	SOURCE
	Facilities Contract		AF 33(600)-31168				
CALDECOTT	784652	EPRI	RP7856-1	01-01-77	12-31-83	947K	03
PETERS	710816	ONR	N00014-78-C-0049	10-01-77	09-30-83	1987K	01
BURNSIDE	710964	NASA/Langley	NSG 1498	01-16-78	06-30-84	349K	02
PETERS/BURNSIDE	711930	NASA/Langley	NSG 1613	05-01-79	04-30-84	676K	02
MARHEFKA/RUDDUCK	712242	NOSC	N00123-79-C-1469	08-01-79	12-31-82	375K	02
COLLINS	712257	NASA/Lewis	NSG 3302	08-01-79	07-30-84	394K	02
YOUNG	712861	TVA	TVA-53983A	04-17-80	12-31-82	163K	01
MOFFATT	713169	ASD/WPAFB	F33615-80-C-1072	08-01-80	02-01-83	193K	01
DAMON	713176	NRL	N00173-80-C-0416	08-01-80	07-31-83	50K	03
MUNK	713206	ASD/WPAFB	F33615-80-C-1086	08-25-80	08-24-83	300K	02
MUNK	713302	NRL	N00173-80-C-0367	09-30-80	12-31-82	98K	03
NEWMAN	713402	ARO	DAAG29-81-K-0020	11-01-80	10-31-83	155K	02
LEVIS	713533	NASA/Lewis	NAG 3-159	01-20-81	07-13-84	113K	01
YOUNG	529623	Gas Research Institute		01-26-81	03-31-83	125K	02
LEVIS	713656	Jet Prop. Lab	NO.956013	03-12-81	03-31-83	310K	02
RUDDUCK	713712	Aerospace Corp	P.O. 27809-AN	04-01-81	12-31-83	105K	02
WALTER	312688	Terra Research		03-15-81	Indefinite	10K	03
PETERS	713768	NSF	ECS-8020636	05-01-81	10-31-83	60K	01
DAMON/LONG	713774	ARO	DAAG29-81-K-0084	06-01-81	11-30-83	200K	01
KSIENSKI	714100	Analytic Sciences	10300	09-01-81	04-15-84	95K	02
MUNK	714119	McDonnell Douglas	P.O. Z10104	09-04-81	11-30-82	35K	03
YOUNG/MOFFATT/ WALTON	714190	ONR	N00014-82-K-0037	10-01-81	10-31-83	960K	01
KSIENSKI	714258	RADC	F30602-82-C-0009	02-04-82	08-03-84	750K	02
PETERS/BURNSIDE	714349	Rockwell	L2XN-11455-915	01-25-82	09-30-83	460K	02
NEWMAN	714381	Southwest Research	PO: 15044-SW	02-27-82	06-27-83	75K	01
SVOBODA	714414	NHTSA	OSU-82-0039	01-01-82	09-30-83	46K	03
MUNK	714428	Boeing	BE5591	03-22-82	12-31-83	25K	02
COMPTON	714505	NASC	N00019-82-C-0190	04-28-82	07-27-83	80K	02
DAMON	312145	Stolle	547928	04-30-82	12-31-83	14K	01
MARHEFKA	714614	Naval Air Station	N0429A-82-C-0396	06-15-82	06-14-84	200K	02
RUDDUCK	714861	NADC	N62269-82-C-0375	09-07-82	09-06-83	35K	03
KSIENSKI	714921	Forsvarets Materialverk	FK 82463-82-018-23-001	10-07-82	09-30-83	80K	02
MUNK	714946	Rockwell	A3EM-900006	10-08-82	03-07-83	40K	01
COLLINS	715010	American Matrix		12-01-82	11-30-83	65K	02
BURNSIDE	715147	NASA/Langley	NAG-1-333	02-08-83	02-07-84	150K	01
PATHAK	715267	Naval Weapons Ctr.	N60530-83-M-40RD	02-01-83	01-31-84	25K	01
YOUNG	715305	General Electric	J85-000516N2416	04-01-83	09-30-83	27K	03

PROJECT ENGINEER	PROJECT NUMBER	SPONSOR	CONTRACT OR GRANT NUMBER	STARTING DATE	ENDING DATE	AWARD AMOUNT	SOURCE
MUNK	715346	Brunswick	PO: DV1-00011	03-22-83	06-20-83	10K	03
MUNK	715354	Brunswick	PO: DV1-00012	04-12-83	12-31-83	20K	03
YOUNG	715370	Westinghouse	P.O. 86 D JHA 3304090 V	05-01-83	12-31-83	84K	02
LEVIS	715498	Jet Prop. Lab	956528	07-01-83	03-31-86	329K	02
RUDDUCK	715559	NASA/Langley	NAS1-17450	07-01-83	09-15-85	151K	01
MUNK	715582	ASD/WPAFB	F33615-83-C-1013	07-18-83	07-18-86	304K	02
COLLINS	715600	Quest Res. Corp.	SC-4171-03	07-13-83	10-12-83	15K	02
RICHMOND	715616	Waterways Exp. Stat.	DACA39-83-K-0001	08-10-83	03-09-84	54K	01
COMPTON	715655	NRL	N00173-83-IPA-07	08-01-83	07-31-84	68K	01
PATHAK	715723	NASA/Lewis	NAG 3-476	09-25-83	03-31-86	138K	01
NEWMAN	715728	E-Systems Corp.	C 5276 K	08-01-83	12-31-83	50K	03
MARHEFKA	715731	Army Missile Command	DAAH01-83-C-1075	10-01-83	09-30-84	50K	02

APPENDIX III

REPORTS PUBLISHED BY ESL OCTOBER 1982 TO OCTOBER 1983

529622-4 DEVELOPMENT OF TECHNIQUES TO PINPOINT NATURAL GAS LEAKS FROM BURIED PIPES WITH AN UNDERGROUND RADAR SYSTEM, J.D. Young, A.K. Dominek, J. Izadian and B.R. Chen, June 1983.

710816-13 TRANSIENT CURRENT DENSITY WAVEFORMS ON A PERFECTLY CONDUCTING SPHERE, E.M. Kennaugh and D.L. Moffatt, January 1983.

710816-12 JOINT SERVICES ELECTRONICS PROGRAM - FIFTH ANNUAL, December 1982.

711930-7 SCATTERING BY THIN DIELECTRIC STRIPS, J.H. Richmond, August 1983.

710964-12 MOMENT METHOD ANALYSIS OF THE CESSNA 150 AIRCRAFT, P.A. Alexandropoulos, E.H. Newman and W.D. Burnside, October 1982.

711679-10 GENERAL 3D AIRBORNE ANTENNA RADIATION PATTERN CODE USER'S MANUAL, H.H. Chung and W.D. Burnside, July 1982.

711964-7 ELECTRICALLY SMALL ANTENNAS, J.H. Richmond and C.H. Walter, December 1982.

712242-11 QUASI-OPTICAL TECHNIQUES FOR ANTENNAS AT UHF AND ABOVE, R.C. Rudduck and R.J. Marhefka, August-October 1981.

712242-12 QUASI-OPTICAL TECHNIQUES FOR ANTENNAS AT UHF AND ABOVE, R.C. Rudduck and R.J. Marhefka, November 1, 1981 - January 31, 1982.

712242-13 QUASI-OPTICAL TECHNIQUES FOR ANTENNAS AT UHF AND ABOVE, R.C. Rudduck and R.J. Marhefka, February 1, 1982 - April 30, 1982.

712242-14 NUMERICAL ELECTROMAGNETIC CODE - BASIC SCATTERING CODE NEC - BSC (VERSION 2) PART I: USER'S MANUAL, R.J. Marhefka and W.D. Burnside, December 1982.

712242-15 NUMERICAL ELECTROMAGNETIC CODE - BASIC SCATTERING CODE NEC - BSC (VERSION 2) PART II: CODE MANUAL, R.J. Marhefka, December 1982.

712242-16 NUMERICAL ELECTROMAGNETIC CODE - REFLECTOR ANTENNA CODE NEC - REF (VERSION 2) PART I: USER'S MANUAL, R.C. Rudduck and Y.C. Chang, December 1982.

712242-17 NUMERICAL ELECTROMAGNETIC CODE - REFLECTOR ANTENNA CODE NEC - REF (VERSION 2) PART II: CODE MANUAL, Y.C. Chang and R.C. Rudduck, December 1982.

712242-18 QUASI-OPTICAL TECHNIQUES FOR ANTENNAS AT UHF AND ABOVE, R.C. Rudduck and R.J. Marhefka, August 1, 1979, - December 31, 1982.

712661-4 ANALYSIS OF ELECTROMAGNETIC BACKSCATTERING FROM AN INLET CAVITY CONFIGURATION - FINAL REPORT, C.C. Huang, P.H. Pathak, E.Y. Lai and D.L. Moffatt, October 1982.

712692-3 A USERS MANUAL FOR ELECTROMAGNETIC SURFACE PATCH (ESP) CODE: VERSION II - POLYGONAL PLATES AND WIRES, E.H. Newman and P. Alexandropoulos, September 1983.

712949-6 THEORY OF FIELD STRUCTURE FOR PORTED COAXIAL CABLE EMBEDDED IN LOSSY MEDIA, J.H. Richmond and R.J. Garbacz, March 1983.

713206-3 USERS MANUAL FOR COMPUTER PROGRAM 'CADLAC', E.K. English and B.A. Munk, January 1983.

713206-4 SCATTERING FROM PERIODIC ARRAYS OF ARBITRARILY ORIENTED DIPOLE ELEMENTS IMBEDDED IN A GENERAL STRATIFIED MEDIUM, E.K. English and B.A. Munk, January 1983.

713206-5 THE SCATTERING OF PLANAR ARRAYS OF ARBITRARILY SHAPED SLOT AND/OR WIRE ELEMENTS IN A STRATIFIED DIELECTRIC MEDIUM, B.A. Munk and L.W. Henderson, July 1983.

713206-6 SCATTERING FROM N ARRAYS OF FLAT, LOSSY ELEMENTS IN A STRATIFIED MEDIUM WITH ARBITRARY μ AND ϵ, B.A. Munk and E.K. English, July 1983.

713206-7 USER'S MANUAL FOR COMPUTER PROGRAM 'INDIAN', E.K. English and B.A. Munk, September 1983.

713206-8 USER'S MANUAL FOR COMPUTER PROGRAM 'FLATBK', E.K. English and B.A. Munk, September 1983.

713774-2 THE EFFECTS OF ATMOSPHERIC WATER VAPOR ABSORPTION ON INFRARED LASER PROPAGATION IN THE 5 MICROMETER BAND, L.G. Walter, May 1983.

713402-5 MICROSTRIP ANALYSIS TECHNIQUES, E.H. Newman, June 1982 - June 1983.

713533-3 ENGINEERING CALCULATIONS FOR COMMUNICATIONS SATELLITE SYSTEMS PLANNING, C.A. Levis C.H. Martin, D. Gonsalvez and C.W. Wang, June 1983.

713581-1 USER'S MANUAL FOR REFLECTOR ANTENNA CODE #2, R.C. Rudduck, and R.J. Paknys, September 1982.

713581-2 COMPUTER CODE FOR SPHERICAL AND PARABOLIC TORUS REFLECTOR ANTENNAS, R.J. Paknys and R.C. Rudduck, September 1982.

713603-8 THE PERFORMANCE OF A TRIPOLE ADAPTIVE ARRAY AGAINST CROSS-POLARIZED JAMMING, R.T. Compton, Jr., October 1982.

713603-9 SOPHISTICATED JAMMERS AND ADAPTIVE ARRAYS - FINAL REPORT, R.T. Compton, Jr., October 1982.

713656-3 RADIOMETRICALLY INFERRED SPACE-DIVERSITY ATTENUATION AT 28.6 GHz: CALIBRATION AND INITIAL RESULTS, B.A. Pigon and C.A. Levis, February 1983.

713671-2 THE CALCULATED PERFORMANCE OF SOME RADAR AND TRANSMISSOMETER SYSTEMS IN RAIN AND FOG AT 35, 94, 140 AND 240 GHz, VOLUMES I AND II - COMPUTER CODES, E.L. Utt and C.A. Levis, December 1982.

713711-1 MEASUREMENTS OF SHIP BACKSCATTER FOR HF SHIP IDENTIFICATION STUDIES - FINAL REPORT, E.K. Walton, October 1982.

713731-1 DATA PROCESSING OF RADAR MEASUREMENTS, E.K. Walton, June 1982.

713768-1 A THEORETICAL AND EXPERIMENTAL STUDY OF A POTENTIAL MOBILE SYSTEM FOR EVALUATING ELECTRICAL PARAMETERS OF THE EARTH, P.K. Hayes and L. Peters, Jr., August 1982.

714190-1 THE OHIO STATE UNIVERSITY NCTR DATA BASE FILE STRUCTURE, F.S. Chen and E.K. Walton, October 1982.

714921-1 PERFORMANCE OF AIRCRAFT MOUNTED ADAPTIVE ARRAYS, I.J. Gupta, January 1983.

714505-1 ADAPTIVE ARRAY BEHAVIOR WITH PERIODIC ENVELOPE MODULATED INTERFERENCE, A.S. Al-Ruwais and R.T. Compton, Jr., December 1982.

714505-2 ADVANCED ADAPTIVE ANTENNA TECHNIQUES, R.T. Compton, Jr., January 1983.

714119-2 USERS MANUAL FOR COMPUTER PROGRAM 'CADFIT', E.K. English and B.A. Munk, November 1982.

714215-4 NEAR FIELD ANALYSIS OF AIRBORNE ANTENNAS, N. Wang and W.D. Burnside, March 1983.

714258-1 EFFECT OF MUTUAL COUPLING ON THE PERFORMANCE OF ADAPTIVE ARRAYS, I.J. Gupta and A.A. Ksienski, October 1982.

714258-2 ADAPTIVE ARRAYS FOR MULTIPLE SIMULTANEOUS DESIRED SIGNALS, I.J. Gupta, November 1982.

714921-2 PERFORMANCE OF AIRCRAFT MOUNTED ADAPTIVE ARRAYS, I.J. Gupta, May 1983.

714119-1 DISCUSSION OF RCS OF MCDONNEL DOUGLAS VEHICLE - FINAL REPORT, R.J. Marhefka, F.L. Volakis, L. Peters, Jr., and W.D. Burnside, August 1982.

714190-2 RESONANT STRUCTURE NCTR, D.L. Moffatt, J.D. Young, E.K. Walton and W. Leeper, January 1983.

714215-1 GEODESIC PATHS FOR THE SIDE-MOUNTED ANTENNA ON AN ELLIPSOID MODEL, J.G. Kim and W.D. Burnside, October 1982.

714215-3 RADIATION PATTERNS OF AN ANTENNA MOUNTED ON THE OFF-MID SECTION OF AN ELLIPSOID, J.G. Kim and W.D. Burnside, June 1983.

714215-2 RADIATION PATTERNS OF AN ANTENNA MOUNTED ON THE MIDSECTION OF AN ELLIPSOID, J.G. Kim and W.D. Burnside, July 1983.

714349-5 A MODEL STUDY OF THE RCS OF AN INLET, R.J. Marhefka and L. Peters, Jr., August 1982.

714349-6 STUDY OF THE 1/40th SCALE B-1, L. Peters, Jr., R.J. Marhefka and W.D. Burnside, September 1983.

714505-3 ADAPTIVE ARRAY BEHAVIOR WITH PERIODIC PHASE MODULATED INTERFERENCE, A.S. Al-Ruwais and R.T. Compton, Jr., July 1983.

714505-4 ADVANCED ADAPTIVE ANTENNA TECHNIQUES, R.T. Compton, Jr., June 1983.

714505-5 THE PERFORMANCE OF AN LMS ADAPTIVE ARRAY WITH FREQUENCY HOPPED SIGNALS, L. Acar and R.T. Compton, Jr., June 1983.

714505-6 ADVANCED ADAPTIVE ANTENNA TECHNIQUES, R.T. Compton, Jr., July 1983.

714505-7 ADVANCED ADAPTIVE ANTENNA TECHNIQUES, R.T. Compton, Jr., July 1983.

715010-1 STEREOLOGICAL COMPUTER-ASSISTED FLUOROMETRY: DEVELOPMENT OF TECHNIQUES FOR ANALYSIS OF BIOLOGICAL MATERIAL, S.A. Collins, Jr., October 1983.

APPENDIX IV

PAPERS PUBLISHED BY ESL OCTOBER 1982 TO OCTOBER 1983

ELECTROMAGNETIC SCATTERING BY OPEN CIRCULAR WAVEGUIDES, D.L. Moffatt and T.W. Johnson, reprinted in Radio Science, Vol. 17, No. 6, pp. 1547-1556, November-December, 1982.

REGGE POLES, NATURAL FREQUENCIES, AND SURFACE WAVE RESONANCES OF A CIRCULAR CYLINDER WITH A CONSTANT SURFACE IMPEDANCE, N. Wang, reprinted in IEEE Transactions on Antennas and Propagation, Vol. AP-30, No. 6, November 1982.

AN APERTURE-MATCHED HORN DESIGN, W.D. Burnside, reprinted IEEE Transactions on Antennas and Propagation, Vol. AP-30, No. 4, July 1982.

A SINGLE-PROBE ON-SITE METHOD OF MEASURING THE DIELECTRIC CONSTANT AND CONDUCTIVITY OF SOFT EARTH MEDIA OVER A 1-GHz BANDWIDTH, P.K. Hayes, reprinted in IEEE Transactions on Geoscience and Remote Sensing, Vol. GE-20, No. 4, October 1982.

A HYBRID MM-GEOMETRICAL OPTICS TECHNIQUE FOR THE TREATMENT OF WIRE ANTENNAS MOUNTED ON A CURVED SURFACE, L.W. Henderson and G.A. Thiele, reprinted in IEEE Transactions on Antennas and Propagation, Vol. AP-30, No. 6, November 1982.

A WIDE-BAND ELECTRICALLY SMALL SUPERDIRECTIVE ARRAY, E.H. Newman and M.R. Schrote, reprinted in IEEE Transactions on Antennas and Propagation, Vol. AP-30, No. 6, November 1982.

THE EFFECT OF RANDOM STEERING VECTOR ERRORS IN THE APPLEBAUM ADAPTABLE ARRAY, R.T. Compton, Jr., reprinted in IEEE Transactions on Aerospace and Electronic Systems, Vol. AES-18, No. 5, September 1982.

HIGH FREQUENCY SCATTERING BY A THIN LOSSLESS DIELECTRIC SLAB, W.D. Burnside and K.W. Burgener, reprinted in IEEE Transactions on Antennas and Propagation, Vol. AP-31, No. 1, January 1983.

IMPROVED IDENTIFICATION OF UNDERGROUND TARGETS USING VIDEO PULSE RADARS BY ELIMINATION OF UNDESIRED NATURAL RESONANCES, J.L. Volakis and L. Peters, Jr., reprinted in IEEE Transactions on Antennas and Propagation, Vol. AP-31, No. 2, March 1983.

ON THE CURRENT DISTRIBUTION FOR OPEN SURFACES, E.H. Newman and M.R. Schrote, reprinted in IEEE Transactions on Antennas and Propagation, Vol. AP-31, No. 3, May 1983.

PREDICTION OF ADAPTIVE ARRAY PERFORMANCE, I.J. Gupta and A.A. Ksienski, reprinted in IEEE Transactions on Aerospace and Electronic Systems, Vol. AE-19, No. 3, May 1983.

EFFECT OF MUTUAL COUPLING ON THE PERFORMANCE OF ADAPTIVE ARRAYS, I.J. Gupta and A.A. Ksienski, reprinted in IEEE Transactions on Antennas and Propagation, Vol. AP-31, No. 5, September 1983.

EIGENFUNCTIONS OF COMPOSITE HERMITIAN OPERATORS WITH APPLICATION TO DISCRETE AND CONTINUOUS RADIATING SYSTEMS, N. Inagaki and R.J. Garbacz, reprinted in IEEE Transactions on Antennas and Propagation, Vol. AP-30, No. 4, pp. 571-575, July 1982.

FIRST-ORDER EQUIVALENT CURRENT AND CORNER DIFFRACTION SCATTERING FROM FLAT PLATE STRUCTURES, F.A. Sikta, W.D. Burnside, T.T. Chu and L. Peters, Jr., reprinted in IEEE Transactions on Antennas and Propagation, Vol. AP-31, No. 4, pp. 584-589, July 1983.

THE PERFORMANCE OF A TRIPOLE ADAPTIVE ARRAY AGAINST CROSS-POLARIZED JAMMING, R.T. Compton, Jr. reprinted in IEEE Transactions on Antennas and Propagation, Vol. AP-31, No. 4, pp. 682-685, July, 1983.

SCATTERING FROM CYLINDRICAL INHOMOGENEITIES IN A LOSSY MEDIUM, L. Peters, Jr. and J.H. Richmond, reprinted in Radio Science, Vol. 17, No. 5, pp. 975-987, September-October 1982.

HIGH FREQUENCY SCATTERING FROM THE EDTES OF IMPEDANCE DISCONTINUITIES ON A FLAT PLANE, R. Tiberio and G. Pelosi, IEEE Transactions on Antennas and Propagation, Vol. AP-31, No. 4, pp. 590-596, July 1983.

AN EXTENSION OF THE UNIFORM GTD FOR THE DIFFRACTOIN BY A WEDGE ILLULMINATED BY A DIPOLE CLOSER TO IT'S EDGE, R.G. Kouyoumjian, G. Pelosi and R. Tiberio, Alta Frequenza, Vol. 52, No. 1, pp. 24-33, 1983.

APPENDIX V

JSEP RELATED ORAL PRESENTATIONS

OCTOBER 1982 TO OCTOBER 1983

RESONANCE REGION BACKSCATTERED SIGNATURES FROM A CONDUCTING ELLIPSOID, J.D. Young and E.K. Walton, 1983 International IEEE/AP-S Symposium and National Radio Science Meeting, Houston, Texas, May 1983.

IDENTIFICATION OF SCATTERING MECHANISMS FROM MEASURED IMPULSE RESPONSE SIGNATURES OS SIMPLE CONDUCTING OBJECTS, W.J. Leeper and J.D. Young, 1983 International IEEE/AP-S Symposium and National Radio Science Meeting, Houston, Texas, May 1983.

MOMENT METHOD MODELING OF REALISTIC STRUCTURES, E.H. Newman, 52nd Interservice Antenna Group (ISAG) Meeting, Annapolis, Maryland, April 1983.

A UNIFORM GTD ANALYSIS OF THE EM DIFFRACTION BY A THIN-DIELECTRIC HALF PLANE, P.H. Pathak and R. Rojas-Teran, 1983 International IEEE/AP-S Symposium and National Radio Science Meeting, Houston, Texas, May 1983.

CONTRIBUTIONS BY EDWARD M. KENNAUGH TO HIGH RESOLUTION BROADBAND RADAR POLARIMETRY, D.L. Moffatt, Second Workshop on Polarimetric Radar Technology Huntsville, Alabama, May 1983. To be published in the Proceedings of the Workshop.

PARAXIAL EDGE DIFFRACTION, R.G. Kouyoumjian and O.M. Buyukdura, 1983 URSI International Symposium in Santiago de Compostela, Spain, August 1983.

THE MODERN GEOMETRICAL THEORY OF DIFFRACTION AND ITS APPLICATION, R.G. Kouyoumjian, Istanbul Technical University, Istanbul, Turkey, September 1983.

TRANSIENT CURRENT DENSITY WAVEFORMS ON A PERFECTLY CONDUCTING SPHERE, E.M. Kennaugh and D.L. Moffatt, NATO Advanced Research Workshop on Inverse Methods in Electromagnetic Imaging, Bad Windsheim, Federal Republic of Germany, September 1983. To be published in the Proceedings of the Workshop.

TIME-DEPENDENT RESPONSE WAVEFORMS AND RECOGNITION OF IMAGING AUTHENTICITY FEATURES, D.L. Moffatt and T.C. Lee, NATO Advanced Research Workshop on Inverse Methods in Electromagnetic Imaging, Bad Windsheim, Federal Republic of Germany, September 1983. To be published in the Proceedings of the Workshop.

THE OHIO STATE UNIVERSITY COMPACT RADAR CROSS-SECTION MEASUREMENT RANGE, E.K. Walton and J.D. Young, 1983 AMTA Annual Meeting, Annapolis, Maryland, September 1983.

August 1982

UNIFORM GEOMETRICAL THEORY OF DIFFRACTION, P.H. Pathak, The International Society for Optical Engineering, San Diego, California, August 1982.

JSEP RELATED DISSERTATIONS

OCTOBER 1982 TO OCTOBER 1983

AN OPEN SURFACE INTEGRAL FORMULATION FOR ELECTROMAGNETIC SCATTERING BY A MATERIAL PLATE, M.R. Schrote.

JSEP RELATED THESES

OCTOBER 1982 TO OCTOBER 1983

ELECTROMAGNETIC MODELING OF ARBITRARY SURFACES BY POLYGONAL PLATES AND/OR WIRES, P. Alexandropoulos.

IDENTIFICATION OF SCATTERING MECHANISMS FROM MEASURED IMPULSE RESPONSE SIGNATURES OF SEVERAL CONDUCTING OBJECTS, W.J. Leeper.

APPENDIX VI

JSEP RELATED PAPERS SUBMITTED FOR PUBLICATION

OCTOBER 1982 TO OCTOBER 1983

CALCULATION OF THE HIGH FREQUENCY DIFFRACTION BY TWO NEARBY EDGES ILLUMINATED AT GRAZING INCIDENCE, R. Tiberio, and R.G. Kouyoumjian, accepted for publication in the IEEE Transactions on Antennas and Propagation.

SCATTERING BY A STRIP WITH TWO FACE IMPEDANCES AT EDGE-ON INCIDENCE, R. Tiberio, F. Bessi, G. Manara and G. Pelosi, accepted for publication in the Journal of Radio Science.

ON THE EIGENFUNCTION EXPANSION OF ELECTROMAGNETIC DYADIC GREEN'S FUNCTIONS, P.H. Pathak, accepted for publication in the IEEE Transactions on Antennas and Propagation.

A UNIFORM GTD APPROACH TO EM SCATTERING AND RADIATION, R.G. Kouyoumjian and P.H. Pathak, to appear in Handbook on Acoustic, Electromagnetic and Elastic Wave Scattering - Theory and Experiment, Vol. I, edited by V.K. Varadan and V.V. Varadan, North Holland.

TECHNIQUES FOR HIGH FREQUENCY PROBLEMS, P.H. Pathak, to appear in the Antenna Handbook, edited by Y.T. Lo and S.W. Lee, ITT Howard W. Sams and Co., Inc.

AN OPEN SURFACE INTEGRAL FORMULATION FOR ELECTROMAGNETIC SCATTERING BY MATERIAL PLATES, E.H. Newman and M.R. Schrote, accepted for publication in the IEEE Transactions on Antennas and Propagation.

POLYGONAL PLATE MODELING OF REALISTIC STRUCTURES, E.H. Newman, P. Alexandropoulos and E.K. Walton, submitted for publication in the IEEE Transactions on Antennas and Propagation.

TIME DOMAIN ELECTROMAGNETIC SCATTERING BY OPEN ENDED CIRCULAR WAVEGUIDE AND RELATED STRUCTURE, D.L. Moffatt, C.Y. Lai and T.C. Lee, accepted for publication in WAVE MOTION.

TRANSIENT RESPONSE CHARACTERISTICS IN IDENTIFICATION AND IMAGING, D.L. Moffatt, J.D. Young and A.A. Ksienski, to appear in Microwave Imaging Techniques a series of books on "Benchmark Papers in Electrical Engineering and Computer Science", edited by J.B. Thomas, Hutchinson Ross Publishing Company, Stroudsburg, Pennsylvania, 1983.

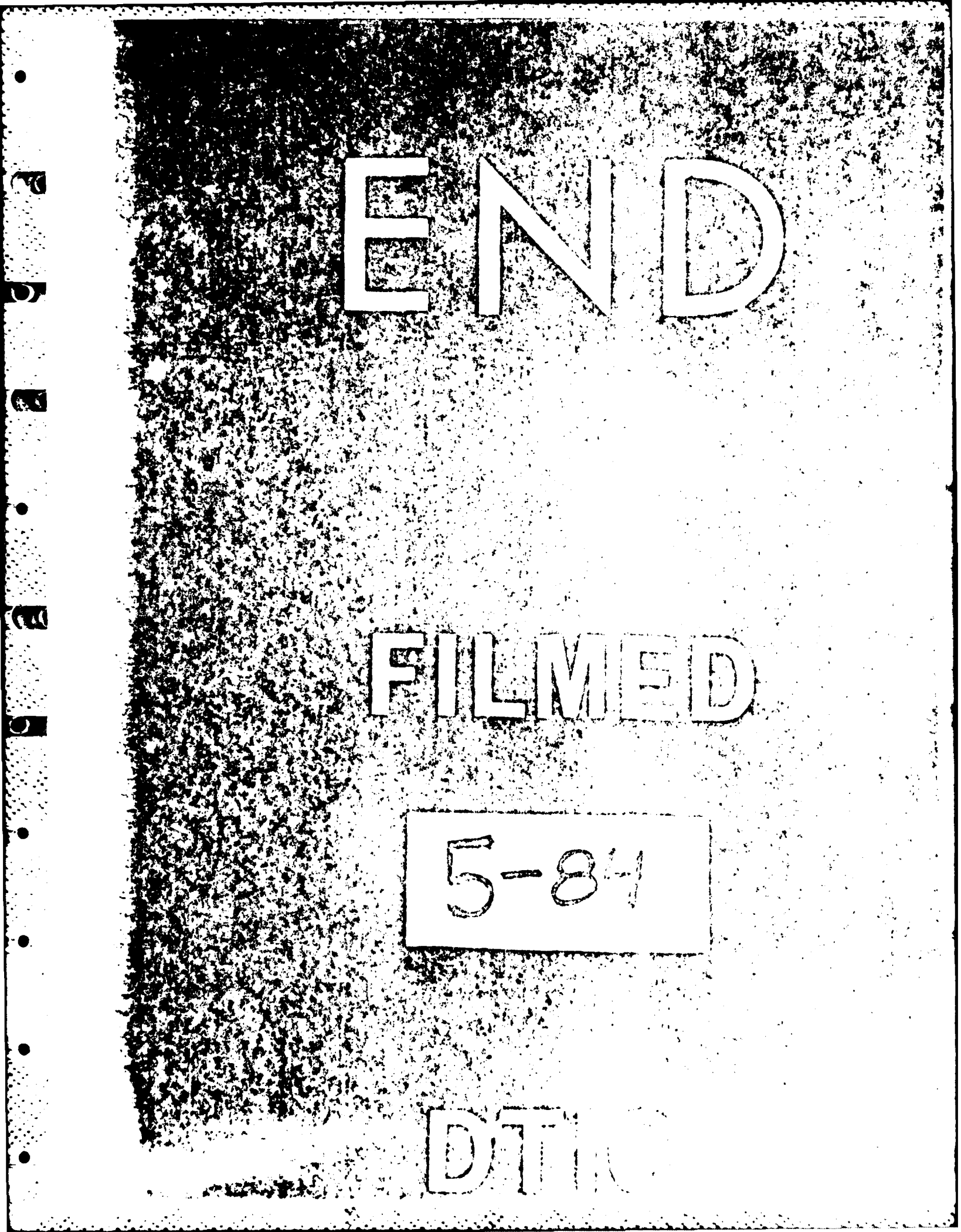
END
FILMED
5-81
DTIC